DESIGN AND ENGINEERING OF A BIO-RESPONSIVE, NANO-ENABLED VITREOUS SUBSTITUTE FOR THE TREATMENT OF RETINAL DISEASES

Kruti Naik

UNIVERSITY OF THE
WITWATERSRAND,
JOHANNESBURG

A dissertation submitted to the Faculty of Health Sciences, University of the Witwatersrand, Johannesburg, in fulfilment of the requirements for the degree of Master of Pharmacy, 2023

Supervisor:

Professor Yahya E. Choonara

Department of Pharmacy and Pharmacology, Faculty of Health Sciences, University of the Witwatersrand, South Africa.

Co-supervisors:

Professor Lisa C. Du Toit

Department of Pharmacy and Pharmacology, Faculty of Health Sciences, University of the Witwatersrand, South Africa.

Doctor Naseer Ally

Division of Ophthalmology, School of Clinical Medicine, Faculty of Health Sciences, University of the Witwatersrand, South Africa

Associate Professor Pierre P.D. Kondiah

Department of Pharmacy and Pharmacology, Faculty of Health Sciences, University of The Witwatersrand, South Africa

Declaration

I, Kruti Naik, hereby declare that this dissertation is my own work, with all other sources of information acknowledged by means of a complete reference list. This dissertation is being submitted in fulfilment of the degree of Master of Pharmacy, at the University of the Witwatersrand, Johannesburg. This work has not been submitted before for any degree or examination to this or any other university.

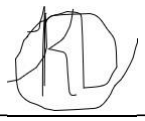

27 July 2023

K Naik Date

Research presentations and publications arising from this study.

1. Kruti Naik, Yahya E. Choonara, Lisa C. Du Toit and Naseer Ally. Design and engineering of a bio-responsive, nano-enabled vitreous substitute for the treatment of retinal diseases, Annual Molecular Biosciences Research Trust (MBRT) Postgraduate Research Day 2021, University of the Witwatersrand, 9 December 2021 (Appendix B)

2. Kruti Naik, Lisa C. Du Toit, Naseer Ally, and Yahya E. Choonara. (2023). Advances in Polysaccharide- and Synthetic Polymer-Based Vitreous Substitutes. *Pharmaceutics* 15(2):566. https://doi.org/10.3390/pharmaceutics15020566
   Note: This review paper forms part of Chapter 2
   Author contribution by the candidate: The candidate assisted with devising and outlining the main ideas of the manuscript. She is the first author of the manuscript, took the lead in writing and modifying the manuscript as well as providing necessary feedback and approving the final manuscript. (Appendix C)

3. Kruti Naik, Lisa C. Du Toit, Naseer Ally, Pierre P.D. Kondiah, and Yahya E. Choonara. A Nanoparticle-loaded Poloxamer-Hyaluronic acid Hydrogel for Potential Vitreous Substitution. (To be submitted)
   Note: This research paper forms part of Chapter 4

Abstract

The vitreous humour is a soft gel between the lens and the retina in the eye. It protects the surrounding ocular tissues functioning as a shock absorber and a vessel for oxygen and metabolite transport. Vitreous liquefaction leads to vitreous detachment resulting in ocular tissue damage such as retinal detachment and vitreous haemorrhage. Current treatment includes total vitreous replacement via pars plana vitrectomy utilising silicone oil. Cataracts, inflammation, and retinal toxicity as a result of silicone oil treatment have led to the need for a more effective long-term vitreous substitute. It is essential to treat vitreoretinal diseases concurrently with vitreous substitution. This study aimed to investigate and design the proposed concept of a thermoresponsive, nano-enabled vitreous substitute for the treatment of retinal diseases. An initial study in the selection of polymers for the hydrogel identified a blend of natural and synthetic polymers. Hyaluronic acid with a blend of two poloxamers of differing molecular weights were identified and optimisation allowed for their selection prior to nanoparticle loading and characterisation. Poly(D,L-lactide-co-glycolide) acid nanoparticles encapsulating triamcinolone acetonide were synthesised with a spherical morphology and mean diameter of 153 nm allowing nanoparticle penetration into the retinal layers from the vitreous. Hydrogel fabrication and nanoparticle loading within the hydrogel was confirmed via physicochemical analysis. Gelation studies indicated that hydrogels formed in nine minutes and 10 minutes for the unloaded and nanoparticle-loaded hydrogels respectively. The hydrogels displayed *in situ* formation properties and rheometric viscoelastic studies indicated the unloaded and loaded hydrogels to have modulus values similar to those of the natural vitreous at 37 °C. Administration of the hydrogels was possible via 26G needles allowing for clinical application and drug release of triamcinolone acetonide from the nanoparticle-loaded hydrogel indicated that a sustained drug release was visible over nine weeks. The hydrogels displayed minimal swelling, reaching equilibrium swelling within 12 hours for the unloaded hydrogel and eight hours for the nanoparticle-loaded hydrogel. Biodegradation in simulated vitreous humour with lysozyme showed < 20% degradation within nine weeks. Biocompatibility of both hydrogels was shown with mouse fibroblast and human retinal pigment epithelium cell lines. Lastly, a pilot *in vivo* study with a New Zealand White rabbit model displayed minimal toxicity with localised drug release behaviour. In conclusion, the unloaded and nanoparticle-loaded hydrogels developed in this research demonstrate their potential as vitreous substitutes that function as drug delivery systems following vitrectomy surgery.

Acknowledgements

At the completion of this dissertation, there are several people for whom I am appreciative. They have all provided immense support and assistance.

To my family, thank you for your endless support, love, and guidance.

To my supervisors Professor Yahya Choonara, Professor Lisa Du Toit, Doctor Naseer Ally, and Professor Pierre Kondiah without whom this could not have been done. I am immensely grateful for your guidance, your time and for seeing the potential in me to achieve this.

To all my wonderful friends, thank you so much. There aren't enough words for how grateful I am for all your support, encouragement, and love.

To all my WADDP colleagues and all the Wits Pharmacy department staff, thank you for your assistance and support in everything.

To Mr Kleinbooi Mohlabi, Mr Hillary Mndlovu, Mr Bafana Temba, Ms Phumzile Moerane, Mr Sello Ramarumo, and Ms Tshidi Mosete, thank you for all your assistance. All your efforts were greatly appreciated.

To Mrs Petra Dinham from the School of Chemical & Metallurgical Engineering and all the staff at the Wits Research Animal Facility (WRAF), all your assistance and support are greatly appreciated.

Financial support received from the National Research Foundation (NRF) for this project is acknowledged.

Table of contents

List of figures

List of tables

List of equations

List of abbreviations

3D – Three dimensional

Abs_C – Control absorbance

Abs_S – Sample absorbance

ADH – Adipic dihydrazide

AMD – Age-related macular degeneration

Anti-VEGF – Anti-vascular endothelial growth factors

APS – Ammonium persulfate

BAC – Bis(acryloyl)cystamine

BMAC – N',N'-bis(methylacryloyl-cystamine)

BSS – Balanced salt solution

CBAA – Carboxybetaine acrylamide

DCM – Dichloromethane

DLS – Dynamic light scattering

DMEM - Dulbecco's Modified Eagle Medium

DSC – Differential scanning calorimeter

EA – Ethyl acetate

ECM – Extracellular matrix

EPC – Tri-component hydrogel

FBS – Fetal Bovine Serum

FCVB – Foldable capsular vitreous body

FTBA – Perfluorotributylamine

FTIR – Fourier Transform Infrared

GAG – Glycosaminoglycan

H&E – Haematoxylin and eosin

HA – Hyaluronic acid

HLB – Hydrophilic-lipophilic balance

HPMC – Hydroxypropyl methylcellulose

hRPE – human Retinal pigment epithelium

IM – Intramuscular

LVR – Linear viscoelastic region

MAM – methacrylamide

MEC – Minimum effective concentration

MW – Molecular weight

NIH/3T3 – mouse fibroblast

NIPAAm – N-isopropylacrylamide

NP – Nanoparticle

NPA – N-phenylacrylamide

NZW – New Zealand White

P188 – Poloxamer 188

P407 – Poloxamer 407

PCL – Poly(ε-caprolactone)

PDI – Polydispersity index

PEG – Polyethylene glycol

PEGDA – Polyethylene glycol diacrylate

PEGMA – Polyethylene glycol methacrylate

PEO – Polyethylene oxide

PEO-PPO-PEO – Poly(ethylene oxide)-*b*-poly(propylene oxide)-*b*-poly(ethylene oxide)

PF-127 – Pluronic polyol F-127

PFCLs – Perfluorocarbon liquids

PGMA – Poly(glyceryl methacrylate)

PHBHx – Poly[(R)-3-hydroxybutyrate-(R)-3-hydroxyhexanoate]

PLGA - Poly(D,L-lactide-co-glycolide) acid

PMAGME – Poly(methyl 2-acrylamido-2-methoxyacetate)

pNIPAAm – Poly(N-isopropylacrylamide)

PPG – Poly(propylene glycol)

PPO – Polypropylene oxide

PPV – Pars plana vitrectomy

PR – Pneumatic retinopexy

PVA – Polyvinyl alcohol

PVA-MA – Methacrylated Polyvinyl alcohol

PVD – Posterior vitreous detachment

PVP – Poly(1-vinyl-2-pyrrolidone)

PVR – Proliferative vitreoretinopathy

RD – Retinal detachment

RPE – Retinal pigment epithelium

RRD – Rhegmatogenous retinal detachment

SEM – Scanning electron microscopy

SFAs – Semifluorinated alkanes

SO – Silicone oil

sol-gel – Solution-gel

SOP – Standard operating procedure

STMP – Trisodium trimetaphosphate

SVH – Simulated vitreous humour

TA – Triamcinolone acetonide

TEMED – N,N,N’,N’ tetramethyl ethylenediamine

TGA – Thermogravimetric analyser

UV – Ultraviolet

W_0 – Initial weight

W_D – Dry weight

WHO – World Health Organisation

WRAF – Wits research animal facility

W_S – Swollen weight

W_t – Weight at each timepoint

XRD – X-Ray Diffraction

β-CD – β-cyclodextrin

Chapter 1 - Introduction

1.1. Background

The vitreous humour is a soft hydrogel that constitutes 80% of the eye. It is a fragile gel that protects the lens and retina from shocks by absorbing and dampening the vibrations (Alovisi *et al.*, 2017). The major components of the vitreous are water, collagen fibres, and hyaluronic acid (Yadav *et al.*, 2021). Alterations in collagen, oxidative damage, and enzymatic digestion lead to a collapse in the gel network of the vitreous. These occur as a result of age causing the vitreous to liquefy (Tram and Swindle-Reilly, 2018; Ankamah *et al.*, 2020).

Vitreous liquefaction leads to varying degrees of posterior vitreous detachment (PVD) as depicted in Figure 1.1 (Le Goff and Bishop, 2008). Posterior vitreous detachment is a process whereby the vitreous humour splits away from the inner surface of the retina (Le Goff and Bishop, 2008; Ankamah *et al.*, 2020). It can result in vitreous haemorrhage, cataracts, macular hole formation, retinal tears, and rhegmatogenous retinal detachment (RRD) (Le Goff and Bishop, 2008; Sebag, 2018). The vitreous is removed by pars plana vitrectomy (PPV) to treat pathologies such as RRD and vitreous haemorrhage (Zhang *et al.*, 2017; Shaikh *et al.*, 2023). During PPV, the vitreous is replaced by silicone oils, perfluorocarbon liquids or gas (Kleinberg *et al.*, 2011; Tram *et al.*, 2020). Silicone oil is the most commonly used vitreous substitute, however, silicone oil substitutes are known to cause many adverse effects such as oxidative damage causing cataracts (Swindle *et al*., 2008; Kleinberg *et al.*, 2011), intraocular inflammation, elevated intraocular pressure (Davis *et al*., 2017) and direct retinal toxicity (Januschowski *et al.*, 2018).

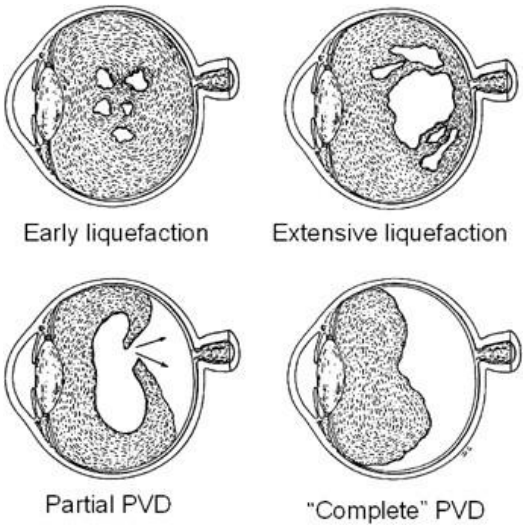

Figure 1.1 – Degrees of PVD from liquefaction to complete PVD (Le Goff and Bishop, 2008).

Proliferative vitreoretinopathy (PVR) can also occur as a result of scarring after retinal detachment or retinal detachment surgery (Idrees *et al*., 2019). There is no effective treatment for PVR currently, however, inflammation, cell proliferation, and fibrosis have been therapeutic targets with the use of corticosteroids (e.g., triamcinolone acetonide and dexamethasone), antiproliferative and antineoplastic agents (e.g. 5-fluorouracil and daunorubicin) and anti-vascular endothelial growth factor (anti-VEGF) agents (e.g. Bevacizumab) (Idrees *et al*., 2019; Charteris, 2020).

Regenerative medicine is a growing discipline that offers sophisticated solutions for the repair, regeneration, and replacement of damaged tissues and cells. Several approaches, including gene therapy, as well as stem cell and progenitor cell therapy can be used. (Vacanti, 2006; Polykandriotis *et al*., 2010). Tissue engineering for tissue regeneration is the development of biodegradable and biocompatible scaffolds for long-term use (Doostmohammadi *et al*., 2020).

Scaffolds developed for ophthalmic tissue regeneration should mimic the extracellular matrix (ECM) resulting in a scaffold that is porous, biodegradable, and biocompatible (Matthyssen *et al.*, 2018; Doostmohammadi *et al*., 2020). Scaffolds for vitreous tissue engineering must be transparent and permeable to allow oxygen, metabolites, and nutrients to diffuse. The natural vitreous acts as a viscoelastic fluid or gel to keep the

shape of the eye (Kleinberg *et al.*, 2011; Davis *et al*., 2017) and a vitreous substitute must simulate this.

Hydrogels are three-dimensional (3D) polymeric scaffolds that can swell in aqueous solutions without dissolving and thermosetting hydrogels are a type of bio-responsive hydrogel that swell to a gel in response to temperature (Kleinberg *et al.*, 2011). Due to their gelation at body temperature, thermosetting hydrogels can be designed to produce an intraocular tamponade effect (Kleinberg *et al.*, 2011; Liu *et al.*, 2019). Currently, there is a need for improved vitreous substitutes, and hydrogels are a promising engineered substitute.

This study proposes to address the need for improved vitreous substitutes following vitrectomy in patients, while simultaneously treating retinal diseases. The purpose of this study is to design a bio-responsive, nano-enabled vitreous substitute for the treatment of retinal diseases.

1.2. Rationale and Motivation

Limitations with current vitreous substitutes have stimulated a need for new vitreous substitutes with reduced side effects (Chang *et al*., 2019). Thermo-responsive, polymeric hydrogels undergo solution-gel (sol-gel) transitions in response to changes in temperature (Soliman *et al.*, 2019). Thus, a thermo-responsive hydrogel as a vitreous substitute is advantageous as it can form a gel once it is injected into the eye.

Synthetic polymers have been considered a more ideal option for long-term substitutes due to more prolonged degradation in comparison to natural polymers such as hyaluronic acid which degrade relatively easily (Kleinberg *et al.*, 2011). Chemical and morphological modifications to natural polymers, such as the introduction of functional groups on reactive groups and the introduction of other polymers to form polymeric complexes, allows for changes in their degradation behaviour (George *et al*., 2019; Tong *et al.*, 2020).

The blood-retinal barrier, the posterior position of the retina, and the inner limiting membrane of the eye present challenges for drug delivery to the retina. Intravitreal drug delivery for retinal diseases has circumvented these challenges, however, it carries its disadvantages. These include the risk of endophthalmitis, vitreous

haemorrhage and retinal detachment (Cabrera *et al.*, 2019). Patient compliance, with the use of intravitreal injections, decreases as a result of the increased frequency of injections due to fast elimination from the vitreous (Huang and Chau, 2019). The bioavailability of these drugs can be increased via encapsulation in polymeric nanoparticles (Imperiale *et al*., 2018). Thus, intravitreal drug-loaded nanoparticles are a potential long-term delivery route for the treatment of retinal diseases.

A thermo-responsive hydrogel that functions as a vitreous substitute, as well as a long-term drug delivery medium, is a novel system for retinal disease treatment. Due to its long-term effects, patient compliance would increase, and adverse effects observed with repeated intravitreal injections would decrease (Ghasemi Falavarjani and Nguyen, 2013).

The bio-responsive vitreous substitute proposed in this study, as shown in Figure 1.2, was a hydrogel composed of natural or synthetic polymers that simulated the properties of the natural vitreous such as refractive index, light transmittance, and viscoelastic properties. The hydrogel was able to be injected into the posterior segment of the eye. This long-term vitreous substitute functioned as a carrier and delivery system for drug-loaded nanoparticles in the treatment of retinal diseases. Triamcinolone acetonide (a steroid used in the management of macular oedema) was used as a model drug with the potential for other drugs such as anti-VEGF agents to be delivered in the same system.

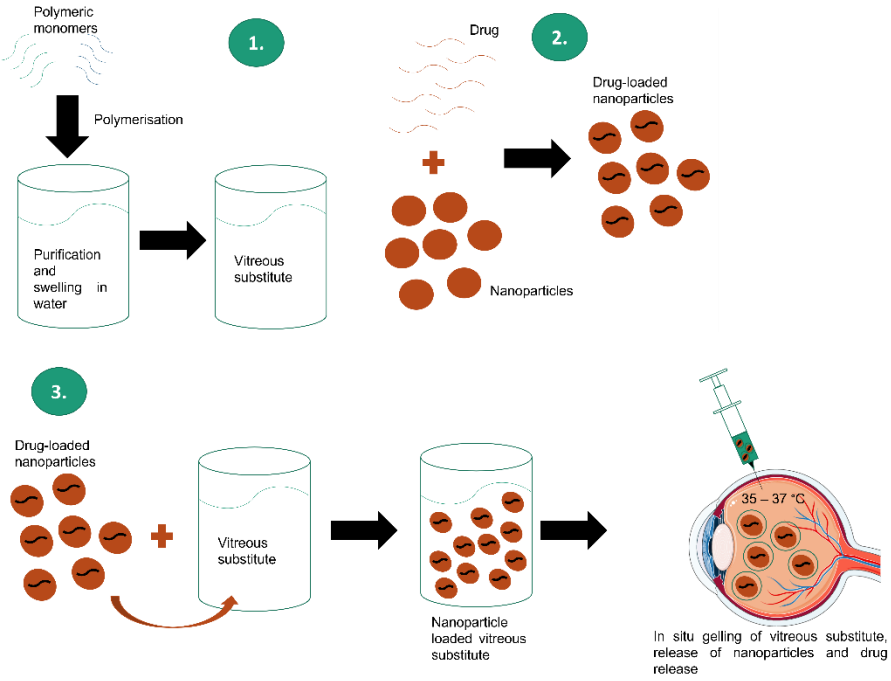

Figure 1.2 - Schematic representation of the proposed bio-responsive, nano-enabled vitreous substitute synthesis process. This figure was partly generated using Servier Medical Art, provided by Servier, licensed under a Creative Commons Attribution 3.0 unported license.

1.3. Aim and Objectives

This research aimed to develop a bio-responsive vitreous substitute which can also function as a delivery system for the controlled release of triamcinolone acetonide-loaded nanoparticles for the treatment of retinal diseases. To achieve the aim of this study, the following objectives were completed:

1. To select appropriate natural or synthetic polymers and to synthesise a bio-responsive vitreous substitute. To screen the formulated vitreous substitute based on transparency and gel formation and to establish the bio-responsive thermo-gelling behaviour of the substitute.
2. To synthesise nanoparticles (NPs), loaded with triamcinolone acetonide, to achieve controlled drug release kinetics, and undertake characterisation studies of the fabricated nanoparticles.
3. To optimise nanoparticle loading in the synthesised vitreous substitute and characterise the physicochemical and mechanical properties of the nanoparticle-

free and nanoparticle-loaded substitutes such as Fourier Transform Infrared (FTIR) spectroscopy, optical transparency, turbidity, density, and rheological analysis.

4. To undertake *in vitro* drug release analysis and establish the polymer degradation behaviour of the vitreous substitute.
5. To undertake *in vitro* compatibility analysis of the nanoparticle-loaded substitute.
6. To perform a pilot *in vivo* analysis using a New Zealand White (NZW) rabbit model to determine the therapeutic efficacy of the nano-enabled vitreous substitute.

1.4. Overview of this dissertation

Chapter one of this dissertation provides an introduction and background to the current study. The disadvantages of current vitreous substitutes and intravitreal drug treatments are discussed, considerations of a vitreous substitute are presented, and the rationale and motivation of this study are discussed. Lastly, the aims and objectives of the study are highlighted.

Chapter two of this dissertation provides a comprehensive review of current clinically used vitreous substitutes along with experimental polymeric vitreous substitutes. The natural human vitreous and its components are discussed along with the properties to consider for an ideal substitute. Additionally, this chapter provides the advantages and disadvantages of all the materials presented.

Chapter three of this dissertation provides the preliminary design and proof-of-concept for the vitreous substitute for this study by evaluating the ability of two synthetic polymers to form a composite thermo-responsive hydrogel with the natural polymer hyaluronic acid that is found in the native eye. This chapter presents the preliminary formulations with various polymer concentrations and finally presents an optimised composite polymer blend as a potential vitreous substitute.

Chapter four of this dissertation describes the characterisation of the nanoparticles, the unloaded hydrogel and the nanoparticle-loaded hydrogel. Optical properties (refractive index and transmittance), viscoelastic properties and physicochemical properties are discussed to confirm the similarities between the hydrogels and to confirm the fabrication of the formulations. Additionally, drug release, swelling and

degradation profiles are discussed. Lastly, a biocompatibility assay with a 3T3 and hRPE cell line is presented.

Chapter five of this dissertation discussed the pilot *in vivo* study conducted using the New Zealand White rabbit model. Methodologies of study design and surgical procedures are discussed. The biocompatibility over 28 days using histomorphological analysis is discussed and the drug release profile over the 28 days of investigation is presented.

Chapter six of this dissertation presents the conclusions of this research. Perspective recommendations with the formulated hydrogel and the field of vitreous substitution are also presented.

1.5. References:

Alovisi, C., Panico, C., Sanctis, U. de & Eandi, C.M. (2017) Vitreous Substitutes: Old and New Materials in Vitreoretinal Surgery. *Journal of Ophthalmology*. 2017, 1–6. doi:10.1155/2017/3172138.

Ankamah, E., Sebag, J., Ng, E. & Nolan, J.M. (2020) Vitreous antioxidants, degeneration, and vitreo-retinopathy: Exploring the links. *Antioxidants*.9 (1) p.7. doi:10.3390/antiox9010007.

Cabrera, F.J., Wang, D.C., Reddy, K., Acharya, G. & Shin, C.S. (2019) Challenges and opportunities for drug delivery to the posterior of the eye. *Drug Discovery Today*. 24 (8), 1679–1684. doi:10.1016/j.drudis.2019.05.035.

Chang, D., Park, K. & Famili, A. (2019) Hydrogels for sustained delivery of biologics to the back of the eye. *Drug Discovery Today*. 24 (8), 1470–1482. doi:10.1016/j.drudis.2019.05.037.

Charteris, D.G. (2020) Proliferative vitreoretinopathy: revised concepts of pathogenesis and adjunctive treatment. *Eye*. 34 (2), 241–245. doi:10.1038/s41433-019-0699-1.

Davis, J.T., Hamilton, P.D. & Ravi, N. (2017) Poly(acrylamide co-acrylic acid) for use as an in situ gelling vitreous substitute. *Journal of Bioactive and Compatible Polymers*. 32 (5), 528–541. doi:10.1177/0883911516688482.

Doostmohammadi, M., Forootanfar, H. & Ramakrishna, S. (2020) Regenerative medicine and drug delivery: Progress via electrospun biomaterials. *Materials Science and Engineering: C*. 109 (April 2019), 110521. doi:10.1016/j.msec.2019.110521.

George, A., Shah, P.A. & Shrivastav, P.S. (2019) Natural biodegradable polymers based nano-formulations for drug delivery: A review. *International Journal of Pharmaceutics*. 561 (March), 244–264. doi:10.1016/j.ijpharm.2019.03.011.

Ghasemi Falavarjani, K. & Nguyen, Q.D. (2013) Adverse events and complications associated with intravitreal injection of anti-VEGF agents: a review of literature. *Eye*. 27 (7), 787–794. doi:10.1038/eye.2013.107.

Huang, X. & Chau, Y. (2019) Intravitreal nanoparticles for retinal delivery. *Drug Discovery Today*. 24 (8), 1510–1523. doi:10.1016/j.drudis.2019.05.005.

Idrees, S., Sridhar, J. & Kuriyan, A.E. (2019) Proliferative Vitreoretinopathy: A Review. *International Ophthalmology Clinics*. 59 (1), 221–240. doi:10.1097/IIO.0000000000000258.

Imperiale, J.C., Acosta, G.B. & Sosnik, A. (2018) Polymer-based carriers for ophthalmic drug delivery. *Journal of Controlled Release*. 285 (June), 106–141. doi:10.1016/j.jconrel.2018.06.031.

Januschowski, K., Irigoyen, C., Pastor, J.C., Srivastava, G.K., Romano, M.R., Heimann, H., Stalmans, P., Van Keer, K., Boden, K., Szurman, P. & Spitzer, M.S. (2018) Retinal Toxicity of Medical Devices Used during Vitreoretinal Surgery: A Critical Overview. *Ophthalmologica*. 240 (4), 236–243. doi:10.1159/000488504.

Kleinberg, T.T., Tzekov, R.T., Stein, L., Ravi, N. & Kaushal, S. (2011) Vitreous Substitutes: A Comprehensive Review. *Survey of Ophthalmology*. 56 (4), 300–323. doi:10.1016/j.survophthal.2010.09.001.

Le Goff, M.M. & Bishop, P.N. (2008) Adult vitreous structure and postnatal changes. *Eye*. 22 (10), 1214–1222. doi:10.1038/eye.2008.21.

Liu, Z., Liow, S.S., Lai, S.L., Alli-Shaik, A., Holder, G.E., et al. (2019) Retinal-detachment repair and vitreous-like-body reformation via a thermogelling polymer

endotamponade. *Nature biomedical engineering*. 3 (8), 598–610. doi:10.1038/s41551-019-0382-7.

Matthyssen, S., van den Bogerd, B., Dhubhghaill, S.N., Koppen, C. & Zakaria, N. (2018) Corneal regeneration: A review of stromal replacements. *Acta Biomaterialia*. 69, 31–41. doi:10.1016/j.actbio.2018.01.023.

Polykandriotis, E., Popescu, L.M. & Horch, R.E. (2010) Regenerative medicine: then and now - an update of recent history into future possibilities. *Journal of Cellular and Molecular Medicine*. 14 (10), 2350–2358. doi:10.1111/j.1582-4934.2010.01169.x.

Sebag, J. (2018) Posterior Vitreous Detachment. *Ophthalmology*. 125 (9), 1384–1385. doi:10.1016/j.ophtha.2018.05.018.

Shaikh, N., Srishti, R., Khanum, A., Thirumalesh, M.B., Dave, V., Arora, A., Bansal, R., Surve, A., Azad, S. & Kumar, V. (2023) Vitreous hemorrhage - Causes, diagnosis, and management. *Indian journal of ophthalmology*. 71 (1), 28–38. doi:10.4103/ijo.IJO_928_22.

Soliman, K.A., Ullah, K., Shah, A., Jones, D.S. & Singh, T.R.R. (2019) Poloxamer-based in situ gelling thermoresponsive systems for ocular drug delivery applications. *Drug Discovery Today*. 24 (8), 1575–1586. doi:10.1016/j.drudis.2019.05.036.

Swindle, K.E., Hamilton, P.D. & Ravi, N. (2008) In situ formation of hydrogels as vitreous substitutes: Viscoelastic comparison to porcine vitreous. *Journal of biomedical materials research. Part A*. 87 (3), 656–665. doi:10.1002/jbm.a.31769.

Tong, X., Pan, W., Su, T., Zhang, M., Dong, W. & Qi, X. (2020) Recent advances in natural polymer-based drug delivery systems. *Reactive and Functional Polymers*. 148 (January), 104501. doi:10.1016/j.reactfunctpolym.2020.104501.

Tram, N.K., Jiang, P., Torres-Flores, T.C., Jacobs, K.M., Chandler, H.L. & Swindle-Reilly, K.E. (2020) A Hydrogel Vitreous Substitute that Releases Antioxidant. *Macromolecular Bioscience*. 20 (2), 1900305. doi:10.1002/mabi.201900305.

Tram, N.K. & Swindle-Reilly, K.E. (2018) Rheological properties and age-related changes of the human vitreous humor. *Frontiers in Bioengineering and Biotechnology*. 6 (DEC), 1–12. doi:10.3389/fbioe.2018.00199.

Vacanti, C. (2006) The history of tissue engineering. *Journal of Cellular and Molecular Medicine*. 1 (3), 569–576. doi:10.2755/jcmm010.003.20.

Yadav, I., Purohit, S.D., Singh, H., Bhushan, S., Yadav, M.K., Velpandian, T., Chawla, R., Hazra, S. & Mishra, N.C. (2021) Vitreous substitutes: An overview of the properties, importance, and development. *Journal of Biomedical Materials Research - Part B Applied Biomaterials*.109 (8) pp.1156–1176. doi:10.1002/jbm.b.34778.

Zhang, Z., Peng, M., Wei, Y., Jiang, X. & Zhang, S. (2017) Pars plana vitrectomy with partial tamponade of filtered air in Rhegmatogenous retinal detachment caused by superior retinal breaks. *BMC Ophthalmology*. 17 (1), 64. doi:10.1186/s12886-017-0459-6.

Chapter 2 - Literature review - Advances in polysaccharide- and synthetic polymer-based vitreous substitutes

2.1. Introduction

The World Health Organisation (WHO) estimates that 2.2 billion people suffer from vision impairment or blindness globally. Of these 2.2 billion, 1 billion people have preventable causes of blindness or visual impairment (World Health Organisation, 2019). Blindness and visual impairment can be caused by, cataracts, glaucoma, diabetic retinopathy, age-related macular degeneration (AMD), and retinal detachment (RD) (Flaxman *et al.*, 2017; World Health Organisation, 2019). The leading cause of global blindness is cataracts, while glaucoma is the leading cause of irreversible visual loss and second to cataracts as a cause of blindness globally (Giangiacomo and Coleman, 2009; Kyari *et al.*, 2013). Worldwide, an estimated 14 million people are affected by age-related macular degeneration (Chappelow and Kaiser, 2008) and one-third of people suffering from diabetes mellitus (285 million) are affected by diabetic retinopathy (Lee *et al*., 2015). Pars plana vitrectomy (PPV) is one of the most commonly used treatments for many retinal diseases especially RD (Vaziri *et al.*, 2016). During PPV the vitreous body is removed after which it is replaced with a vitreous substitute (Murtagh *et al.*, 2020). Certain types of RD can also be treated with pneumatic retinopexy (PR) (Chan *et al.*, 2008). PR is an outpatient procedure that involves the induction of retinopexy around the retinal breaks or tears and intravitreal injection of a long-acting expansive gas (Figure 2.1) (Gupta *et al.*, 1997).

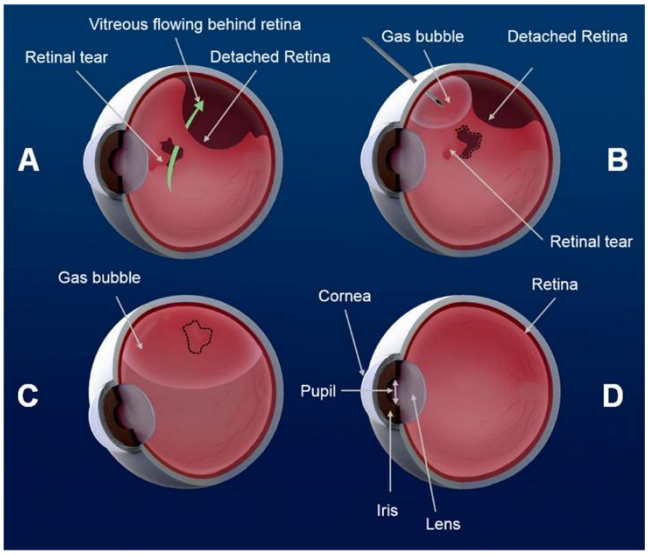

Figure 2.1 - Endotamponade caused by an intraocular gas bubble during pneumatic retinopexy. (A) Fluid enters behind the retina causing detachment (B, C) Retinal reattachment is facilitated through gas bubble tamponade (D) Reattachment of the retina. Reprinted with permission from (Su *et al.*, 2015) Copyright 2015 American Chemical Society.

The purpose of the vitreous substitute is to fill the vitreous cavity and to help reattach the vitreous and the retina after vitrectomy surgery (Figure 2.2) by providing tension on the eye and promoting healing (Kleinberg *et al.*, 2011; Murtagh *et al.*, 2020). Silicone oil and gases are commonly used for medium and long-term tamponade effects, while perfluorocarbons are utilised as intraoperative tamponades. Currently, the only post-operative choice for long-term vitreous substitution is silicone oil (Kleinberg *et al.*, 2011; Vaziri *et al.*, 2016). The optical clarity and chemical inertness of these compounds are favourable, but many disadvantages and adverse effects have prompted researchers to develop a vitreous substitute using polymers.

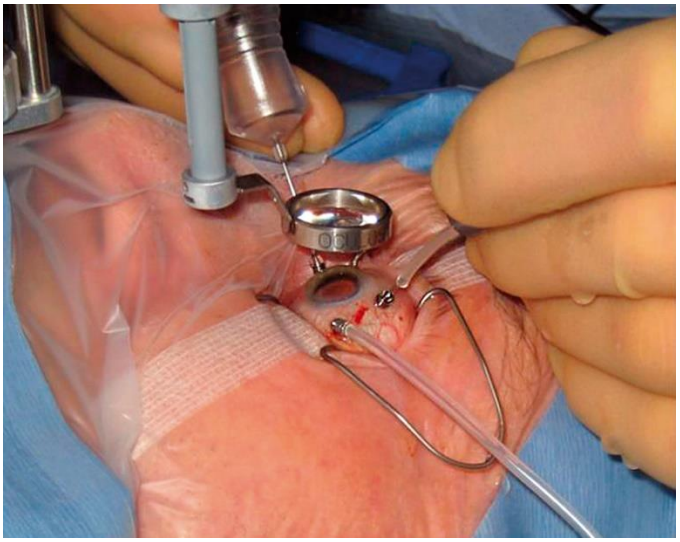

Figure 2.2 - During vitrectomy surgery microsurgical instruments are placed in the eye through incisions in the sclera. A suitable substitute is used to replace the native vitreous (Astbury et al., 2008).

The development of an ideal vitreous substitute is one of the most intricate and difficult disciplines of ophthalmic research and a suitable polymeric substitute is yet to be developed. This review presents and critically evaluates current vitreous substitutes with emphasis placed on developments in polysaccharide and synthetic polymer hydrogels that show promise. For this review, a literature search was conducted for the keywords “vitreous substitute,” “artificial vitreous,” “experimental vitreous,” “polymeric vitreous,” “vitreous mimetic,” “vitreous humour,” “retinal tamponade,” “retinal detachment,” “silicone oil substitute,” and “hydrogel vitreous”. Databases utilised for the search include SCOPUS, Google Scholar, and PubMed. Papers from 1950 were included in the search and references in the relevant articles were also used. Articles in languages other than English were excluded.

2.2. The Natural Vitreous

The vitreous is a transparent, gel-like structure, with a volume of approximately 4 millilitres, occupying the majority of each eye (Snell and Lemp, 1997). The vitreous provides a clear passage of light, provides oxygen transport through the eye, and also functions to hold the retina in place, dampen eye movements, and create a barrier against biochemical substances (Snell, 2000; Chirila and Harkin, 2016; Alovisi *et al.*, 2017). The gelatinous structure of the vitreous is based on the polysaccharide, hyaluronic acid, and the peptide, collagen, which, along with 98% water, are the main

components of the vitreous (Donati *et al.*, 2014; Chirila and Harkin, 2016). Structural stability of the vitreous is provided through the binding of water to proteins and glycosaminoglycans (GAGs) (Alovisi *et al.*, 2017). The proteins, GAGs, metabolites, and cells found in the vitreous are shown in Table 2.1 (Donati *et al.*, 2014; Alovisi *et al.*, 2017).

Table 2.1 - Biochemical composition of the vitreous (Donati *et al.*, 2014)

Biochemical Group	**Molecule**
Proteins	Albumin Transferrin (iron-binding protein) Collagen (type II, IV, V, VI, IX, XI)
Glycosaminoglycans	Hyaluronic acid Chondroitin sulfate
Metabolites	Ascorbic acid Glucose Lactic acid Amino acids Unsaturated fatty acids Prostaglandins PGE2 PGF2 alpha Prostacyclin Thromboxane
Cells	Hyalocytes Fibrocytes/fibroblasts Macrophages

The vitreous has a density of 1.0053 – 1.008 g/cm^3, a refractive index of 1.3345 – 1.3348, and a pH of 7.0 – 7.4 (Donati *et al.*, 2014). A high hyaluronic acid concentration with suspended collagen fibres within the vitreous allows for the viscosity of the vitreous (300 – 2000 cP) and absorbs the stress and strain created during the movement of the eye during the day. The viscosity of the vitreous is highest close to the posterior pole of the eye and decreases as you move anteriorly. (Chirila and Harkin, 2016). Collagen, GAGs, and water in the vitreous ensure transparency and support the mechanism responsible for vision and accommodation of the eye (Donati *et al.*, 2014; Chirila and Harkin, 2016). Ascorbic acid in the vitreous has been found to act as a neovascularisation inhibitor, it can increase the proliferation of hyalocytes and

act as an antioxidant to reduce free oxygen in the vitreous (Kleinberg *et al.*, 2011; Donati *et al.*, 2014).

The vitreous humour is a viscoelastic gel or solid displaying both solid and liquid-like behaviour. The storage shear modulus (G') of the vitreous is higher than the loss shear modulus (G''). The storage modulus represents the recoverable or elastic component while the loss modulus represents the viscous component (Swindle *et al*., 2008; Tram and Swindle-Reilly, 2018). Therefore, under static loading, the vitreous will respond as an elastic body but during rapid unloading events, such as trauma, the vitreous will be capable of dissipating substantial energy (Chirila and Harkin, 2016).

2.3. The Ideal Vitreous Substitute

The ideal vitreous substitute should have analogous viscoelastic properties to the natural vitreous. It should maintain intraocular pressure within a normal range, and it should be able to support the surrounding ocular tissue such as the retina without causing toxicity (Kleinberg *et al.*, 2011). Vitreous substitutes must be transparent and permeable. The natural vitreous maintains the shape of the eye by behaving as a viscoelastic fluid or gel (Kleinberg *et al.*, 2011; Davis *et al.*, 2017) and a vitreous substitute must mimic this. An ideal vitreous substitute should also not degrade with time (Chirila and Harkin, 2016).

2.4. Current Vitreous Substitutes

During pars plana vitrectomy, the vitreous is removed to repair a retinal detachment or clear a vitreous haemorrhage. Silicone oils, perfluorocarbon liquids, gases, air, and balanced salt solutions are substitutes that are currently used following vitrectomy (Kleinberg *et al.*, 2011; Tram *et al.*, 2020). These substitutes work as short-term or long-term tamponades that keep the retina in place. Table 2.2 shows various gas and liquid tamponade agents used. Polymeric vitreous substitutes are currently only used for sustained drug delivery mainly for posterior segment diseases and have not yet been employed as permanent vitreous substitutes (Swindle and Ravi, 2007).

Table 2.2 - Tamponade agents used in the treatment of retinal detachment. (Adapted from Vaziri *et al.*, 2016)

Silicone Oil (SO) tamponades	**Chemical Composition**	**Viscosity (centistoke)**	**Specific gravity (g/cm^3)**	**Interfacial tension (mN/m)**	**Refractive Index**
Conventional SO					
1000 cSt SO	100% PDMS	1000	0.97	35	1.4
5000 cSt SO	100% PDMS	5000	0.97	35	1.4
Heavy SO					
Oxane HD	88.1% 5700 cSt	3300	1.02	45	1.4
Densiron 68	Oxane/11.9% RMN-3 69.5% 5 000 cSt PDMS/30.5% F_6H_8	1400	1.06	41	1.4

Gas Tamponades	**Chemical formula and molecular weight (g/mol)**	**100% gas expansivity**	**100% maximum gas expansion**	**Tamponade duration**	**Isoexpansile concentration**	**Interfacial tension (mN/m)**
Air	N/A 28.97	N/A	N/A	5-7 days	N/A	70
Sulfur hexafluoride	SF_6 146.06	2×	1-2 days	2 weeks	20%	70
Perfluoro-ethane	C_2F_6 138.01	3×	1-3 days	4-5 weeks	16%	70
Perfluoro-propane	C_3F_8 188.02	4×	3-4 days	8 weeks	14%	70

Perfluorocarbon liquids	**Chemical formula and molecular weight (g/mol)**	**Specific gravity (g/cm^3)**	**Viscosity (mPas)**	**Interfacial tension (mN/m)**	**Refractive Index**
Perfluoro-*n*-octane	C_8F_{18} 438.06	1.76	1.20	55.0	1.3
Perfluorodecalin	$C_{10}F_{18}$ 462.08	1.33	5.68	57.8	1.3

2.4.1. Gases

Vitreous substitutes with gases are used for pneumatic retinopexy and post-operative endotamponade. These include the use of air and expansile gases such as sulfur hexafluoride (SF_6), perfluoroethane (C_2F_6) and perfluoropropane (C_3F_8) (Marcus *et al*., 1994; Gurunadh *et al.*, 2010; Kleinberg *et al.*, 2011).

2.4.1.1. Air

Treatment of retinal detachment (RD) was first conducted by Ohm in 1911 using sterile air in an intravitreal injection (Vaziri *et al.*, 2016). Air is readily available, inexpensive and does not need to be removed as it is replaced with aqueous humour once absorbed (Donati *et al.*, 2014). However, the refractive index of air is incompatible with ocular tissue, and it has a decreased residence time (Marcus *et al*., 1994). Thus, air is only used when no other substitutes are available (Kleinberg *et al.*, 2011), but recent studies show that air can be considered in vitrectomy for simple RD with sufficient removal of subretinal fluid (Pak *et al.*, 2017) and pars plana vitrectomy with a partial air tamponade (Zhang *et al.*, 2017).

2.4.1.2. Expansile Gases

Expansile gases such as SF_6 and C_3F_8 are used more commonly for vitrectomy, and both are heavier than air. These gases are also colourless, odourless, and nontoxic rendering them ideal for use as vitreous substitutes (Donati *et al.*, 2014; Alovisi *et al.*, 2017). The buoyancy of these gases maintains the position of the retina against retinal pigment epithelium (RPE) (Neffendorf *et al*., 2018). Expansile gases will be spontaneously reabsorbed in 6 to 80 days and replaced with aqueous humour as seen with air, avoiding a secondary surgery for the removal of the gas (Thompson, 1992). SF_6 expands within 2 days lasting for 1 to 2 weeks in the vitreous cavity while C_3F_8 expands within 96 hours and can last for 6 to 8 weeks (Lee *et al.*, 1991; Vaziri *et al.*, 2016). This expansive property of these gases requires patients to avoid high altitudes (including air travel) for 2 weeks and 6 weeks respectively following the administration of these gases (Mateo-Montoya and de Smet, 2013). Adverse effects of expansile gases include a raised intraocular pressure after surgery, cataract formation, foveal sensitivity, and endothelial changes to the cornea (Kleinberg *et al.*, 2011; Kanclerz and Grzybowski, 2018; Scheerlinck *et al.*, 2018). Temporary vision impairment due to the difference in refractive indexes between the gas and surrounding ocular tissue is also observed (Kanclerz and Grzybowski, 2018; Neffendorf *et al*., 2018). When vitrectomy is performed under general anaesthesia, and these gases are used as a tamponade, dinitrogen monoxide (N_2O) must be avoided. Studies show that due to the strong diffusion tendency of N_2O, a rapid expansion of expansile gases is caused leading to a fast increase in intraocular pressure and in some cases the retinal artery

is occluded resulting in a temporary or permanent loss of vision (Hart *et al.*, 2002). Expansile gases are suitable short-term vitreous substitutes, but alternatives should be used for long-term substitution.

2.4.2. Liquids

Liquid vitreous substitutes include balanced salt solutions (BSS), perfluorocarbon liquids (PFCLs), semi-fluorinated alkanes, silicone oil and heavy silicones. They have been studied and used as endotamponades that can respond to head movement without being absorbed and degraded.

2.4.2.1. Balanced Salt Solutions (BSS)

Physical characteristics of balanced salt solutions (BSS) such as the refractive index, density and optical transparency are similar to those of the aqueous humour (Donati *et al.*, 2014). These solutions are used as irrigating solutions rather than vitreous substitutes and may change once injected due to proteins, metabolites, and cells in the vitreous cavity (de Bustros *et al*., 1985; Asaria *et al.*, 2001). Balanced salt solutions have a low surface tension leading to no tamponade properties on the retina that are required by an ideal vitreous substitute (Kleinberg *et al.*, 2011).

2.4.2.2. Perfluorocarbon Liquids (PFCLs)

Perfluorocarbon liquids (PFCLs) are chemicals in which fluorine atoms replace all the hydrogen atoms (Yu *et al.*, 2014). Because of their physical features such as high specific gravity, low surface tension, low viscosity, and optical transparency, PFCLs are an appropriate alternative for vitreoretinal surgery. (Peyman *et al*., 1995; Yu *et al.*, 2014; Eiger-Moscovich *et al.*, 2017). Due to the long-term toxicity, PFCLs are limited to intraoperative use where they flatten the retina temporarily allowing for the repair of retinal detachments (Chang *et al.*, 1989; Peyman *et al*., 1995; Vaziri *et al.*, 2016). This toxicity results in mechanical damage to cells, disorganisation of the retina, and ocular inflammation (Peyman *et al*., 1995; Malchiodi-Albedi *et al.*, 2002; Mertens *et al*., 2002). The low viscosity of PFCLs allows for injection, removal, and tissue manipulation (Peyman *et al*., 1995). PFCLs have a high oxygen solubility and a study with perfluorotributylamine (FTBA) as a vitreous substitute in rabbits showed that FTBA had a neuroprotective effect (Wilson *et al*., 1995).

2.4.2.3. Semifluorinated Alkanes (SFAs)

Semifluorinated alkanes (SFAs) are physically and chemically inert, colourless, and immiscible in water. SFAs have a lower specific gravity than PFCLs and this allows them to produce less retinal damage than that observed with PFCLs (Matteucci *et al.*, 2007). SFAs can be used as long-term tamponades as their refractive index is close to that of the vitreous in the human eye (Kirchhof *et al.*, 2002; Roider *et al.*, 2002). Adverse effects linked with the use of SFAs include emulsification and cataract formation (Kirchhof *et al.*, 2002; Wetterqvist *et al.*, 2004). The solubility of SFAs in silicone oil has led to their combined use to overcome the emulsification of SFAs alone (Ozdek *et al.*, 2011).

2.4.2.4. Silicone Oil

Silicone oil (SO) is the gold-standard for long-term vitreous substitution (Kleinberg *et al.*, 2011). SO is a polymerised liquid siloxane that is hydrophobic. SO polymers are the most used vitreous substitute as they have high surface tension and viscosity, are easy to remove, have low toxicity, and are transparent (Gurunadh *et al.*, 2010; Barca *et al*., 2014; Vaziri *et al.*, 2016). These properties make SO substitutes the ideal long-term vitreous replacement. SOs are used for complicated RD, in uncooperative patients such as children and adults with physical impairment, and when postoperative air travel is planned (Kim and Baumal, 2004; Kleinberg *et al.*, 2011). Viscosities of 1000 to 5000 centistokes of SO are used (Barca *et al*., 2014). SO removal is typically performed between 3-6 months after the initial surgery when the retina is deemed to be adequately attached (Kleinberg *et al.*, 2011; Barca *et al*., 2014). SOs have a tamponade effect on the superior retina while preserving anatomical integrity because of their high surface tension and low specific gravity (Azen *et al.*, 1998).

Patients need to be monitored closely following SO administration as it has many disadvantages. Its low specific gravity means that it is difficult for SO to tamponade the inferior retina. SO has a refractive index higher than that of ocular tissue and thus optical adjustments need to be made. Other disadvantages include emulsification, increased intraocular pressure, intraocular inflammation, decreased choroidal thickness, oxidative damage causing cataracts, and glaucoma (Kim and Baumal, 2004; Barca *et al*., 2014; Eibenberger *et al.*, 2020; Kars *et al.*, 2020). Complications

that may arise following SO administration require the SO to be removed. Removal of SO can also lead to recurrent RD, corneal abnormalities, hypotony, and a loss in the clarity and sharpness of the patient's vision (Xie and Lei, 2013; Eibenberger *et al.*, 2020).

2.4.2.5. Heavy Silicone Oil

Heavy silicone oil is created by mixing silicone oil and SFAs forming a homogenous tamponade (Kleinberg *et al.*, 2011; Donati *et al.*, 2014). The combination of the two creates an effective tamponade that is heavier than water and has minimal emulsification in comparison to SFAs alone (Wetterqvist *et al.*, 2004; Joussen *et al.*, 2011). Heavy silicone oil has been used for complex RD involving inferior proliferative vitreoretinopathy (Lim and Vote, 2008; Li *et al.*, 2010; Ozdek *et al.*, 2011). Complications associated with heavy silicone oil include cataract formation, emulsification, elevated intraocular pressure, and anterior segment inflammation (Berker *et al.*, 2007; Morescalchi *et al.*, 2014).

2.5. Experimental Polymeric Vitreous Substitutes

Hydrogels are three dimensional (3D) polymers. Without dissolving, they can swell in aqueous solutions, and thermosetting hydrogels are a type of bio-responsive hydrogel that swell to a gel (undergo sol-gel, solution-gel, transitions) in response to a change in temperature (Kleinberg *et al.*, 2011; Soliman *et al.*, 2019). Due to their ability to gel at physiological temperatures, thermosetting hydrogels can be developed to have a tamponade effect in the eye(Kleinberg *et al.*, 2011; Z. Liu *et al.*, 2019).

Polymeric hydrogels have the potential to be the ideal vitreous substitute as they can be injected as aqueous solutions, after which they form a gel *in situ* in response to a change in temperature. An *in situ* gel is a solution that can transition into a semisolid gel in response to a physiological change such as pH and temperature (Kleinberg *et al.*, 2011). This ability to form a gel *in situ* is advantageous as it overcomes the problem of shearing and degradation when a hydrogel is injected through a small gauge needle (Chirila and Hong, 1998; Swindle *et al*., 2008). Some disadvantages that need to be overcome when using polymeric hydrogels include short degradation times (Kleinberg *et al.*, 2011), retinal toxicity (Davidorf *et al.*, 1990; de Jong *et al.*, 2000; Hwang *et al.*,

2013), polymer fragmentation (Pruett *et al*., 1972, 1974; Chirila and Hong, 1998), and an increased time to form a gel within the eye (Katagiri *et al.*, 2005).

2.5.1. Natural Polymers (Polysaccharides and Proteins) - Structural Vitreous Substitutes

Natural polymers are proteins (silk, collagen, gelatin, fibrinogen, elastin, keratin, actin and myosin), polysaccharides (cellulose, amylose, dextran, chitin and glycosaminoglycans) or polynucleotides. Natural polymers degrade relatively easily, and thus synthetic polymers have been considered a more ideal option for long-term substitutes due to more prolonged degradation (Kleinberg *et al.*, 2011). However, natural polysaccharides and proteins can be modified to retard their degradation (George *et al*., 2019). These modifications include chemical and morphological modifications such as the introduction of functional groups on reactive groups and the introduction of other polymers to form polymeric complexes (Tong *et al.*, 2020). Studies utilising natural polysaccharides and polymers for vitreous substitution were conducted due to the similar molecular structures between these polymers and the natural vitreous. The focus of these studies was to fabricate a vitreous substitute that would mimic the structure of the natural vitreous in its chemical composition. Natural polysaccharides and polymers such as hyaluronic acid and collagen are components of the natural vitreous making them the ideal first choice to study for vitreous substitution (Pruett *et al*., 1972; Necas *et al*., 2008).

2.5.1.1. Hyaluronic Acid

Hyaluronic acid (HA) is a natural polysaccharide that is found in the vitreous of the eye (Necas *et al.*, 2008). HA is biocompatible, mucoadhesive and biodegradable making it ideal for ocular drug delivery (Y. Liu *et al.*, 2019). Since the 1970s HA has been studied as a vitreous substitute (Pruett *et al*., 1979). Through the extraction and purification of sodium hyaluronate, a highly viscous, clear, and injectable HA solution was derived. This solution was then found to be biocompatible in a clinical trial. However, the study that was conducted could not substantiate its application following vitrectomy surgery.

HA is an ineffective intraocular tamponade due to its short degradation time. Several studies have been conducted to extend the degradation period and make HA a

suitable vitreous substitute through the functionalisation of HA via crosslinking and copolymerisation. To extend the degradation period of HA, it was crosslinked with another chemical, adipic dihydrazide (ADH), by two different groups. Su *et al*. (2011) oxidized HA to form oxi-HA after which a clear, colourless, and transparent hydrogel was formed following cross-linking with ADH. This hydrogel had a refractive index similar to that of the natural vitreous, the gel matrix could be maintained over 35 days, and it was found to be non-toxic when evaluated on RPE cells. Preliminary studies of this hydrogel in rabbits showed no significant irregular reactions for 3 weeks. Schramm *et al*. (2012) assembled different hydrogels by crosslinking HA with ADH and by photo-crosslinking HA with N-vinyl-pyrrolidinone and UV-light. Both hydrogels that were assembled were clear, transparent, and found to have refractive indexes similar to that of the natural vitreous. Degradation studies of the hydrogels showed only slight degradation over 1 month. No toxicity was observed in RPE cells for the UV-crosslinked hydrogels, however, the ADH crosslinked hydrogel showed mild toxicity unlike that in the study by Su *et al*. Schramm *et al*. concluded that hydrogels based on UV-crosslinked HA may be promising vitreous substitutes.

Healaflow® is a commercially available implant that is used in glaucoma surgery as a space-filler to limit post-operative fibrosis (Roy *et al.*, 2012). It is a transparent hydrogel that consists of over 97% water and crosslinked sodium HA, with a refractive index of 1.34. These properties of Healaflow® led researchers to study it as a vitreous substitute following PPV in rabbits. Their findings indicated that the hydrogel maintained its viscous structure for a few weeks following vitrectomy and following long-term follow-up, retinal detachments were found to be self-limiting. These results lead the researchers to believe that Healaflow® may potentially be an effective short-term tamponade but more studies need to be conducted to prolong the structural integrity of the hydrogel (Barth *et al.*, 2016).

Enzymatic crosslinking of silk fibroin with HA has also recently been done to form a hydrogel for vitreous substitution. Using horseradish peroxidase and H_2O_2, crosslinked silk-HA hydrogels were formed. Crosslinking of these two polymers resulted in a hydrogel that overcame the limitations placed on the individual polymers with increased stability of the hydrogel and tunability of the rate of gelation of the hydrogel. The resultant silk-HA hydrogel had a refractive index of 1.336 and light transmission

of up to 91% (Raia *et al.*, 2020) but more research needs to be done to improve degradation and to assess the cytotoxicity of the hydrogels for it to be considered for use as a vitreous substitute.

Vitreous substitutes based on crosslinked thiolated HA have also been studied. The first study, by Schnichels *et al*. (2017), prepared two different hydrogels, soft (1% HA) and strong (2.2% HA), from thiolated HA by the formation of disulphide bridges. The researchers found that the thiol-modified HA had the capability to form stable hydrogels by the natural formation of disulphide bridges without the addition of any chemical crosslinkers. Both hydrogels displayed all characteristics required of an ideal vitreous substitute. In addition to this, both hydrogels also showed superiority to silicone oil in that cataract formation was less frequent with the hydrogels. The soft hydrogel prepared by Schnichels *et al*. with 1% HA was then further studied by Januschowski *et al*. (2019). The purpose of the second study was to characterise the biophysical properties (intraocular pressure and retinal integrity) of the prepared substitute. Their results showed no significant increase in intraocular pressure and no significant toxicity which justifies *in vivo* studies of the hydrogel for biocompatibility.

Other modifications to HA include the introduction of other polymers to form polymeric complexes. Nakagawa *et al*. (1997) used HA and collagen showing that the concomitant use of collagen and HA is capable of a tamponade effect. Their study showed that the mixture is safe and effective for 3 months in rabbit eyes as a vitreous substitute. They also found that the half-life of collagen was enhanced by HA, but an accumulation of collagen was seen on the retina. The concomitant use of HA with gellan as a vitreous substitute has also been studied. The study found that although a gel formed, its application was limited due to the diminished mechanical properties of the gel. $CaCl_2$ was added to form a crosslinked hydrogel which resulted in a substitute that could act as short-term tamponade, circumventing the limiting rheological properties displayed by the previous gel (Suri and Banerjee, 2006).

2.5.1.2. Collagen and Its Derivatives

In the 1960s, polygeline, a derivative of gelatin which itself is a derivative of hydrolysed collagen, was implanted in rabbit and human eyes. A 3.5% solution initially was opaque but remained clear thereafter for 3 months. However, RD and haemorrhages

were seen in the rabbit eyes. The retention rate of polygeline decreased to 22.5% by the tenth day and higher concentrations of polygeline cause white dots and inflammation. Copolymerisation with other polymers caused cloudiness and it was concluded that the inflammation caused by polygeline made it unacceptable as a vitreous substitute (Oosterhuis *et al.*, 1966). Studies conducted by Pruett *et al*. (1972, 1974) reported many adverse effects following the administration of collagen as a vitreous substitute. These include inflammation, blurred vision due to opacification of the vitreous, and decreased mechanical properties of the gel due to fragmentation.

As discussed previously, a study by Nakagawa *et al*. found that the hydrogel copolymer of collagen and HA was capable of tamponade and the half-life of collagen was enhanced by HA, but collagen accumulated on the retina (Nakagawa *et al*., 1997). The use of methylated collagen was then studied to determine its efficacy in overcoming previously found disadvantages with collagen. A solution of Type I/II collagen and acidified anhydrous methanol was produced. This solution had no surface tension preventing a tamponade effect making it unsuitable for retinal detachment (Liang *et al.*, 1998). Overall, the inflammation and ocular pain caused by collagen and its derivatives render them unsuitable as vitreous substitutes.

2.5.1.3. Gellan Gum

Gellan gum is a microbial heteropolysaccharide used in the food industry. Gellan gum can form a gel *in situ* and is capable of maintaining a gel structure at body temperature (Giavasis *et al*., 2000; Osmałek *et al*., 2014). Suri and Banerjee (2006) studied polymers of gellan gum and hyaluronic acid as discussed previously. The resultant gel was crosslinked with $CaCl_2$ which formed a stronger hydrogel that could be a short-term tamponade.

2.5.1.4. Chitosan

Chitosan is a partially deacetylated derivative of the polysaccharide, chitin, and has been extensively used due to its favourable biological properties (Huang *et al*., 2017; Tang *et al.*, 2017). An *in vivo* rabbit eye study with chitosan and HA showed no significant effect on the intraocular tissue and no changes in the intraocular pressure were observed. The intra-vitreous chitosan also had a longer biodegradation time than

HA with similar inflammatory effects, making chitosan more suitable than HA (Yang *et al.*, 2008).

Hydroxypropyl chitosan, a derivative of chitosan, has enhanced solubility, stability, and biocompatibility compared with chitosan (Peng *et al.*, 2005; Huang *et al*., 2017). Jiang *et al*. (2018) studied an *in situ*-forming hydrogel by crosslinking hydroxypropyl chitosan with alginate dialdehyde. Properties such as the refractive index, light transmittance, and density of the prepared hydrogel were comparable to that of the natural vitreous and biocompatibility studies showed the hydrogel to be nontoxic. *In vivo* rabbit studies showed that the hydrogel caused no change in intraocular pressure 90 days post-operation. A minor decline in vision was seen along with a decrease in the densities of photoreceptors in the eyes, indicating that further studies of this hydrogel need to be conducted.

2.5.2. Synthetic Polymers – Functional Vitreous Substitutes

Some of the shortcomings of polysaccharides for long-term vitreous substitution have led to more research into the use of synthetic polymeric hydrogels. The extensive studies utilising synthetic polymers for vitreous substitution have centred on reproducing the mechanical and viscoelastic properties of the natural vitreous. The focus of these studies was to design a vitreous substitute that would mimic the function of the natural vitreous. The synthetic polymers discussed below have varying chemical structures and properties that allow for tuning of their functions. Synthetic polymers are synthesised via chemical reactions such as polymerisation that utilise harsh solvents and other polymers that could be incompatible with ocular cells. Therefore, due to the use of polymers that may vary notably in composition from the chemical make-up of the natural vitreous such as polyacrylamide (Nardo *et al.*, 2017) and polyethylene glycol (Hayashi et al., 2017), in addition to the chemical processes involved in the synthesis of these polymers, intensive biocompatibility studies are essential for clinical application of these substitutes (Davidorf *et al.*, 1990; de Jong *et al*., 2000).

2.5.2.1. Poly(1-Vinyl-2-Pyrrolidone)

First studied by Scuderi in 1954, Poly(1-vinyl-2-pyrrolidone) (PVP) was the first synthetic polymer to be studied as a potential vitreous substitute. Variable

concentrations of PVP solutions were injected into rabbit eyes and no histological reactions were seen but opacification in the eyes occurred (Scuderi, 1954).

Researchers subsequently studied a selection of PVP gels to select the most suitable materials that have the potential to be vitreous substitutes through various characterisation studies (Hong *et al.*, 1996). The 1-vinyl-2-pyrrolidine monomer was then chosen and polymerised with divinyl glycol as a crosslinker. The transparent hydrogel that formed had a similar viscosity and density to the natural vitreous with a refractive index of 1.339 and a shear storage modulus higher than the shear loss modulus (Hong *et al.*, 1996). The hydrogels were then tested in rabbit eyes. Macrophages were present after 4 weeks indicating inflammation, and biodegradation of the hydrogel was also seen (Vijayasekaran *et al.*, 1996; Hong *et al.*, 1998). PVP hydrogels displayed similar properties to the natural vitreous, however, polymer fragmentation from small-gauge needle injection resulted in a decrease in the mechanical properties of the hydrogel (Chirila and Hong, 1998).

2.5.2.2. Hydroxypropyl Methylcellulose and Methylcellulose

One of the most abundant naturally occurring polysaccharides is cellulose and synthetic modifications to cellulose are easily accomplished. These modifications have resulted in polymers with improved properties (Tylkowski *et al.*, 2017). Examples of modified cellulose that have been used as potential vitreous substitutes include hydroxypropyl methylcellulose and methylcellulose.

Hydroxypropyl methylcellulose (HPMC) is prepared by treating the alkali cellulose fibres with propylene oxide and methyl chloride (Tylkowski *et al.*, 2017). A solution of HPMC was injected in rabbit eyes by Fernandez-Vigo *et al*. (1990). In their study, it was observed that HPMC elimination occurred within 10 weeks after implantation deeming the solution unsuitable for long-term vitreous substitution and the sealing of retina holes in RD. The residence time of HPMC was controlled by varying the molecular weight of HPMC in another study. The results indicated that HPMC with a molecular weight of 120 kDa had a half-life of 38 days. However, HPMC was still unsuitable for long-term vitreous substitution (Fernandez-Vigo *et al.*, 1990).

Heating of cellulose fibres followed by treatment with methyl chloride or methyl iodide forms methylcellulose (Tylkowski *et al.*, 2017). Methylcellulose can form reverse

thermo-responsive hydrogels that can undergo a sol-gel transition when heated (Contessi *et al.*, 2017). Katagiri *et al.* (2005) prepared a thermosetting gel with methylcellulose mixed with polyethylene glycol. Various gel concentrations were prepared until a final, optimised preparation, WTG-127, was used for further studies. WTG-127 formed a gel at 36 °C and retained transparency upon gelation. However, the time to form a gel was 50 min which resulted in the drifting of WTG-127 under the retina through the retinal tear. WTG-127 is hydrophobic and could not provide a tamponade effect. Thus, WTG cannot be a suitable long-term vitreous substitute, but research can be done on the application of WTG-127 as a drug delivery medium.

2.5.2.3. Adcon-L

Adcon-L is a polymer that has been used in neurosurgery formed with proteoglycan esters in gelatin saturated with water (Tribolet *et al.*, 1998). Adcon-L was studied by de Jong *et al*. (2000) as a vitreous substitute in rabbits. After 1-day ocular inflammation was observed, lens capsules were thickened after 2 weeks, and after 3 weeks, corneal opacity and additional thickening of the lens capsule were observed. Additionally, after 3 weeks, the hydrogels were no longer visible and retinal toxicity was indicated rendering Adcon-L an unsuitable vitreous substitute.

2.5.2.4. Pluronic Polyol

An aqueous solution of pluronic polyol F-127 (PF-127) is liquid at low temperatures forming a clear gel at physiological temperature. Davidorf *et al*. evaluated PF-127 in rabbits as a vitreous substitute. Although it formed a gel *in situ*, severe retinal toxicity was observed, making PF-127 clinically unsafe to use (Davidorf *et al.*, 1990). Severe retinal toxicity of PF-127 was also observed by Hwang *et al.* (2013).

2.5.2.5. Poly(N-Isopropylacrylamide)

Strotmann *et al.* (2011) studied a polyelectrolyte hydrogel composed of sodium acryloyldimethyltaurate and acrylic functionalised poly(N-isopropylacrylamide) macromonomer crosslinked with glycerol dimethacrylate. They observed that the crosslinked polyelectrolyte was thermosensitive and enabled the hydrogel to form a gel *in situ* and the developed hydrogel was also biocompatible. Following the promising results from the 2011 study, Strotmann *et al.* (2013) investigated the stability of the developed polyelectrolyte hydrogel against enzymatic biodegradation and

conducted further biocompatibility studies. In this study, an absence of cell proliferation was observed suggesting that the integrity of the retinal barrier is not affected by the hydrogel. These studies, however, did not evaluate the optical and mechanical properties of the hydrogel and further studies would need to be conducted to evaluate the capability of these hydrogels as vitreous substitutes.

2.5.2.6. Polyacrylamide

Acrylamide is toxic and carcinogenic. However, polymerised acrylamide, poly(acrylamide), is biocompatible, hydrophilic and viscoelastic making it an advantageous polymer for vitreous substitution (Nardo *et al.*, 2017). Reversible hydrogels composed of acrylamide and bis(acryloyl)cystamine (BAC) with disulphide crosslinkers were developed (Figure 2.3). Reduction of the disulphide bonds to thiol groups resulted in the removal of the toxic monomer. As is needed with current substitutes, following vitrectomy with this hydrogel, a patient would be required to remain face down due to the swelling nature of the hydrogel (Aliyar *et al.*, 2004). After injection into human cadaver eyes as well as porcine eyes *ex vivo,* studies indicated that the gel elasticity of the developed hydrogel was maintained (Foster *et al.*, 2006; Chirila and Harkin, 2016). Foster *et al*. (2006) also confirmed that the developed hydrogels form gels in the eye and osmotic pressure in the vitreous cavity is generated. Further studies showed that the addition of N-phenylacrylamide (NPA) to the previously developed hydrogel increased biocompatibility. Rheological testing of the new hydrogel indicated that the storage and loss moduli matched that of the porcine vitreous (Swindle *et al*., 2008). *In vivo* rabbit studies of the hydrogel indicated no inflammation or toxicity after 1 week (Swindle-Reilly *et al.*, 2009). Recently, Davis *et al*., (2017) incorporated acrylic acid into the hydrogel formulation. Various concentrations of this hydrogel were developed and characterised. Results of this study indicated that this new hydrogel could form a gel at lower concentrations while remaining optically clear and biocompatible, thus making it an ideal potential for vitreous substitution.

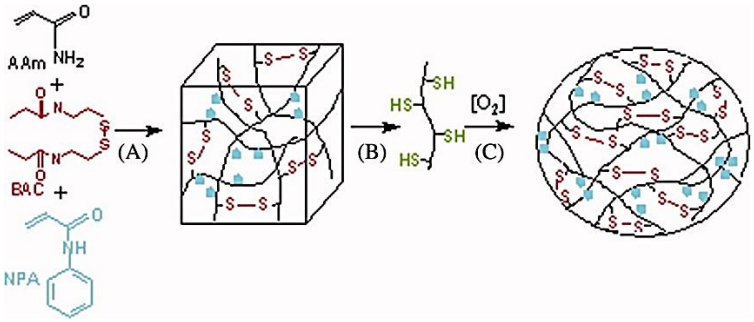

Figure 2.3 - Polymerised acrylamide reversible hydrogel; (A) Polymerization and crosslinking (B) reduction, and (C) *in situ* regelation. (Aliyar *et al.*, 2004)

2.5.2.7. Methacrylamide

Liang *et al*. (2017) studied and formulated copolymers composed of methacrylamide (MAM), methylacrylic acid and N',N'-bis(methylacryloyl-cystamine) (BMAC). Methacrylic acid increases the anionic charge of the copolymer system while also increasing the swell ability. This allowed the researchers to modify the hydrogel to have comparable mechanical properties to the natural vitreous. Liang *et al*. (2017) modified the storage modulus of the hydrogel by changing the copolymer concentration and thiol content. They found that the hydrogels with a lower BMAC concentration were biocompatible while those with a higher concentration were not. However, the biocompatible hydrogels with a lower BMAC concentration were too soft to be used as vitreous substitutes.

2.5.2.8. Poly(Glyceryl Methacrylate)

Studies with Poly(glyceryl methacrylate) (PGMA) have been conducted by Daniele *et al*. (1968) and Hogen-Esch *et al*. (1976). These studies both found that the resultant hydrogel was soft and swelled with analogous optical properties to the natural vitreous. The hydrogel in both studies was also biocompatible, however, the dehydration process in the study by Daniele *et al*. was found to be too slow and the polymer has been found to fragment upon injection (Daniele *et al.*, 1968; Hogen-Esch *et al*., 1976; Kleinberg *et al.*, 2011) making PGMA unusable as a polymer for vitreous substitution.

2.5.2.9. Poly(Methyl 2-Acrylamido-2-Methoxyacetate)

Poly(methyl 2-acrylamido-2-methoxyacetate) (PMAGME) was used to formulate hydrogels that would be stimuli-responsive by Chirila *et al.* (1994). Various polymers and copolymers of PMAGME were synthesised and tested in rabbits. There was no

fragmentation of the polymer when injected; however, the PMAGME hydrogel was found to induce inflammation and scarring, along with being toxic to neural tissue causing the shrinking of nerves in the eye. This study showed that PMAGME is an unsuitable polymer for vitreous substitution.

2.5.2.10. Polyvinyl Alcohol (PVA)

Polyvinyl alcohol (PVA) has good optical properties which makes it an ideal polymer choice for a vitreous substitute (Donati *et al.*, 2014). PVA was investigated and studied extensively by Yamauchi (1991). They first developed γ-irradiated PVA hydrogels that were injected into rabbit eyes and compared to a saline solution. Although the polymer had effective optical properties, inflammation in the rabbit eyes was seen. Yamauchi then formulated a PVA hydrogel mixed with chondroitin sulfate. This hydrogel absorbed more water and displayed a transparency higher than that observed in the previously formulated PVA hydrogel. However, they found that the PVA/chondroitin sulfate hydrogel was less biocompatible than the first hydrogel.

Formulation of PVA hydrogels by gamma-irradiation was also done by Maruoka *et al*. (2006). In this study, the polymer was autoclaved before gamma-irradiation and injection into the eyes of crab-eating macaques. The purification improved the biocompatibility of the PVA hydrogel. Although an increase in intraocular pressure was seen 1-2 weeks after the operation, normal intraocular pressure and retinal activity were seen after 3 months. Some vacuolizations of the inner retina and low toxicity were observed following the operation, and difficulties were experienced with the injection of the preformed hydrogel.

Methacrylated PVA (PVA-MA) hydrogels were synthesised by Cavalieri *et al*. (2004). A photo-initiator in the PVA-MA polymer enabled the gel network to be formed when irradiated. Changing the concentration of the photo-initiator as well as changing the irradiation time controlled the degree of crosslinking. Low degrees of crosslinking displayed partial degradation and the storage modulus of the hydrogel was higher than that of the physiological vitreous. Low polymer concentrations could not form a gel and high polymer concentrations formed gels that were much stiffer than the natural vitreous making this hydrogel unsuitable as a substitute.

Leone *et al*. (2010) and Lamponi *et al*. (2012) synthesised PVA hydrogels with a non-toxic crosslinker, trisodium trimetaphosphate (STMP). Leone *et al.* synthesised PVA/STMP hydrogels of varying concentrations to determine the hydrogel most similar to the natural vitreous. The 1:8 (STMP/PVA) molar ratio hydrogel was recognised as the most suitable following rheological testing and other characterisation tests. This 1:8 ratio hydrogel also showed suitable injectability with no change in its viscoelastic properties. Biocompatibility studies of the STMP/PVA hydrogel were conducted by Lamponi *et al*. Three ratios of the STMP/PVA hydrogel (1:4, 1:6, and 1:8) were analysed for their effects on various mouse and human cell lines. The 1:8 STMP/PVA hydrogel demonstrated the best biocompatibility to the cell lines used and histopathology examinations of the retina showed no loss of tissue with all retinal layers remaining intact. The hydrogels also demonstrated stability during swelling for 6 months at physiological temperatures indicating their suitability for long-term substitution. The 1:8 STMP/PVA hydrogel also showed no change in its biocompatibility following injection through a 19-gauge needle. The results from the two studies conducted show promising results for the PVA/STMP hydrogels as long-term vitreous substitutes.

2.5.2.11. Polyethylene Glycol (PEG)

Polyethylene glycol (PEG) is a polymer that is formed by radical polymerisation, and it is hydrophilic. It is biocompatible, resistant to protein absorption, and can form hydrogels making them a good polymer choice for vitreous substitution *(Mukherjee et al.*, 2019; Zarrintaj *et al.*, 2020). In the last 10 years, researchers have extensively studied PEG-based hydrogels as vitreous substitutes. Pritchard *et al*. (2011) studied a 5% PEG solution in a rabbit-eye model. Seven days following PPV with a 20-gauge needle showed no change in the translucence, however, complications such as transient hypotony, retinal detachment, and cataracts were observed. The viscosity of the substitute was also observed to have reduced over the follow-up period. All of these complications were likely due to not using any crosslinker with the polymer.

Annaka *et al*. (2011) functionalised PEG with hydrophobic ends to develop a thermo-responsive *in situ*-forming hydrogel. The hydrogel was clear, transparent, and biologically and chemically inert. The hydrogel was shown to be rigid enough to act as

a tamponade; it was nonabsorbable, nonbiodegradable, and injectable through a small-gauge needle. *In vivo* testing of the hydrogel showed no retinal toxicity and normal intraocular pressure. High polymer concentrations in the hydrogel resulted in moduli higher than the natural vitreous; thus, more research is required for this hydrogel to be a suitable vitreous substitute. A different approach was studied by Tao *et al.* (2013). They developed a system composed of two PEG-based components. Each PEG-based component had a different functionalised end group (thiol and active vinyl). The two components were then mixed and injected into rabbit eyes where they then crosslink *in situ*. The hydrogel, composed of the two components, has similar mechanical and optical properties to the human vitreous. Furthermore, the hydrogel was transparent and stable during the 9-month study period. No significant adverse effects were observed during the *in vivo* rabbit study, demonstrating that chemically crosslinked PEG hydrogels may be suitable long-term vitreous substitutes.

Chang *et al.* (2014) recognised drawbacks in the two-component hydrogel developed by Tao *et al.* and noted that PEG with the active vinyl end group, PEG methacrylate (α-PEG-MA), can form a gel via free radical crosslinking. This observation resulted in the development of an *in situ*-forming hydrogel based on α-PEG-MA. The hydrogel had a gelation time of 28 min and the stability at body temperature, gel swelling, and gelation kinetics were regarded as suitable for a vitreous substitute. Preliminary *in vivo* rabbit studies indicated that the hydrogel remained transparent at an acceptable inflammation level. More studies need to be done to fully evaluate the potential of this hydrogel as a vitreous substitute.

To overcome the swelling of hydrogels induced by degradation and high osmotic pressure, Hayashi *et al.* (2017) designed a hydrogel with low polymeric concentrations. The designed hydrogel, Oligo-Tetra-PEG, was developed in a two-step process. The first step forms two Oligo-PEG clusters, Tetra-PEG-SH and Tetra-PEG-MA, by stopping the crosslinking process before the gelation point. The second step involved the mixing of the two clusters to form the hydrogel. By varying the initial polymer concentrations, the researchers managed to control the gelation and mechanical properties of the hydrogel. The osmotic pressure of the hydrogel was lower than eye pressure and it was compatible with small gauge needle surgery. The hydrogel showed biocompatibility before and after degradation and was able to

function as a vitreous substitute, treating RD, for over a year in rabbit eyes with no adverse effects seen. The results of this study make this Oligo-Tetra-PEG hydrogel a potential long-term vitreous substitute.

Biodegradation *in vivo* due to hydrolases (Hong *et al.*, 1998) resulted in Z. Liu *et al.* (2019) designing a tri-component hydrogel (EPC) that can facilitate vitreous regeneration during the biodegradation of the hydrogel. The EPC hydrogel was formed by linking PEG, poly(propylene glycol) (PPG), and poly(ε-caprolactone) (PCL) with urethane bonds. By changing the polymer concentrations, the researchers were able to tune the gelation temperature of the EPC hydrogel to form a gel at physiological temperatures. The EPC hydrogel was able to form a gel *in situ* following vitrectomy with a small gauge needle and the hydrogel achieved a surface tension high enough to form across retinal tears. The hydrogel was biocompatible long-term, remained optically clear, caused no intraocular pressure changes or inflammation, and restored normal retinal architecture in RD models. Three months post vitrectomy, total degradation of the hydrogels was observed; however, a vitreous-like body formed in response to this degradation. The vitreous-like body displayed biophysical properties similar to the natural vitreous (Z. Liu *et al.*, 2019). This study indicates that EPC hydrogel can function as a vitreous substitute and also enable the regeneration of a vitreous-like body.

During vitrectomy, as the natural vitreous is removed, the oxygen balance in the eye is disrupted, causing oxidative stress resulting in cataract formation. Tram *et al.* (2020) addressed this as a design standard for a vitreous substitute. They designed a hydrogel loaded with an antioxidant to function as a substitute. The hydrogel was prepared by free radical polymerisation of PEG-MA and PEG-diacrylate (PEG-DA). The resultant hydrogels showed comparable optical and mechanical properties to the natural vitreous; it was injectable and showed biocompatibility with human ocular cells. Vitamin C, an antioxidant, was added to the hydrogel to restore oxygen balance to the eye. It was seen that the hydrogel with added Vitamin C had a synergetic effect in protecting retinal and lens cells from reactive oxygen species, indicating that these hydrogels had the potential to act as vitreous substitutes that can prevent the formation of post-vitrectomy cataracts. This is the first reported hydrogel mimicking the chemical function of the vitreous along with optical and mechanical functions.

2.5.2.12. Other Synthetic Polymers

Other synthetic polymers have also been used to develop vitreous substitutes. Böhm *et al*. (2012) designed hydrogels based on a mixture of polymeric β-cyclodextrin (β-CD) and poly{(2-acrylamido-2-methyl-1-propanesulfonic acid sodium salt)-co-[6-(acrylamido)-N-adamantylhexaneamide]}. The two components of the mixture are cytotoxic but the mixture of the two as a hydrogel was biocompatible. This hydrogel, though biocompatible, is not suitable as a vitreous substitute as the administration of the components is done individually and can lead to cytotoxic effects.

To circumvent the biodegradation of PEG, Chang *et al*. (2015) designed zwitterionic hydrogel that forms *in situ*. Poly(MPDSA-co-AC), was designed as a copolymer composed of sulfobetaine methacrylamide and acryloyl cystamine. *In vitro* studies indicated that the hydrogel had suitable gelation properties, viscoelastic properties, and light transmittance for use as a vitreous substitute. *In vivo* studies showed that the hydrogel remained transparent and displayed no inflammation after 1 month. More studies need to be conducted to assess the viability of this hydrogel as a vitreous substitute.

A zwitterionic monomer unit, carboxybetaine acrylamide (CBAA) was used by Wang *et al.* (2018). They synthesised a supramolecular copolymer hydrogel composed of poly(N-acryloyl glycinamide-co-carboxybetaine acrylamide). The synthesised hydrogel could hold a water content of greater than 98% and it was stable during swelling by tuning the monomer ratios. The refractive index, modulus, and light transmittance were similar to the physiological vitreous. *In vivo* rabbit testing indicated that the hydrogel functioned as an ideal vitreous substitute without any adverse effects. This novel approach for a vitreous substitute can be a potential substitute but more studies are required.

Uesugi *et al*. (2017) evaluated a gel composed of a self-assembling peptide, PanaceaGel SPG-127. The physical properties of the gel were comparable to those of the natural vitreous, the gel was biocompatible, and no fragmentation following injection through a 27-gauge needle was observed. Three months after administration, the gel remained transparent, and no complications were seen. The researchers could not verify the tamponade effect of the hydrogel and additional studies need to be

conducted before this hydrogel can be a potential vitreous substitute (Uesugi *et al.*, 2017).

Xue *et al.* (2020) developed a more optically transparent hydrogel based on Poly[(R)-3-hydroxybutyrate-(R)-3-hydroxyhexanoate] (PHBHx). The physicochemical properties of this polymer along with its ideal machinability were the reason for this choice. The PHBHx hydrogel demonstrated high light transmittance, good sol-gel transition, and rheological properties as a vitreous substitute. Xue *et al*. (2020) showed that increasing the concentration of PHBHx resulted in hydrogel cloudiness. *In vivo* rabbit studies showed that the hydrogel could maintain transparency when implanted and displayed preservation of the retina and negligible inflammation of ocular tissue over 6 months (Xue *et al.*, 2020). This study can be a new direction for research on vitreous substitutes.

2.5.3. Composite Polymers

Hydrogels composed of synthetic polymers alone may not provide a biomimetic effect. Thus, researchers have studied composite hydrogels composed of a combination of synthetic and natural polymers. Ideally, these composite hydrogels would hold the biomimetic properties seen in hydrogels composed of natural polymers and the long-term viability properties observed with synthetic hydrogels.

Lin *et al.* (2013) synthesised a copolymer of HA with Pluronic® F-127. It is an *in situ* vitreous substitute with ideal chemical, rheological, and optical properties. Biodegradation studies of this substitute indicated that the hydrogel maintained 60% of its mass after 7 days and cytotoxicity studies with RPE cells indicated that the hydrogel did not have any cytotoxic or adverse effects.

Three studies conducted since 2016 have evaluated a hydrogel composed of gellan and poly(methacrylamide-co-methacrylate) that forms *in situ*. Santhanam *et al.* (2016) considered 17 possible hydrogels with varying concentrations of the two polymers to determine how each polymer affects the properties of the final hydrogel. The developed hydrogels had optical and physical properties comparable to that of the natural vitreous with a sol-gel transition temperature range from 35.5 to 43 °C. Degradation studies showed that the hydrogels remained swollen for 4 weeks *in vitro* and biocompatibility studies with RPE cells showed no toxicity. The hydrogel was

found to allow for the optimising of swelling, mechanical properties, and transition temperature to obtain hydrogels similar to the vitreous. Eleven of these hydrogels were then further studied by Santhanam *et al.* (2019) and the two formulations that were most similar to the vitreous were studied further. The concentrations of thiolated gellan and poly(methacrylamide-co-methacrylate) in each of the two formulations were 0.9 $g \cdot L^{-1}$ and 12 $g \cdot L^{-1}$, and 1.5 $g \cdot L^{-1}$ and, 10 $g \cdot L^{-1}$ respectively. Both hydrogels were compared to silicone oil and were found to be clinically acceptable as vitreous replacements. The hydrogels were also biocompatible in rabbits and retained optical clarity and physiological intraocular pressure. The researchers concluded that further long-term *in vivo* studies of both hydrogels should be conducted (Santhanam *et al.*, 2019). Recently, Laradji *et al.* (2020) further studied the two optimised hydrogels and found them both to closely mimic the natural vitreous. Toxicity studies with various cell lines show biocompatibility, and preclinical studies 4 months after pars plana vitrectomy on rabbits showed no signs of inflammation. The lens was clear apart from partial opacities at the site of surgery. None of the rabbits developed cataracts in the four-month post-operative period. Further evaluation of the hydrogels is ongoing, but it promises to be a superior alternative to current substitutes.

Morozova *et al.* (2016) synthesised a vitreous substitute composed of the methacrylamide (MAM), methylacrylic acid and N',N'-bis(methylacryloyl-cystamine) (BMAC); however, unlike Liang *et al.* (2017) they also crosslinked gellan to the copolymer system. They proposed that the addition of anionic charges and a structural component that is fibrous would improve the structural integrity and the density of the vitreous substitute. The synthesised hydrogels swelled and were reinforced by the gellan fibres. Characterisation studies showed that the formulated hydrogel with crosslinked gellan had similar water content, transport properties and responsiveness to light to the natural vitreous. These results render this substitute a possible ideal long-term vitreous substitute.

2.6. Foldable Capsular Vitreous Body

An alternative to *in situ* hydrogels has been studied and assessed by a group of researchers. They developed a foldable capsular vitreous body (FCVB) that can be implanted in the ocular cavity and filled. The capsule of the FCVB, with a thickness of

0.01 mm, was composed of a liquid silicone rubber that was vulcanised once the FCVB mold was dipped in it. The liquid silicone rubber material was a crosslinked mixture of polyvinylsiloxane and polyhydrosiloxane (Gao *et al.*, 2008). The developed FCVB demonstrated good optical, mechanical, and biocompatible properties while effectively mimicking the physiological and structural functions of the natural vitreous (Liu *et al.*, 2010; Chen *et al.*, 2011; Lin *et al.*, 2011). The FCVB can be filled with solutions or hydrogels to regulate intraocular pressure, function as a tamponade for the retina, and act as a vitreous substitute. It has been filled with SO, PVA and PEG (Figure 2.4) (Wang *et al.*, 2012; Chen *et al.*, 2013; Feng *et al.*, 2013). Twelve-month and three-year follow-up studies of silicone oil (SO) filled FCVB show promising results. Retinal reattachment was seen at the three-year follow-up. Although some fluctuations in visual acuity were observed, no SO leakage or emulsification was seen, and no glaucoma or other complications occurred (Lin *et al.*, 2012, 2016). The FCVB has also been studied as a drug delivery system (Liu, *et al.*, 2010; Jiang *et al.*, 2011, 2012; Zheng *et al.*, 2012). All the FCVB studies indicate an ideal vitreous substitute, and any subsequent studies may result in a new therapeutic strategy for the treatment of RD.

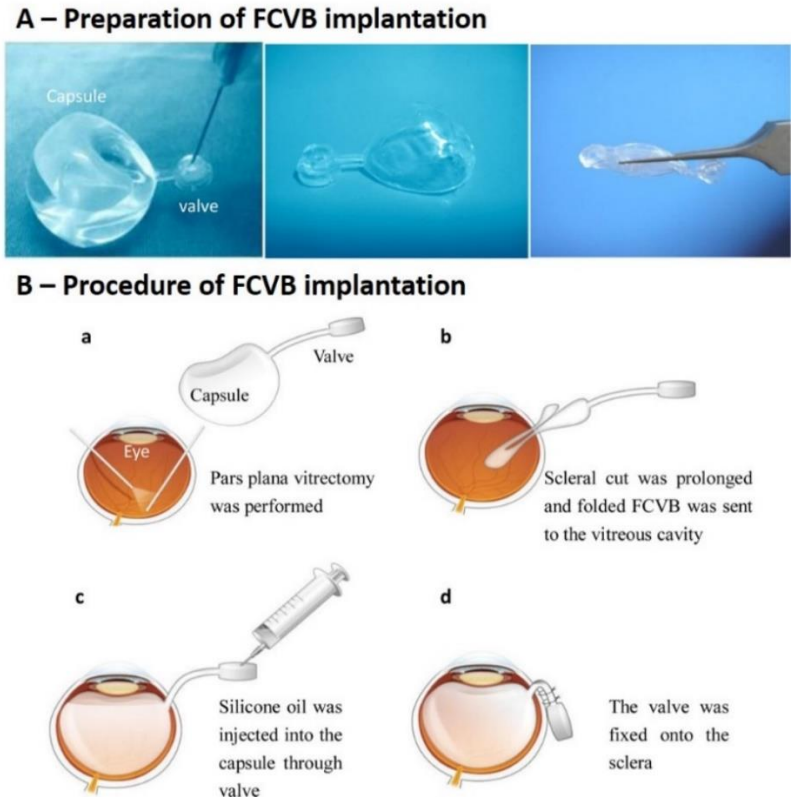

Figure 2.4 - (A) Preparation of the FCVB. The airtightness of the FCVB capsule was checked and the capsule was then three-folded like a spindle. (B) Procedure for the implantation surgery. (a) PPV (b) Placement of the FCVB in the vitreous cavity. (c) Injection of SO into the capsule (d) Fixing of the valve onto the sclera. (Lin *et al.*, 2016)

2.7. Future perspectives on the design of an ideal vitreous substitute

2.7.1. Drug Delivery

Drug delivery to the retina is a challenge due to the position of the retina in the eye along with the blood-retinal barrier. Intravitreal delivery of drugs for retinal diseases is a direct drug delivery route, however, it still carries the risk of endophthalmitis, vitreous haemorrhage, and retinal detachment (Cabrera *et al.*, 2019). The quick drug elimination from the vitreous requires frequent injections and this would decrease patient compliance (Huang and Chau, 2019). Polymeric nanoparticles retain drugs at the site of absorption for extended periods thus increasing the bioavailability of ocular drugs (Imperiale *et al*., 2018). Drug delivery via drug encapsulation in nanoparticles is a potentially sustainable long-term delivery route for retinal disease treatment. However, the uncontrolled burst release of drugs from encapsulation (Elsaid *et al.*,

2016) and the frequent need for intravitreal injections (Xue *et al.*, 2019) are disadvantages to the use of nanoparticles alone.

Using a vitreous substitute as a reservoir during drug delivery is a novel delivery system that should be further studied. Such a system can be used long-term and thus increase patient compliance while decreasing adverse effects such as intraocular inflammation, endophthalmitis and intraocular pressure elevation seen in repeated intravitreal injection administration (Ghasemi Falavarjani and Nguyen, 2013). The ideal vitreous substitute should be compatible with therapeutic agents to treat common adverse effects seen following vitrectomy such as cataract formation (Chirila and Harkin, 2016; Tram *et al.*, 2020). A vitreous substitute with high water content would be able to facilitate drug delivery and drug diffusion through ocular tissues. A vitreous substitute that can act as a drug delivery system will have to be similar to the natural vitreous while also being compatible with therapeutic agents allowing the controlled release of those agents.

2.7.2. Regenerative/Tissue Engineering

Regenerative medicine is a developing field that provides advanced solutions in the repair, regrowth, and replacement of tissues, cells or organs that are damaged. Several techniques can be utilised such as gene therapy, stem cell and progenitor cell therapy and tissue engineering (Vacanti, 2006; Polykandriotis *et al*., 2010). Tissue engineering for the regeneration of tissues consists of the development of scaffolds and nano-scaffolds that are biodegradable and biostable for long-term use (Doostmohammadi *et al.,* 2020). Scaffolds for ocular tissue regeneration should have the ability to mimic the extracellular matrix (ECM) and should be porous, biodegradable, and biocompatible to improve the integration of the scaffold into the ocular environment (Matthyssen *et al.*, 2018; Doostmohammadi *et al*., 2020).

Regeneration of the vitreous humour (Figure 2.5) would solve many disadvantages that are observed with current artificial vitreous substitutes such as lack of biocompatibility with surrounding tissue, inadequate transport of nutrients and poor biomechanical properties. The 3D structure of the vitreous is complex and would pose a challenge in the regeneration of the vitreous. Some researchers have investigated vitreal regeneration via hyalocyte control. The researchers controlled hyalocyte

proliferation using growth factors and evaluated HA production (Nishitsuka *et al.*, 2007; Sommer *et al.*, 2008). Regeneration of a vitreous-like body has spontaneously occurred in rabbit eyes following the biodegradation of a PEG-based hydrogel (Z. Liu *et al.*, 2019) which, together with other research, brings researchers closer to regenerating the natural vitreous.

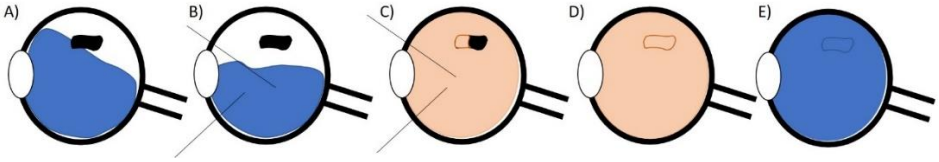

Figure 2.5 - Schematic diagrams illustrating the potential mechanism of vitreous body regeneration following vitreous substitution. (A) Retinal detachment with a retinal tear. (B) Vitrectomy (surgical removal of the vitreous). (C) Intravitreal injection of a gel allowing for chorioretinal adhesion to occur. (D) The gel supports the retina as an ideal vitreous substitute. (E) The vitreous substitute biodegrades and is replaced by a regenerated vitreous body.

Challenges with vitreous regeneration are evident in ocular diseases, such as proliferative diabetic retinopathy, that cause damage to the retina and its vasculature (Lee *et al*., 2015). Damage to ocular tissues may affect hyalocyte and collagen regeneration and thus vitreous regeneration. The hyaluronan-collagen network is responsible for the gel nature of the vitreous, which is necessary for its function to maintain the eye's structure and as a shock absorber. This stiffness of the gel has also been reported to impact stem cell differentiation essential for tissue regeneration (Sommer *et al.*, 2008).

2.8. Conclusions

The vitreous is an essential part of the eye. It has various functions, from filling and shaping the eye to providing stability to the retina. Long-term vitreous substitution is currently only performed using silicone oil while gas substitutes may be used as temporary substitutes. Current long-term vitreous substitutes present disadvantages that have led researchers to study and evaluate other substitutes that may be more ideal. The ideal vitreous substitute must be comparable to the natural vitreous in optical and mechanical properties, demonstrate long-term viability and biocompatibility, and maintain transparency. Recent research on vitreous substitutes has focussed on *in situ*-forming polymeric hydrogels that are injectable via small gauge

needles. Hydrogels are an ideal choice for vitreous substitution because they are biocompatible and can act as viscoelastic dampeners like the natural vitreous. Natural polysaccharide-based hydrogels, although structurally similar to the natural vitreous are unable to provide the correct mechanical strength required for vitreous substitution; and synthetic polymer-based hydrogels, while able to function similarly to the natural vitreous, have resulted in retinal toxicity. Manipulation of polymeric hydrogels allows for the tuning of various properties to prevent adverse effects. Substitutes composed of a mixture of natural and synthetic polymers are advantageous as they have the biomimetic and increased degradation profiles required for vitreous substitution. Polymeric hydrogels are a promising future as vitreous substitutes to fulfil patient needs and surgeon requirements.

2.9. References

Aliyar, H.A., Foster, W.J., Hamilton, P.D. & Ravi, N. (2004) Towards the development of an artificial human vitreous. *Polym Prep*. 45, 469–470.

Alovisi, C., Panico, C., Sanctis, U. de & Eandi, C.M. (2017) Vitreous Substitutes: Old and New Materials in Vitreoretinal Surgery. *Journal of Ophthalmology*. 2017, 1–6. doi:10.1155/2017/3172138.

Annaka, M., Mortensen, K., Vigild, M.E., Matsuura, T., Tsuji, S., Ueda, T. & Tsujinaka, H. (2011) Design of an Injectable in Situ Gelation Biomaterials for Vitreous Substitute. *Biomacromolecules*. 12 (11), 4011–4021. doi:10.1021/bm201012f.

Asaria, R.H.Y., Kon, C.H., Bunce, C., Charteris, D.G., Wong, D., Khaw, P.T. & Aylward, G.W. (2001) Adjuvant 5-fluorouracil and heparin prevents proliferative vitreoretinopathy. *Ophthalmology*. 108 (7), 1179–1183. doi:10.1016/S0161-6420(01)00589-9.

Astbury, N., Wood, M., Gajiwala, U., Patel, R., In the Sewa Rural Team, Chen, Y., Benjamin, L. & Abuh, S.O. (2008) Management of capsular rupture and vitreous loss in cataract surgery. *Community eye health*. 21 (65), 6–8. http://www.ncbi.nlm.nih.gov/pubmed/18504467.

Azen, S.P., Scott, I.U., Flynn, H.W., Lai, M.-Y., Topping, T.M., Benati, L., Trask, D.K. & Rogus, L.A. (1998) Silicone oil in the repair of complex retinal detachments. *Ophthalmology*. 105 (9), 1587–1597. doi:10.1016/S0161-6420(98)99023-6.

Barca, F., Caporossi, T. & Rizzo, S. (2014) Silicone Oil: Different Physical Proprieties and Clinical Applications. *BioMed Research International*. 2014, 1–7. doi:10.1155/2014/502143.

Barth, H., Crafoord, S., Andréasson, S. & Ghosh, F. (2016) A cross-linked hyaluronic acid hydrogel (Healaflow®) as a novel vitreous substitute. *Graefe's Archive for Clinical and Experimental Ophthalmology*. 254 (4), 697–703. doi:10.1007/s00417-015-3256-z.

Berker, N., Batman, C., Ozdamar, Y., Eranil, S., Aslan, O. & Zilelioglu, O. (2007) Long-term outcomes of heavy silicone oil tamponade for complicated retinal detachment. *European journal of ophthalmology*. 17 (5), 797–803. doi:10.1177/112067210701700518.

Böhm, I., Strotmann, F., Koopmans, C., Wolf, I., Galla, H.-J. & Ritter, H. (2012) Two-component in situ forming supramolecular hydrogels as advanced biomaterials in vitreous body surgery. *Macromolecular bioscience*. 12 (4), 432–437. doi:10.1002/mabi.201100357.

Cabrera, F.J., Wang, D.C., Reddy, K., Acharya, G. & Shin, C.S. (2019) Challenges and opportunities for drug delivery to the posterior of the eye. *Drug Discovery Today*. 24 (8), 1679–1684. doi:10.1016/j.drudis.2019.05.035.

Cavalieri, F., Miano, F., D'Antona, P. & Paradossi, G. (2004) Study of Gelling Behavior of Poly(vinyl alcohol)-Methacrylate for Potential Utilizations in Tissue Replacement and Drug Delivery. *Biomacromolecules*. 5 (6), 2439–2446. doi:10.1021/bm049654g.

Chan, C.K., Lin, S.G., Nuthi, A.S.D. & Salib, D.M. (2008) Pneumatic Retinopexy for the Repair of Retinal Detachments: A Comprehensive Review (1986–2007). *Survey of Ophthalmology*. 53 (5), 443–478. doi:10.1016/j.survophthal.2008.06.008.

Chang, J., Tao, Y., Wang, B., Guo, B., Xu, H., Jiang, Y. & Huang, Y. (2015) An in situ-forming zwitterionic hydrogel as vitreous substitute. *Journal of Materials Chemistry B*. 3 (6), 1097–1105. doi:10.1039/C4TB01775G.

Chang, J., Tao, Y., Wang, B., Yang, X., Xu, H., Jiang, Y., Guo, B. & Huang, Y. (2014) Evaluation of a redox-initiated in situ hydrogel as vitreous substitute. *Polymer*. 55 (18), 4627–4633. doi:10.1016/j.polymer.2014.07.031.

Chang, S., Reppucci, V., Zimmerman, N.J., Heinemann, M.-H. & Coleman, D.J. (1989) Perfluorocarbon Liquids in the Management of Traumatic Retinal Detachments. *Ophthalmology*. 96 (6), 785–792. doi:10.1016/S0161-6420(89)32812-0.

Chappelow, A. v & Kaiser, P.K. (2008) Neovascular Age-Related Macular Degeneration. *Drugs*. 68 (8), 1029–1036. doi:10.2165/00003495-200868080-00002.

Chen, H., Feng, S., Liu, Y., Huang, Z., Sun, X., Zhou, L., Lu, X. & Gao, Q. (2013) Functional evaluation of a novel vitreous substitute using polyethylene glycol sols injected into a foldable capsular vitreous body. *Journal of Biomedical Materials Research Part A*. 101A (9), 2538–2547. doi:10.1002/jbm.a.34560.

Chen, J., Gao, Q., Liu, Y., Ge, J., Cao, X., Luo, Y., Huang, D., Zhou, G., Lin, S., Lin, J., To, C.H. & Siu, A.W. (2011) Clinical device-related article evaluation of morphology and functions of a foldable capsular vitreous body in the rabbit eye. *Journal of Biomedical Materials Research Part B: Applied Biomaterials*. 97B (2), 396–404. doi:10.1002/jbm.b.31812.

Chirila, T. v. & Harkin, D.G. (2016) *Biomaterials and Regenerative Medicine in Ophthalmology*. 2nd edition. Elsevier. doi:10.1016/C2014-0-01443-8.

Chirila, T. v. & Hong, Y. (1998) Poly(1-vinyl-2-pyrrolidinone) hydrogels as vitreous substitutes: a rheological study. *Polymer International*. 46 (3), 183–195. doi:10.1002/(SICI)1097-0126(199807)46:3<183::AID-PI941>3.3.CO;2-0.

Chirila, T. v., Tahija, S., Hong, Y., Vijayasekaran, S. & Constable, I.J. (1994) Synthetic Polymers as Materials for Artificial Vitreous Body: Review and Recent Advances. *Journal of Biomaterials Applications*. 9 (2), 121–137. doi:10.1177/088532829400900203.

Contessi, N., Altomare, L., Filipponi, A. & Farè, S. (2017) Thermo-responsive properties of methylcellulose hydrogels for cell sheet engineering. *Materials Letters*. 207, 157–160. doi:10.1016/j.matlet.2017.07.023.

Daniele, S., Refojo, M.F., Schepens, C.L. & Freeman, H.M. (1968) Glyceryl methacrylate hydrogel as a vitreous implant. An experimental study. *Archives of ophthalmology (Chicago, Ill.: 1960)*. 80 (1), 120–127. doi:10.1001/archopht.1968.00980050122020.

Davidorf, F.H., Chambers, R.B., Kwon, O.W., Doyle, W., Gresak, P. & Frank, S.G. (1990) Ocular toxicity of vitreal pluronic polyol F-127. *Retina (Philadelphia, Pa.)*. 10 (4), 297–300. doi:10.1097/00006982-199010000-00013.

Davis, J.T., Hamilton, P.D. & Ravi, N. (2017) Poly(acrylamide co-acrylic acid) for use as an in situ gelling vitreous substitute. *Journal of Bioactive and Compatible Polymers*. 32 (5), 528–541. doi:10.1177/0883911516688482.

de Bustros, S., Glaser, B.M. & Johnson, M.A. (1985) Thrombin Infusion for the Control of Intraocular Bleeding During Vitreous Surgery. *Archives of Ophthalmology*. 103 (6), 837–839. doi:10.1001/archopht.1985.01050060097034.

de Tribolet, N., Porchet, F., Lutz, T.W., Gratzl, O., Brotchi, J., van Alphen, H.A., van Acker, R.E., Benini, A., Strommer, K.N., Bernays, R.L., Goffin, J., Beuls, E.A. & Ross, J.S. (1998) Clinical assessment of a novel antiadhesion barrier gel: prospective, randomized, multicenter, clinical trial of ADCON-L to inhibit postoperative peridural fibrosis and related symptoms after lumbar discectomy. *American journal of orthopedics (Belle Mead, N.J.)*. 27 (2), 111–120. http://www.ncbi.nlm.nih.gov/pubmed/9506196.

Donati, S., Caprani, S.M., Airaghi, G., Vinciguerra, R., Bartalena, L., Testa, F., Mariotti, C., Porta, G., Simonelli, F. & Azzolini, C. (2014) Vitreous Substitutes: The Present and the Future. *BioMed Research International*. 2014 (May), 1–12. doi:10.1155/2014/351804.

Doostmohammadi, M., Forootanfar, H. & Ramakrishna, S. (2020) Regenerative medicine and drug delivery: Progress via electrospun biomaterials. *Materials Science and Engineering: C*. 109 (April 2019), 110521. doi:10.1016/j.msec.2019.110521.

Eibenberger, K., Sacu, S., Rezar-Dreindl, S., Schmidt-Erfurth, U. & Georgopoulos, M. (2020) Silicone Oil Tamponade in Rhegmatogenous Retinal Detachment: Functional and Morphological Results. *Current Eye Research*. 45 (1), 38–45. doi:10.1080/02713683.2019.1652917.

Eiger-Moscovich, M., Gershoni, A., Axer-Siegel, R., Weinberger, D. & Ehrlich, R. (2017) Short-Term Vitreoretinal Tamponade with Heavy Liquid Following Surgery for Giant Retinal Tear. *Current Eye Research*. 42 (7), 1074–1078. doi:10.1080/02713683.2016.1266664.

Elsaid, N., Jackson, T.L., Elsaid, Z., Alqathama, A. & Somavarapu, S. (2016) PLGA Microparticles Entrapping Chitosan-Based Nanoparticles for the Ocular Delivery of Ranibizumab. *Molecular Pharmaceutics*. 13 (9), 2923–2940. doi:10.1021/acs.molpharmaceut.6b00335.

Feng, S., Chen, H., Liu, Y., Huang, Z., Sun, X., Zhou, L., Lu, X. & Gao, Q. (2013) A Novel Vitreous Substitute of Using a Foldable Capsular Vitreous Body Injected with Polyvinylalcohol Hydrogel. *Scientific Reports*. 3 (1), 1838. doi:10.1038/srep01838.

Fernandez-Vigo, J., Refojo, M.F. & Verstraeten, T. (1990) Evaluation of a viscoelastic solution of hydroxypropyl methylcellulose as a potential vitreous substitute. *Retina (Philadelphia, Pa.)*. 10 (2), 148–152. doi:10.1097/00006982-199004000-00012.

Fernandez-Vigo, J., Sabugal, J.F., Diaz Rey, A., Concheiro, A. & Martinez, R. (1990) Molecular weight dependence of the pharmacokinetic of hydroxypropyl methylcellulose in the vitreous. *Journal of ocular pharmacology*. 6 (2), 137–142. doi:10.1089/jop.1990.6.137.

Flaxman, S.R., Bourne, R.R.A., Resnikoff, S., Ackland, P., Braithwaite, T., et al. (2017) Global causes of blindness and distance vision impairment 1990–2020: a systematic review and meta-analysis. *The Lancet Global Health*. 5 (12), e1221–e1234. doi:10.1016/S2214-109X(17)30393-5.

Foster, W.J., Aliyar, H.A., Hamilton, P. & Ravi, N. (2006) Internal Osmotic Pressure as a Mechanism of Retinal Attachment in a Vitreous Substitute. *Journal of Bioactive and Compatible Polymers*. 21 (3), 221–235. doi:10.1177/0883911506064368.

Gao, Q., Mou, S., Ge, J., To, C., Hui, Y., Liu, A., Wang, Z., Long, C. & Tan, J. (2008) A new strategy to replace the natural vitreous by a novel capsular artificial vitreous body with pressure-control valve. *Eye*. 22 (3), 461–468. doi:10.1038/sj.eye.6702875.

George, A., Shah, P.A. & Shrivastav, P.S. (2019) Natural biodegradable polymers based nano-formulations for drug delivery: A review. *International Journal of Pharmaceutics*. 561 (March), 244–264. doi:10.1016/j.ijpharm.2019.03.011.

Ghasemi Falavarjani, K. & Nguyen, Q.D. (2013) Adverse events and complications associated with intravitreal injection of anti-VEGF agents: a review of literature. *Eye*. 27 (7), 787–794. doi:10.1038/eye.2013.107.

Giavasis, I., Harvey, L.M. & McNeil, B. (2000) Gellan Gum. *Critical Reviews in Biotechnology*. 20 (3), 177–211. doi:10.1080/07388550008984169.

Gupta, R.P., Deshpande, M., Bharadwaj, A. & Baranwal, V.K. (1997) PNEUMATIC RETINOPEXY IN RHEGMATOGENOUS RETINAL DETACHMENT. *Medical journal, Armed Forces India*. 53 (4), 255–258. doi:10.1016/S0377-1237(17)30747-5.

Gurunadh, V., Banarji, A., Patyal, S., Upadhyay, A., Ahluwalia, T., Gupta, R. & Bhaduria, M. (2010) Evaluation of Vitreous Substitutes in Managing Complicated Vitreo-retinal Surgeries. *Medical Journal Armed Forces India*. 66 (2), 125–128. doi:10.1016/S0377-1237(10)80123-6.

Hart, R.H., Vote, B.J., Borthwick, J.H., McGeorge, A.J. & Worsley, D.R. (2002) Loss of vision caused by expansion of intraocular perfluoropropane (C3F8) gas during nitrous oxide anesthesia. *American Journal of Ophthalmology*. 134 (5), 761–763. doi:10.1016/S0002-9394(02)01654-9.

Hayashi, K., Okamoto, F., Hoshi, S., Katashima, T., Zujur, D.C., Li, X., Shibayama, M., Gilbert, E.P., Chung, U., Ohba, S., Oshika, T. & Sakai, T. (2017) Fast-forming hydrogel with ultralow polymeric content as an artificial vitreous body. *Nature Biomedical Engineering*. 1 (3), 0044. doi:10.1038/s41551-017-0044.

Hogen-Esch, T.E., Shah, K.R. & Fitzgerald, C.R. (1976) Development of injectable poly(glyceryl methacrylate) hydrogels for vitreous prosthesis. *Journal of Biomedical Materials Research*. 10 (6), 975–976. doi:10.1002/jbm.820100615.

Hong, Y., Chirila, T. v., Cuypers, M.J.H. & Constable, I.J. (1996a) Polymers of 1-Vinyl-2-Pyrrolidinone as Potential Vitreous Substitutes: Physical Selection. *Journal of Biomaterials Applications*. 11 (2), 135–181. doi:10.1177/088532829601100202.

Hong, Y., Chirila, T. v., Vijayasekaran, S., Dalton, P.D., Tahija, S.G., Cuypers, M.J.H. & Constable, I.J. (1996b) Crosslinked poly (1-vinyl-2-pyrrolidinone) as a vitreous substitute. *Journal of Biomedical Materials Research*. 30 (4), 441–448. doi:10.1002/(SICI)1097-4636(199604)30:4<441::AID-JBM2>3.0.CO;2-P.

Hong, Y., Chirila, T. v., Vijayasekaran, S., Shen, W., Lou, X. & Dalton, P.D. (1998) Biodegradation in vitro and retention in the rabbit eye of crosslinked poly(1-vinyl-2-pyrrolidinone) hydrogel as a vitreous substitute. *Journal of Biomedical Materials Research*. 39 (4), 650–659. doi:10.1002/(SICI)1097-4636(19980315)39:4<650::AID-JBM21>3.0.CO;2-9.

Huang, G., Liu, Y. & Chen, L. (2017) Chitosan and its derivatives as vehicles for drug delivery. *Drug Delivery*. 24 (2), 108–113. doi:10.1080/10717544.2017.1399305.

Huang, X. & Chau, Y. (2019) Intravitreal nanoparticles for retinal delivery. *Drug Discovery Today*. 24 (8), 1510–1523. doi:10.1016/j.drudis.2019.05.005.

Hwang, Y.-S., Chiang, P.-R., Hong, W.-H., Chiao, C.-C., Chu, I.-M., Hsiue, G.-H. & Shen, C.-R. (2013) Study In Vivo Intraocular Biocompatibility of In Situ Gelation Hydrogels: Poly(2-Ethyl Oxazoline)-Block-Poly(ε-Caprolactone)-Block-Poly(2-Ethyl Oxazoline) Copolymer, Matrigel and Pluronic F127 W.-C. Chin (ed.). *PLoS ONE*. 8 (7), e67495. doi:10.1371/journal.pone.0067495.

Imperiale, J.C., Acosta, G.B. & Sosnik, A. (2018) Polymer-based carriers for ophthalmic drug delivery. *Journal of Controlled Release*. 285 (June), 106–141. doi:10.1016/j.jconrel.2018.06.031.

Januschowski, K., Schnichels, S., Hurst, J., Hohenadl, C., Reither, C., Rickmann, A., Pohl, L., Bartz-Schmidt, K.-U. & Spitzer, M.S. (2019) Ex vivo biophysical characterization of a hydrogel-based artificial vitreous substitute T. Langmann (ed.). *PLOS ONE*. 14 (1), e0209217. doi:10.1371/journal.pone.0209217.

Jiang, X., Peng, Y., Yang, C., Liu, W. & Han, B. (2018) The feasibility study of an in situ marine polysaccharide-based hydrogel as the vitreous substitute. *Journal of biomedical materials research. Part A*. 106 (7), 1997–2006. doi:10.1002/jbm.a.36403.

Jiang, Z., Wang, P., Pan, B., Xie, Z., Li, D., Wang, T., Liu, Y., Yuan, Z. & Gao, Q. (2012a) Evaluation of Levofloxacin Release Characteristics from a Human Foldable Capsular Vitreous Body *In Vitro*. *Journal of Ocular Pharmacology and Therapeutics*. 28 (1), 33–40. doi:10.1089/jop.2011.0109.

Jiang, Z., Wang, T., Pan, B., Xie, Z., Wang, P., Liu, Y. & Gao, Q. (2012b) Evaluation of the levofloxacin release characters from a rabbit foldable capsular vitreous body. *International journal of nanomedicine*. 7, 1–10. doi:10.2147/IJN.S25268.

de Jong, C., Bali, E., Libert, J. & Caspers-Velu, L. (2000) ADCON-L hydrogel as a vitreous substitute: preliminary results. *Bulletin de la Societe belge d'ophtalmologie*. (278), 71–75. http://www.ncbi.nlm.nih.gov/pubmed/11761565.

Joussen, A.M., Rizzo, S., Kirchhof, B., Schrage, N., Li, X., Lente, C. & Hilgers, R.-D. (2011) Heavy silicone oil versus standard silicone oil in as vitreous tamponade in inferior PVR (HSO Study): interim analysis. *Acta Ophthalmologica*. 89 (6), e483–e489. doi:10.1111/j.1755-3768.2011.02139.x.

Kanclerz, P. & Grzybowski, A. (2018) Complications Associated with the Use of Expandable Gases in Vitrectomy. *Journal of Ophthalmology*. 2018, 1–7. doi:10.1155/2018/8606494.

Kars, M.E., Toklu, Y., Arıkan Yorgun, M., Neşelioğlu, S. & Eren, F. (2020) Electrolyte, Nitric Oxide and Oxidative Stress Levels of Aqueous Humor in Patients with Retinal Detachment and Silicone Oil Tamponade. *Current Eye Research*. 45 (11), 1443–1450. doi:10.1080/02713683.2020.1749668.

Katagiri, Y., Iwasaki, T., Ishikawa, T., Yamakawa, N., Suzuki, H. & Usui, M. (2005) Application of Thermo-setting Gel as Artificial Vitreous. *Japanese Journal of Ophthalmology*. 49 (6), 491–496. doi:10.1007/s10384-005-0255-3.

KIM, R. & BAUMAL, C. (2004) Anterior segment complications related to vitreous substitutes. *Ophthalmology Clinics of North America*. 17 (4), 569–576. doi:10.1016/j.ohc.2004.06.011.

Kirchhof, B., Wong, D., van Meurs, J., Hilgers, R.D., Macek, M., Lois, N. & Schrage, N.F. (2002) Use of perfluorohexyloctane as a long-term internal tamponade agent in complicated retinal detachment surgery. *American journal of ophthalmology*. 133 (1), 95–101. doi:10.1016/s0002-9394(01)01295-8.

Kleinberg, T.T., Tzekov, R.T., Stein, L., Ravi, N. & Kaushal, S. (2011) Vitreous Substitutes: A Comprehensive Review. *Survey of Ophthalmology*. 56 (4), 300–323. doi:10.1016/j.survophthal.2010.09.001.

Kyari, F., Abdull, M.M., Bastawrous, A., Gilbert, C.E. & Faal, H. (2013) Epidemiology of glaucoma in sub-saharan Africa: prevalence, incidence and risk factors. *Middle East African journal of ophthalmology*. 20 (2), 111–125. doi:10.4103/0974-9233.110605.

Lamponi, S., Leone, G., Consumi, M., Greco, G. & Magnani, A. (2012) In Vitro Biocompatibility of New PVA-Based Hydrogels as Vitreous Body Substitutes. *Journal of Biomaterials Science, Polymer Edition*. 23 (1–4), 555–575. doi:10.1163/092050611X554499.

Laradji, A., Shui, Y.-B., Karakocak, B.B., Evans, L., Hamilton, P. & Ravi, N. (2020) Bioinspired Thermosensitive Hydrogel as a Vitreous Substitute: Synthesis, Properties, and Progress of Animal Studies. *Materials*. 13 (6), 1337. doi:10.3390/ma13061337.

Lee, D.A., Wilson, M.R., Yoshizumi, M.O. & Hall, M. (1991) The ocular effects of gases when injected into the anterior chamber of rabbit eyes. *Archives of ophthalmology (Chicago, Ill. : 1960)*. 109 (4), 571–575. doi:10.1001/archopht.1991.01080040139045.

Lee, R., Wong, T.Y. & Sabanayagam, C. (2015) Epidemiology of diabetic retinopathy, diabetic macular edema and related vision loss. *Eye and Vision*. 2 (1), 17. doi:10.1186/s40662-015-0026-2.

Leone, G., Consumi, M., Aggravi, M., Donati, A., Lamponi, S. & Magnani, A. (2010) PVA/STMP based hydrogels as potential substitutes of human vitreous. *Journal of*

Materials Science: Materials in Medicine. 21 (8), 2491–2500. doi:10.1007/s10856-010-4092-7.

Li, W., Zheng, J., Zheng, Q., Wu, R., Wang, X. & Xu, M. (2010) Clinical complications of Densiron 68 intraocular tamponade for complicated retinal detachment. *Eye*. 24 (1), 21–28. doi:10.1038/eye.2009.57.

Liang, C., Peyman, G.A., Serracarbassa, P., Calixto, N., Chow, A.A. & Rao, P. (1998) An evaluation of methylated collagen as a substitute for vitreous and aqueous humor. *International ophthalmology*. 22 (1), 13–18. doi:10.1023/a:1006016809070.

Liang, J., Struckhoff, J.J., Du, H., Hamilton, P.D. & Ravi, N. (2017) Synthesis and characterization of in situ forming anionic hydrogel as vitreous substitutes. *Journal of Biomedical Materials Research Part B: Applied Biomaterials*. 105 (5), 977–988. doi:10.1002/jbm.b.33632.

Lim, B.L. & Vote, B. (2008) Densiron intraocular tamponade: a case series. *Clinical & Experimental Ophthalmology*. 36 (3), 261–264. doi:10.1111/j.1442-9071.2008.01721.x.

Lin, X., Ge, J., Gao, Q., Wang, Z., Long, C., He, L., Liu, Y. & Jiang, Z. (2011) Evaluation of the Flexibility, Efficacy, and Safety of a Foldable Capsular Vitreous Body in the Treatment of Severe Retinal Detachment. *Investigative Opthalmology & Visual Science*. 52 (1), 374. doi:10.1167/iovs.10-5869.

Lin, X., Sun, X., Wang, Z., Jiang, Z., Liu, Y., Wang, P. & Gao, Q. (2016) Three-Year Efficacy and Safety of a Silicone Oil-Filled Foldable-Capsular-Vitreous-Body in Three Cases of Severe Retinal Detachment. *Translational Vision Science & Technology*. 5 (1), 2. doi:10.1167/tvst.5.1.2.

Lin, X., Wang, Z., Jiang, Z., Long, C., Liu, Y., Wang, P., Jin, C., Yi, C. & Gao, Q. (2012) Preliminary efficacy and safety of a silicone oil-filled foldable capsular vitreous body in the treatment of severe retinal detachment. *Retina (Philadelphia, Pa.)*. 32 (4), 729–741. doi:10.1097/IAE.0b013e31822b1f80.

Lin, Y.-K., Chen, K.-H. & Kuan, C.-Y. (2013) The synthesis and characterization of a thermally responsive hyaluronic acid/Pluronic copolymer and an evaluation of its

potential as an artificial vitreous substitute. *Journal of Bioactive and Compatible Polymers*. 28 (4), 355–367. doi:10.1177/0883911513491181.

Liu, Y., Jiang, Z., Gao, Q., Ge, J., Chen, J., Cao, X., Shen, Q. & Ma, P. (2010a) Technical standards of a foldable capsular vitreous body in terms of mechanical, optical, and biocompatible properties. *Artificial organs*. 34 (10), 836–845. doi:10.1111/j.1525-1594.2010.01006.x.

Liu, Y., Ke, Q., Chen, J., Wang, Z., Xie, Z., Jiang, Z., Ge, J. & Gao, Q. (2010b) Sustained Mechanical Release of Dexamethasone Sodium Phosphate from a Foldable Capsular Vitreous Body. *Investigative Opthalmology & Visual Science*. 51 (3), 1636. doi:10.1167/iovs.09-4134.

Liu, Y., Wang, Y., Yang, J., Zhang, H. & Gan, L. (2019a) Cationized hyaluronic acid coated spanlastics for cyclosporine A ocular delivery: Prolonged ocular retention, enhanced corneal permeation and improved tear production. *International Journal of Pharmaceutics*. 565, 133–142. doi:10.1016/j.ijpharm.2019.05.018.

Liu, Z., Liow, S.S., Lai, S.L., Alli-Shaik, A., Holder, G.E., et al. (2019b) Retinal-detachment repair and vitreous-like-body reformation via a thermogelling polymer endotamponade. *Nature biomedical engineering*. 3 (8), 598–610. doi:10.1038/s41551-019-0382-7.

Malchiodi-Albedi, F., Morgillo, A., Formisano, G., Paradisi, S., Perilli, R., Scalzo, G.C., Scorcia, G. & Caiazza, S. (2002) Biocompatibility assessment of silicone oil and perfluorocarbon liquids used in retinal reattachment surgery in rat retinal cultures. *Journal of Biomedical Materials Research*. 60 (4), 548–555. doi:10.1002/jbm.10079.

Marcus, D.M., D'Amico, D.J. & Mukai, S. (1994) Pneumatic retinopexy versus scleral buckling for repair of primary rhegmatogenous retinal detachment. *International ophthalmology clinics*. 34 (3), 97–108. doi:10.1097/00004397-199403430-00011.

Maruoka, S., Matsuura, T., Kawasaki, K., Okamoto, M., Yoshiaki, H., Kodama, M., Sugiyama, M. & Annaka, M. (2006) Biocompatibility of Polyvinylalcohol Gel as a Vitreous Substitute. *Current Eye Research*. 31 (7–8), 599–606. doi:10.1080/02713680600813854.

Mateo-Montoya, A. & de Smet, M.D. (2014) Air as Tamponade for Retinal Detachments. *European Journal of Ophthalmology*. 24 (2), 242–246. doi:10.5301/ejo.5000373.

Matteucci, A., Formisano, G., Paradisi, S., Carnovale-Scalzo, G., Scorcia, G., Caiazza, S., Hoerauf, H. & Malchiodi-Albedi, F. (2007) Biocompatibility Assessment of Liquid Artificial Vitreous Replacements: Relevance of In Vitro Studies. *Survey of Ophthalmology*. 52 (3), 289–299. doi:10.1016/j.survophthal.2007.02.004.

Matthyssen, S., van den Bogerd, B., Dhubhghaill, S.N., Koppen, C. & Zakaria, N. (2018) Corneal regeneration: A review of stromal replacements. *Acta Biomaterialia*. 69, 31–41. doi:10.1016/j.actbio.2018.01.023.

Mertens, S., Bednarz, J. & Engelmann, K. (2002) Evidence of toxic side effects of perfluorohexyloctane after vitreoretinal surgery as well as in previously established in vitro models with ocular cell types. *Graefe's Archive for Clinical and Experimental Ophthalmology*. 240 (12), 989–995. doi:10.1007/s00417-002-0561-0.

Morescalchi, F., Costagliola, C., Duse, S., Gambicorti, E., Parolini, B., Arcidiacono, B., Romano, M.R. & Semeraro, F. (2014) Heavy Silicone Oil and Intraocular Inflammation K. Li (ed.). *BioMed Research International*. 2014, 1–16. doi:10.1155/2014/574825.

Morozova, S., Hamilton, P., Ravi, N. & Muthukumar, M. (2016) Development of a Vitreous Substitute: Incorporating Charges and Fibrous Structures in Synthetic Hydrogel Materials. *Macromolecules*. 49 (12), 4619–4626. doi:10.1021/acs.macromol.6b00885.

Mukherjee, P., Rani, A. & Saravanan, P. (2019) Polymeric Materials for 3D Bioprinting. In: *3D Printing Technology in Nanomedicine*. Elsevier. pp. 63–81. doi:10.1016/B978-0-12-815890-6.00004-9.

Murtagh, P.J., Stephenson, K.A., Rhatigan, M., McElnea, E.M., Connell, P.P. & Keegan, D.J. (2020) Rhegmatogenous retinal detachments: primary reattachment rates and visual outcomes over a 4-year period. *Irish Journal of Medical Science (1971 -)*. 189 (1), 355–363. doi:10.1007/s11845-019-02084-7.

Nakagawa, M., Tanaka, M. & Miyata, T. (1997) Evaluation of Collagen Gel and Hyaluronic Acid as Vitreous Substitutes. *Ophthalmic Research*. 29 (6), 409–420. doi:10.1159/000268042.

Nardo, T., Carmagnola, I., Ruini, F., Caddeo, S., Calzone, S., Chiono, V. & Ciardelli, G. (2017) Synthetic Biomaterial for Regenerative Medicine Applications. In: *Kidney Transplantation, Bioengineering and Regeneration*. Elsevier. pp. 901–921. doi:10.1016/B978-0-12-801734-0.00065-5.

Necas, J., Bartosikova, L., Brauner, P. & Kolar, J. (2008) Hyaluronic acid (hyaluronan): a review. *Veterinární medicína*. 53 (8), 397–411. doi:10.17221/1930-VETMED.

Neffendorf, J.E., Gupta, B. & Williamson, T.H. (2018) THE ROLE OF INTRAOCULAR GAS TAMPONADE IN RHEGMATOGENOUS RETINAL DETACHMENT: A Synthesis of the Literature. *Retina (Philadelphia, Pa.)*. 38 Suppl 1 (1), S65–S72. doi:10.1097/IAE.0000000000002015.

Nishitsuka, K., Kashiwagi, Y., Tojo, N., Kanno, C., Takahashi, Y., Yamamoto, T., Heldin, P. & Yamashita, H. (2007) Hyaluronan production regulation from porcine hyalocyte cell line by cytokines. *Experimental Eye Research*. 85 (4), 539–545. doi:10.1016/j.exer.2007.07.006.

Oosterhuis, J.A., van Haeringen, N.J., Jeltes, I.G. & Glasius, E. (1966) Polygeline as a vitreous substitute. I. Observations in rabbits. *Archives of ophthalmology (Chicago, Ill. : 1960)*. 76 (2), 258–265. doi:10.1001/archopht.1966.03850010260018.

Osmałek, T., Froelich, A. & Tasarek, S. (2014) Application of gellan gum in pharmacy and medicine. *International Journal of Pharmaceutics*. 466 (1–2), 328–340. doi:10.1016/j.ijpharm.2014.03.038.

Ozdek, S., Yuksel, N., Gurelik, G. & Hasanreisoglu, B. (2011) High-density silicone oil as an intraocular tamponade in complex retinal detachments. *Canadian Journal of Ophthalmology*. 46 (1), 51–55. doi:10.3129/i10-107.

Pak, K.Y., Lee, S.J., Kwon, H.J., Park, S.W., Byon, I.S. & Lee, J.E. (2017) Exclusive Use of Air as Gas Tamponade in Rhegmatogenous Retinal Detachment. *Journal of Ophthalmology*. 2017, 1–5. doi:10.1155/2017/1341948.

Peng, Y., Han, B., Liu, W. & Xu, X. (2005) Preparation and antimicrobial activity of hydroxypropyl chitosan. *Carbohydrate research*. 340 (11), 1846–1851. doi:10.1016/j.carres.2005.05.009.

Peyman, G.A., Schulman, J.A. & Sullivan, B. (1995) Perfluorocarbon liquids in ophthalmology. *Survey of ophthalmology*. 39 (5), 375–395. doi:10.1016/s0039-6257(05)80093-1.

Polykandriotis, E., Popescu, L.M. & Horch, R.E. (2010) Regenerative medicine: then and now - an update of recent history into future possibilities. *Journal of Cellular and Molecular Medicine*. 14 (10), 2350–2358. doi:10.1111/j.1582-4934.2010.01169.x.

Pritchard, C.D., Crafoord, S., Andréasson, S., Arnér, K.M., O'Shea, T.M., Langer, R. & Ghosh, F.K. (2011) Evaluation of viscoelastic poly(ethylene glycol) sols as vitreous substitutes in an experimental vitrectomy model in rabbits. *Acta Biomaterialia*. 7 (3), 936–943. doi:10.1016/j.actbio.2010.11.013.

Pruett, R.C. (1979) Hyaluronic Acid Vitreous Substitute. *Archives of Ophthalmology*. 97 (12), 2325. doi:10.1001/archopht.1979.01020020541006.

Pruett, R.C., Calabria, G.A. & Schepens, C.L. (1972) Collagen vitreous substitute. I. Experimental study. *Archives of ophthalmology (Chicago, Ill. : 1960)*. 88 (5), 540–543. doi:10.1001/archopht.1972.01000030542015.

Pruett, R.C., Schepens, C.L. & Freeman, H.M. (1974) Collagen vitreous substitute. II. Preliminary clinical trials. *Archives of ophthalmology (Chicago, Ill. : 1960)*. 91 (1), 29–32. doi:10.1001/archopht.1974.03900060033008.

Raia, N.R., Jia, D., Ghezzi, C.E., Muthukumar, M. & Kaplan, D.L. (2020) Characterization of silk-hyaluronic acid composite hydrogels towards vitreous humor substitutes. *Biomaterials*. 233 (July 2019), 119729. doi:10.1016/j.biomaterials.2019.119729.

Roider, J., Hoerauf, H., Kobuch, K. & Gabel, V.-P. (2002) Clinical findings on the use of long-term heavy tamponades (semifluorinated alkanes and their oligomers) in complicated retinal detachment surgery. *Graefe's Archive for Clinical and Experimental Ophthalmology*. 240 (12), 965–971. doi:10.1007/s00417-002-0574-8.

Roy, S., do Thi, H., Feusier, M. & Mermoud, A. (2012) Crosslinked Sodium Hyaluronate Implant in Deep Sclerectomy for the Surgical Treatment of Glaucoma. *European Journal of Ophthalmology*. 22 (1), 70–76. doi:10.5301/ejo.5000054.

Santhanam, S., Liang, J., Struckhoff, J., Hamilton, P.D. & Ravi, N. (2016) Biomimetic hydrogel with tunable mechanical properties for vitreous substitutes. *Acta Biomaterialia*. 43, 327–337. doi:10.1016/j.actbio.2016.07.051.

Santhanam, S., Shui, Y.-B., Struckhoff, J., Karakocak, B.B., Hamilton, P.D., Harocopos, G.J. & Ravi, N. (2019) Bioinspired Fibrillary Hydrogel with Controlled Swelling Behavior: Applicability as an Artificial Vitreous. *ACS Applied Bio Materials*. 2 (1), 70–80. doi:10.1021/acsabm.8b00376.

Scheerlinck, L.M., Schellekens, P.A., Liem, A.T., Steijns, D. & van Leeuwen, R. (2018) Retinal sensitivity following intraocular silicone oil and gas tamponade for rhegmatogenous retinal detachment. *Acta Ophthalmologica*. 96 (6), 641–647. doi:10.1111/aos.13685.

Schnichels, S., Schneider, N., Hohenadl, C., Hurst, J., Schatz, A., Januschowski, K. & Spitzer, M.S. (2017) Efficacy of two different thiol-modified crosslinked hyaluronate formulations as vitreous replacement compared to silicone oil in a model of retinal detachment A. Wedrich (ed.). *PLOS ONE*. 12 (3), e0172895. doi:10.1371/journal.pone.0172895.

Schramm, C., Spitzer, M.S., Henke-Fahle, S., Steinmetz, G., Januschowski, K., Heiduschka, P., Geis-Gerstorfer, J., Biedermann, T., Bartz-Schmidt, K.U. & Szurman, P. (2012) The Cross-linked Biopolymer Hyaluronic Acid as an Artificial Vitreous Substitute. *Investigative Opthalmology & Visual Science*. 53 (2), 613. doi:10.1167/iovs.11-7322.

Schwartz, S., Vaziri, K., Kishor, K. & Flynn, H. (2016) Tamponade in the surgical management of retinal detachment. *Clinical Ophthalmology*. 10, 471. doi:10.2147/OPTH.S98529.

Scuderi, G. (1954) [Experimental vitreous transplantation: attempted partial replacement with homologous vitreous, heterologous liquor and polyvinylpyrrolidone

solutions]. *Annali di ottalmologia e clinica oculistica*. 80 (4), 213–220. http://www.ncbi.nlm.nih.gov/pubmed/13189251.

Snell, R.S. (2000) *Clinical anatomy for medical students*. 6th edition. Lippincott Williams & Wilkins.

Snell, R.S. & Lemp, M.A. (1997) *Clinical Anatomy of the Eye*. 2nd edition. Oxford, UK, Blackwell Science Ltd,. doi:10.1002/9781118690987.

Soliman, K.A., Ullah, K., Shah, A., Jones, D.S. & Singh, T.R.R. (2019) Poloxamer-based in situ gelling thermoresponsive systems for ocular drug delivery applications. *Drug Discovery Today*. 24 (8), 1575–1586. doi:10.1016/j.drudis.2019.05.036.

Sommer, F., Pollinger, K., Brandl, F., Weiser, B., Teßmar, J., Blunk, T. & Göpferich, A. (2008) Hyalocyte proliferation and ECM accumulation modulated by bFGF and TGF-β1. *Graefe's Archive for Clinical and Experimental Ophthalmology*. 246 (9), 1275–1284. doi:10.1007/s00417-008-0846-z.

Strotmann, F., Bezdushna, E., Ritter, H. & Galla, H.-J. (2011) In Situ Forming Hydrogels: A Thermo-Responsive Polyelectrolyte as Promising Liquid Artificial Vitreous Body Replacement. *Advanced Engineering Materials*. 13 (5), B172–B180. doi:10.1002/adem.201080104.

Strotmann, F., Wolf, I. & Galla, H.-J. (2013) The biocompatibility of a polyelectrolyte vitreous body substitute on a high resistance *in vitro* model of the blood-retinal barrier. *Journal of Biomaterials Applications*. 28 (3), 334–342. doi:10.1177/0885328212450597.

Su, W.-Y., Chen, K.-H., Chen, Y.-C., Lee, Y.-H., Tseng, C.-L. & Lin, F.-H. (2011) An Injectable Oxidated Hyaluronic Acid/Adipic Acid Dihydrazide Hydrogel as a Vitreous Substitute. *Journal of Biomaterials Science, Polymer Edition*. 22 (13), 1777–1797. doi:10.1163/092050610X522729.

Su, X., Tan, M.J., Li, Z., Wong, M., Rajamani, L., Lingam, G. & Loh, X.J. (2015) Recent Progress in Using Biomaterials as Vitreous Substitutes. *Biomacromolecules*. 16 (10), 3093–3102. doi:10.1021/acs.biomac.5b01091.

Suri, S. & Banerjee, R. (2006) In vitro evaluation of in situ gels as short term vitreous substitutes. *Journal of biomedical materials research. Part A*. 79 (3), 650–664. doi:10.1002/jbm.a.30917.

Swindle, K.E., Hamilton, P.D. & Ravi, N. (2008) In situ formation of hydrogels as vitreous substitutes: Viscoelastic comparison to porcine vitreous. *Journal of biomedical materials research. Part A*. 87 (3), 656–665. doi:10.1002/jbm.a.31769.

Swindle, K.E. & Ravi, N. (2007) Recent advances in polymeric vitreous substitutes. *Expert Review of Ophthalmology*. 2 (2), 255–265. doi:10.1586/17469899.2.2.255.

Swindle-Reilly, K.E., Shah, M., Hamilton, P.D., Eskin, T.A., Kaushal, S. & Ravi, N. (2009) Rabbit Study of an In Situ Forming Hydrogel Vitreous Substitute. *Investigative Opthalmology & Visual Science*. 50 (10), 4840. doi:10.1167/iovs.08-2891.

Tang, Q., Luo, C., Lu, B., Fu, Q., Yin, H., Qin, Z., Lyu, D., Zhang, L., Fang, Z., Zhu, Y. & Yao, K. (2017) Thermosensitive chitosan-based hydrogels releasing stromal cell derived factor-1 alpha recruit MSC for corneal epithelium regeneration. *Acta Biomaterialia*. 61, 101–113. doi:10.1016/j.actbio.2017.08.001.

Tao, Y., Tong, X., Zhang, Y., Lai, J., Huang, Y., Jiang, Y.-R. & Guo, B.-H. (2013) Evaluation of an in situ chemically crosslinked hydrogel as a long-term vitreous substitute material. *Acta Biomaterialia*. 9 (2), 5022–5030. doi:10.1016/j.actbio.2012.09.026.

Thompson, J.T. (1992) The absorption of mixtures of air and perfluoropropane after pars plana vitrectomy. *Archives of ophthalmology (Chicago, Ill.: 1960)*. 110 (11), 1594–1597. doi:10.1001/archopht.1992.01080230094028.

Tong, X., Pan, W., Su, T., Zhang, M., Dong, W. & Qi, X. (2020) Recent advances in natural polymer-based drug delivery systems. *Reactive and Functional Polymers*. 148 (January), 104501. doi:10.1016/j.reactfunctpolym.2020.104501.

Tram, N.K., Jiang, P., Torres-Flores, T.C., Jacobs, K.M., Chandler, H.L. & Swindle-Reilly, K.E. (2020) A Hydrogel Vitreous Substitute that Releases Antioxidant. *Macromolecular Bioscience*. 20 (2), 1900305. doi:10.1002/mabi.201900305.

Tram, N.K. & Swindle-Reilly, K.E. (2018) Rheological properties and age-related changes of the human vitreous humor. *Frontiers in Bioengineering and Biotechnology*. 6 (DEC), 1–12. doi:10.3389/fbioe.2018.00199.

Tylkowski, B., Wieszczycka, K., Jastrzab, R., Nogalska, A., Trojanowska, A., et al. (2017) *Polymer Engineering*. Berlin, Boston, De Gruyter. doi:10.1515/9783110469745.

Uesugi, K., Sakaguchi, H., Hayashida, Y., Hayashi, R., Baba, K., Suganuma, Y., Yokoi, H., Tsujikawa, M. & Nishida, K. (2017) A Self-Assembling Peptide Gel as a Vitreous Substitute: A Rabbit Study. *Investigative Opthalmology & Visual Science*. 58 (10), 4068. doi:10.1167/iovs.17-21536.

Vacanti, C. (2006) The history of tissue engineering. *Journal of Cellular and Molecular Medicine*. 1 (3), 569–576. doi:10.2755/jcmm010.003.20.

Vijayasekaran, S., Chirila, T. v, Hong, Y., Tahija, S.G., Dalton, P.D., Constable, I.J. & McAllister, I.L. (1996) Poly(1-vinyl-2-pyrrolidinone) hydrogels as vitreous substitutes: histopathological evaluation in the animal eye. *Journal of biomaterials science. Polymer edition*. 7 (8), 685–696. doi:10.1163/156856296x00453.

Villain, M.-A. (2005) [The epidemiology of glaucoma]. *Journal francais d'ophtalmologie*. 28 Spec No 2, 2S9-2S12. http://www.ncbi.nlm.nih.gov/pubmed/16208234.

Wang, H., Wu, Y., Cui, C., Yang, J. & Liu, W. (2018) Antifouling Super Water Absorbent Supramolecular Polymer Hydrogel as an Artificial Vitreous Body. *Advanced Science*. 5 (11), 1800711. doi:10.1002/advs.201800711.

Wang, P., Gao, Q., Jiang, Z., Lin, J., Liu, Y., Chen, J., Zhou, L., Li, H., Yang, Q. & Wang, T. (2012) Biocompatibility and retinal support of a foldable capsular vitreous body injected with saline or silicone oil implanted in rabbit eyes. *Clinical & Experimental Ophthalmology*. 40 (1), e67–e75. doi:10.1111/j.1442-9071.2011.02664.x.

Wetterqvist, C., Wong, D., Williams, R., Stappler, T., Herbert, E. & Freeburn, S. (2004) Tamponade efficiency of perfluorohexyloctane and silicone oil solutions in a model

eye chamber. *The British journal of ophthalmology*. 88 (5), 692–696. doi:10.1136/bjo.2003.024737.

Wilson, C.A., Berkowitz, B.A. & Srebro, R. (1995) Perfluorinated organic liquid as an intraocular oxygen reservoir for the ischemic retina. *Investigative ophthalmology & visual science*. 36 (1), 131–141. http://www.ncbi.nlm.nih.gov/pubmed/7822140.

World Health Organisation (2019) *Blindness and vision impairment*. 2019. World Health Organisation. https://www.who.int/en/news-room/fact-sheets/detail/blindness-and-visual-impairment [Accessed: 12 February 2020].

Xie, A. & Lei, J. (2013) Pars Plana Vitrectomy and Silicone Oil Tamponade as a Primary Treatment for Retinal Detachment Caused by Macular Holes in Highly Myopic Eyes: A Risk-Factor Analysis. *Current Eye Research*. 38 (1), 108–113. doi:10.3109/02713683.2012.722742.

Xue, K., Liu, Z., Jiang, L., Kai, D., Li, Z., Su, X. & Loh, X.J. (2020) A new highly transparent injectable PHA-based thermogelling vitreous substitute. *Biomaterials Science*. 8 (3), 926–936. doi:10.1039/C9BM01603A.

Xue, K., Zhao, X., Zhang, Z., Qiu, B., Tan, Q.S.W., Ong, K.H., Liu, Z., Parikh, B.H., Barathi, V.A., Yu, W., Wang, X., Lingam, G., Hunziker, W., Su, X. & Loh, X.J. (2019) Sustained delivery of anti-VEGFs from thermogel depots inhibits angiogenesis without the need for multiple injections. *Biomaterials science*. 7 (11), 4603–4614. doi:10.1039/c9bm01049a.

Yamauchi, A. (1991) Synthetic Vitreous Body of PVA Hydrogel. In: *Polymer Gels*. Boston, MA, Springer US. pp. 127–134. doi:10.1007/978-1-4684-5892-3_8.

Yang, H., Wang, R., Gu, Q. & Zhang, X. (2008) Feasibility study of chitosan as intravitreous tamponade material. *Graefe's Archive for Clinical and Experimental Ophthalmology*. 246 (8), 1097–1105. doi:10.1007/s00417-008-0813-8.

Yu, Q., Liu, K., Su, L., Xia, X. & Xu, X. (2014) Perfluorocarbon Liquid: Its Application in Vitreoretinal Surgery and Related Ocular Inflammation. *BioMed Research International*. 2014, 1–6. doi:10.1155/2014/250323.

Zarrintaj, P., Saeb, M.R., Jafari, S.H. & Mozafari, M. (2020) Application of compatibilized polymer blends in biomedical fields. In: *Compatibilization of Polymer Blends*. Elsevier. pp. 511–537. doi:10.1016/B978-0-12-816006-0.00018-9.

Zhang, Z., Peng, M., Wei, Y., Jiang, X. & Zhang, S. (2017) Pars plana vitrectomy with partial tamponade of filtered air in Rhegmatogenous retinal detachment caused by superior retinal breaks. *BMC Ophthalmology*. 17 (1), 64. doi:10.1186/s12886-017-0459-6.

Zheng, H., Wang, Z., Wang, P., Liu, Y., Jiang, Z. & Gao, Q. (2012) Evaluation of 5-fluorouracil released from a foldable capsular vitreous body in vitro and in vivo. *Graefe's Archive for Clinical and Experimental Ophthalmology*. 250 (5), 751–759. doi:10.1007/s00417-011-1862-y.

3.1. Introduction

The ideal choice of material for any tissue engineering application is essential as it will integrate with native tissue and will form the basis of native tissue regeneration (Da Silva *et al.*, 2020). The vitreous is described as being a fragile and transparent gel, between the lens and retina of the eye (Nickerson *et al.*, 2008; Tram and Swindle-Reilly, 2018; Yadav *et al.*, 2021). It is reported that the vitreous is predominantly composed of water with collagen fibrils and hyaluronic acid (Sebag, 2002; Kleinberg *et al.*, 2011). As the vitreous liquefies with age, various diseases such as retinal tears and detachment, macular hole formation, and cataracts occur (Sebag, 2018; Ankamah *et al.*, 2020), rendering it essential that a vitreous substitute formed with the appropriate materials is used.

In recent years polymer-based hydrogels have been increasingly studied for tissue substitution and regeneration. As discussed in Chapter 2, natural polymer-based hydrogels have limitations such as poor mechanical strength and fast degradation (Kleinberg *et al.*, 2011), while synthetic polymers are limited by low biocompatibility and poor cell-binding ability (Donati *et al.*, 2014). Composite polymer blends of natural and synthetic polymers have thus been used to overcome these limitations. Any polymer used to create a hydrogel for vitreous substitution must satisfy the requirements discussed in Table 3.1.

Table 3.1 - Summary of the requirements for the design of a vitreous substitute (Kleinberg *et al.*, 2011; Tram *et al.*, 2020).

Hydrogel requirements	Vitreous substitute requirements
Viscous	Transparent
Shear thinning behaviour	Biodegradable
Undergoes yield stress	Biocompatible
Quick gelation	Permeable to oxygen, metabolite, and nutrient transport
Injectability	
Post-injection stability and flow	Shape integrity of the eye

Polymer-based hydrogels are a promising strategy for vitreous substitution as hydrogels have the ability to absorb water without dissolving and they can be manipulated to fit biological specifications (Cooper and Yang, 2019; Mondal *et al*.,

2020). Swelling of the hydrogel creates a soft polymer gel ideal for soft tissue engineering as is the case with the vitreous. Furthermore, once the hydrogel has reached swelling equilibrium, further expansion of the hydrogel does not occur (Wang *et al.*, 2021). This is important for vitreous substitution so that the hydrogel does not cause damage to surrounding ocular tissue.

In situ-forming hydrogels are hydrogels that change phase in response to an external stimulus (Al-Tahami and Singh, 2007; Almeida *et al*., 2012). This phase change from liquid to semi-solid or solid is advantageous for injectable systems. The stimuli responsible for the phase change can be temperature (thermo-responsive), light (photo-responsive), pH, or enzymes (Almeida *et al*., 2012; Mahlumba *et al.*, 2016; Lu *et al.*, 2019). Thermo-responsive *in situ*-forming hydrogels are ideal for vitreous substitution.

The present study set out to design a polymeric, thermo-responsive *in situ*-forming hydrogel vitreous substitute using the criteria discussed in Table 3.1 with consideration to the hydrogel properties described above and rheological properties of the human vitreous. It is proposed that the properties of the chosen polymers along with the properties of the hydrogel formed will provide for a vitreous substitute that is similar to the native vitreous discussed in Chapter 2. This work involved the preparation of polymeric hydrogels through the blending of the natural polymer and native vitreous glycosaminoglycan, hyaluronic acid (de Smet *et al.,* 2013; Silva *et al.,* 2017) with synthetic polymers shown to exhibit good thermo-responsive properties, namely, poly(N-isopropylacrylamide) (pNIPAAm) and Poloxamers.

3.2. Potential polymers for hydrogel vitreous substitute

3.2.1. poly(N-isopropylacrylamide) (pNIPAAm)

Poly(N-isopropylacrylamide) (pNIPAAm) based polymers have been used for many tissues. Poly(N-isopropylacrylamide) is a thermo-responsive polymer that exhibits solution-to-gel phase changes at around 32 °C (Lehmann *et al.*, 2019; L. Wang *et al.*, 2021). To improve the temperature at which pNIPAAm hydrogels form a gel they have been copolymerised with hydrophilic monomers (Son and Lee, 2016). Poly(ethylene glycol) (PEG) based polymers, specifically poly(ethylene glycol) diacrylate (PEGDA),

have been used in scaffolds to mimic the ECM for many tissues. Despite being a synthetic polymer, PEGDA is non-toxic, biodegradable, and biocompatible. Studies by Zellander *et al.* (2014), McAvoy *et al*. (2018), and Tram *et al.* (2020) have shown the biocompatibility of PEGDA with ocular tissue. Poly(ethylene glycol) diacrylate with a MW of 700 Da was chosen due to its water solubility while PEGDA with a molecular weight of 575 Da was selected as it has shown to have good thermoresponsive properties. In this study, pNIPAAm was co-polymerised with PEGDA to overcome the brittleness observed with PEGDA hydrogels (Frost *et al.*, 2019) and to improve the thermo-gelling properties of pNIPAAm.

3.2.2. Poloxamers

Poloxamers, also known by their trademark name, Pluronics®, are widely used synthetic polymers in the preparation of hydrogels. Poloxamers are triblock copolymers, poly(ethylene oxide)-*b*-poly(propyleneoxide)-*b*-poly(ethylene oxide) (PEO-PPO-PEO), that undergo a reversible sol-gel transition in response to changes in temperature (Moon *et al.*, 2012; Ow and Loh, 2022). Features of poloxamers that make them a popular choice for the design of hydrogels are their thermo-gelling properties, solubilising capacity, and low toxicity (Shastri *et al*., 2010; Almeida *et al.*, 2013). Poloxamers also have good compatibility with other polymers and biomolecules (Almeida *et al.*, 2014; Fakhari *et al.*, 2017) rendering them an ideal polymer choice for this study. A variety of poloxamers with differing molecular weights of the PEO and PPO blocks are available (Alexandridis and Alan Hatton, 1995; Singh-Joy and McLain, 2008). Variations between the molecular weights of the PEO and PPO blocks create differences in the hydrophobic-hydrophilic ratio (Gioffredi *et al.*, 2016). This allows for the development of poloxamer hydrogels with their unique properties in terms of their gelation concentration and gelation time. Common poloxamers and their properties are shown in Table 3.2 (Jeong *et al*., 2012; Almeida *et al.*, 2018). Of these poloxamers, P188, P237, P338 and P407 are freely soluble in water (Russo and Villa, 2019). The poloxamers, P407 and P188 are commonly used in ophthalmic administration because of their good water solubility and clarity when in solution, optimal viscosity and good biocompatibility with ocular tissues (Qi *et al.*, 2007; Al Khateb *et al.*, 2016; Fathalla *et al.*, 2017). Therefore, P188 and P407 were chosen for this study.

Table 3.2 - Properties of common poloxamers (Jeong *et al*., 2012; Almeida *et al.*, 2018).

Poloxamer	Average Molecular Weight	PEO (%$^{w}/_{v}$)	Viscosity (Pa.s)	Melting Point (°C)	Surface tension (dyn cm^{-1})	Hydrophilic-Lipophilic balance (HLB)
P108	4700	80	0.26	48	52	>24
P122	1630	20	0.28	-26	46	7-12
P185	3400	50	0.18	27	46	12-18
P188	8400	80	1.00	52	50	>24
P237	7700	70	0.70	49	44	>24
P238	11 400	80	2.30	54	48	>24
P335	6500	50	0.75	35	39	12-18
P338	14 600	80	2.80	57	41	>24
P403	5750	30	0.35	31	34	7-12
P407	12 600	70	3.10	56	41	18-23

3.3. Design approach for hydrogel development

In this study, a known synthetic polymer – pNIPAAm, P188 or P407 – was blended with the natural polysaccharide Hyaluronic acid (HA) to create a composite hydrogel (composed of a blend of a synthetic and natural polymer). Hyaluronic acid was chosen as it is a component of the human vitreous. As highlighted in Chapter 2, HA is limited by its short degradation time. To overcome this, HA was blended with pNIPAAm and P407 in an attempt to improve the degradation time of HA. A hydrogel would be considered to be a successful candidate if it has a sol-gel transition temperature greater than 30 °C while remaining transparent as a solution and a gel.

3.4. Materials and Methods

3.4.1. Materials

All chemicals were used as received from Sigma Aldrich (St Louis, MI, USA) and were of analytical grade. These chemicals were Poly(ethylene glycol) diacrylate MW 575 (PEGDA 575), Poly(ethylene glycol) diacrylate MW 700 (PEGDA 700), N-isopropylacrylamide (NIPAAm), ammonium persulfate (APS), N,N.N',N' tetramethyl ethylenediamine (TEMED), cellulose dialysis tubing (MW cut-off 14 000 Da), Poloxamer 407 (P407), Poloxamer 188 (P188), and hyaluronic acid sodium salt (from *Streptococcus equi*).

3.4.2. Evaluation of composite polymer blends

All composite polymer blends were formulated and assessed for their transparency before and after gelation, and their ability to gel via the vial inversion test. For the inversion test, 4 mL of all prepared formulations were placed in 10 mL glass vials. These were then immersed in a water bath where the temperature was increased from 10 °C to 50 °C. The temperature and the time for the sol-gel phase change were visualised by the inversion of the vial. The time and temperature at which no flow of the sample was observed were considered to be indicative of the formation of the gel.

3.4.2.1. pNIPAAm and HA composite blend

NIPAAm (40 mg) and varying concentrations of HA (0.2%, 0.5%, 0.7% and 1% $^{w}/_{v}$) were dissolved in 1 mL of deionised water. Various concentrations, namely 1%, 5%, 10% and 20% $^{w}/_{v}$, PEGDA 575 and PEGDA 700 (individually and in conjunction) were added and gently mixed. APS (4 mg) and 20 µL TEMED (free radical crosslinking agents) were added to the solution and the solution was gently vortexed (Fisherbrand™ ZX3 Vortex Mixer, Fisher Scientific, Leicestershire, England). The mixture was then dialysed at 4 °C for 24 hours to allow for NIPAAm polymerisation and crosslinking to occur as well as to remove excess crosslinker.

3.4.2.2. Poloxamer and HA composite blend

Poloxamer-HA composite hydrogels were fabricated by adding various concentrations (0.2%, 0.5%, 0.7% and 1% $^{w}/_{v}$) HA in P188 and P407, either alone or in combination with one another at concentrations shown in Table 3.3. The cold method (stirring at 4 °C) was used to dissolve the poloxamers and HA until completely dissolved.

Table 3.3 - Concentrations of Poloxamer 407 and Poloxamer 188 evaluated in this study.

Concentration of P407 (% $^{w}/_{v}$)	Concentration of P188 (% $^{w}/_{v}$)
10	5
15	10
20	15
25	
30	

3.4.3. Statistical analysis

All analyses were conducted in triplicate (n = 3). All results were expressed as the mean and standard deviation and data was analysed using Microsoft EXCEL. The level of significance was determined using a student t-test. P values of less than 0.05 ($p < 0.05$) were considered as an indication of statistically significant differences. All graphs were plotted using SigmaPlot 12.0.

3.5. Results and Discussion

3.5.1. pNIPAAm and HA composite bend

3.5.1.1. pNIPAAM, PEGDA 575 and HA

As shown in Table 3.4, despite the various hyaluronic acid combinations tested with pNIPAAm and different concentrations of PEGDA 575, none of the resulting hydrogels were good candidates for vitreous substitution. At low concentrations of HA and PEGDA 575, the formulation did not change from its liquid consistency while formulations with higher concentrations formed a gel/solid. The gel formed with HA concentrations of 0.5%, 0.7% and 1% $^{w}/_{v}$ was a solid gel that could not be extruded via a needle, while the gel that formed with PEGDA 575 concentrations of 10% and 20% $^{w}/_{v}$ had a cloudy colour. A higher concentration of the crosslinking agents could not be used as that would lead to cytotoxicity. The colour change, from transparent to cloudy, of the gel can be attributed to leaching out of pNIPAAm (Egbu *et al.,* 2018).

Table 3.4 - Evaluation of pNIPAAm with PEGDA 575 as a potential composite polymer hydrogel.

Concentration of HA (% $^{w}/_{v}$)	**Concentration of PEGDA 575 (%$^{w}/_{v}$)**			
	1	**5**	**10**	**20**
0.2	Formulation remains a liquid at all temperature ranges studied (4 °C to 40 °C).		Formulation forms a gel at temperatures higher than 30 °C, and colour change when a gel is formed.	
0.5 **0.7** **1**	Formulation forms a cloudy gel immediately after the addition of APS and TEMED. Cooling the formulation at 4 °C did not change the viscosity of the gel.			

3.5.1.2. pNIPAAm, PEGDA 700 and HA

PEGDA 700 was selected as it displayed better water solubility than PEGDA 575 and the longer PEG chains in PEGDA 700 improve its viscosity (Zhao *et al.*, 2015). Table 3.5 depicts that as with PEGDA 575, at low concentrations of HA and PEGDA 700,

the formulation remains a liquid. It was observed that at higher concentrations of PEGDA 700 and HA, the hydrogel has sol-gel characteristics. However, the gel formation also results in a colour change that is not suitable for a vitreous substitute candidate.

Table 3.5 - Evaluation of pNIPAAm with PEGDA 700 as a potential composite polymer hydrogel.

Concentration of HA (%$^{w}/_{v}$)	**Concentration of PEGDA 700 (%$^{w}/_{v}$)**			
	1	**5**	**10**	**20**
0.2	Formulation remains a liquid at all temperature ranges studied (4 °C to 40 °C).	Formulation forms a gel at temperatures higher than 30 °C, and colour change when a gel is formed.		
0.5 **0.7** **1**	Formulation forms a gel immediately after the addition of APS and TEMED. Cooling the formulation at 4 °C changed the viscosity to a liquid. Thereafter, the liquid formed a gel when kept at room temperature (~22 °C). The formulation changed colour when a gel formed.			

3.5.1.3. pNIPAAm, PEGDA 575, PEGDA 700 and HA

Since PEGDA 575 and PEGDA 700 individually could not produce a suitable hydrogel with pNIPAAm, a mixture of the two PEGDA polymers was tested in an attempt to alter their chemistry. PEGDA 575 was maintained at a constant concentration of 10% $^{w}/_{v}$ while the HA and PEGDA 700 concentrations were varied. The results of this polymer blend, shown in Table 3.6, are similar to the results of PEGDA 700 alone. A slight increase in viscosity was observed at lower PEGDA 700 concentrations when blended with PEGDA 575 in comparison to PEGDA 700 alone. However, these viscosity changes are not enough for the hydrogel to be a successful candidate as a colour change was observed as viscosity increased.

Table 3.6 - Evaluation of pNIPAAm with PEGDA 575 and 700 as a potential composite polymer hydrogel.

Concentration of HA (% $^{w}/_{v}$)	**Concentration of PEGDA 700 (%$^{w}/_{v}$)**			
	1	**5**	**10**	**20**
0.2	Formulation forms a gel immediately after the addition of APS and TEMED. Cooling the formulation at 4 °C changed the viscosity to a liquid. Thereafter, the liquid showed a slight increase in viscosity with colour change.		Formulation forms a gel immediately after the addition of APS and TEMED. Cooling the formulation at 4 °C changed the viscosity to a liquid. Thereafter, the liquid formed a gel when kept at room temperature (~22 °C). The formulation changed colour when a gel formed.	
0.5 **0.7** **1**	Formulation forms a gel immediately after the addition of APS and TEMED. Cooling the formulation at 4 °C changed the viscosity to a liquid. Thereafter, the			

	liquid formed a gel when kept at room temperature (~22 °C). The formulation changed colour when a gel formed.
	10% $^{w}/_{v}$ Concentration of PEGDA 575

3.5.2. Poloxamer and HA blend

P188 and HA formulations at varying concentrations as shown in Table 3.7 were first investigated. However, at all concentrations and with varying temperatures, the formulations remained liquid. Thereafter, as depicted in Table 3.7, various P407 concentrations were studied with changing HA concentrations. At low concentrations of P407, the formulation did not change in viscosity despite high HA concentrations, while low HA concentrations with high P407 concentrations also remained liquid. Slight viscosity increases were observed when the concentrations of HA and P407 were increased, yielding liquid-like gels that were further studied as shown in Table 3.8.

Table 3.7 - Evaluation of Poloxamer 188 and Poloxamer 407 as potential composite polymer hydrogels individually.

Concentration of HA **(%$^{w}/_{v}$)**	Concentration of P188 **(%$^{w}/_{v}$)**			Concentration of P407 **(%$^{w}/_{v}$)**				
	5%	**10%**	**15%**	**10%**	**15%**	**20%**	**25%**	**30%**
0.2	The formulation remains a liquid at all temperature ranges studied (4 °C to 40 °C).							
0.5	The formulation remains a liquid at all temperature ranges studied (4 °C to 40 °C).						Formulation starts to increase in viscosity above ~30 °C.	
0.7								
1								

Following studies of HA with P407 and P188 individually, P407 at concentrations of 25% and 30% $^{w}/_{v}$ were mixed with varying concentrations of P188 and HA as depicted in Table 3.8Table 3.8. Low P188 concentrations resulted in liquid formulations at varying temperatures as seen when P188 was not mixed with P407. However, P188 concentrations of 10% and 15% $^{w}/_{v}$ with all HA concentrations and both P407 concentrations, showed formulations that increased in viscosity when the temperature was increased. These liquid-like and solid gels were transparent and showed thermo-responsive properties. Ideal results were seen when HA was at a concentration of 0.5% $^{w}/_{v}$, P407 had a concentration of 25% $^{w}/_{v}$ and P188 concentrations were at 10% and 15% $^{w}/_{v}$ (depicted in green in Table 3.8Table 3.8). These two formulations formed gels at temperatures within a physiological range and were transparent. Therefore,

these two formulations were tested further to identify the preferred system for nanoparticle loading.

Table 3.8 - Evaluation of 30% $^{w}/_{v}$ Poloxamer 407 and 25% $^{w}/_{v}$ Poloxamer 407 with Poloxamer 188 as a potential composite polymer hydrogel.

Concentration of HA (% $^{w}/_{v}$)	**Concentration of P188 (% $^{w}/_{v}$)**			**Concentration of P188 (% $^{w}/_{v}$)**		
	5	**10**	**15**	**5**	**10**	**15**
0.5	The formulation remains a liquid at all temperature ranges studied (4 °C to 40 °C)	The formulation begins to form a gel from ~20 °C.		The formulation remains a liquid at all temperature ranges studied (4 °C to 40 °C).	The formulation begins to form a gel from ~30 °C.	
0.7					The formulation begins to form a gel from ~20 °C.	
1						
	30% $^{w}/_{v}$			**25% $^{w}/_{v}$**		
	Concentration of P407			**Concentration of P407**		

3.6. Poloxamer and HA composite blend optimisation

The successful P407-P188-HA composite polymer blends (P1 and P2 shown in Table 3.9Table 3.9) obtained in the pre-formulation stage underwent further studies to compare them to the natural vitreous. These were undertaken to obtain the index of refraction, light transmittance, gelling time, and colour post-injection via a small gauge needle.

Table 3.9 - Individual polymer concentrations in each composite hydrogel.

Polymer	**P1 (% $^{w}/_{v}$)**	**P2 (% $^{w}/_{v}$)**
HA	0.5	0.5
P407	25	25
P188	10	15

The refractive index of each hydrogel was determined using the Anton Paar refractometer (Anton Paar OptoTec GmbH, Germany). It was observed that each hydrogel formulation had a similar refractive index to the human vitreous (1.3349) (Santhanam *et al*., 2016; Tram *et al*., 2020). P1 had a refractive index of 1.3350 ±0.002 ($p < 0.05$) and the refractive index of P2 was 1.3336 ±0.004 ($p < 0.05$). The transparency of the hydrogels was determined using the Implen Nanophotometer (NP80, UV//Vis spectrophotometer, Munich, Germany). The transparency of both hydrogels within the visible spectrum was above 90% ($p < 0.05$) (shown in Figure 3.1) which is an acceptable transparency, with P1 more transparent than P2. As with the

human vitreous, the transmittance of both hydrogels dropped within the UV range (~230 nm). These optical properties of the hydrogels are considered to be due to the high water content of the hydrogels.

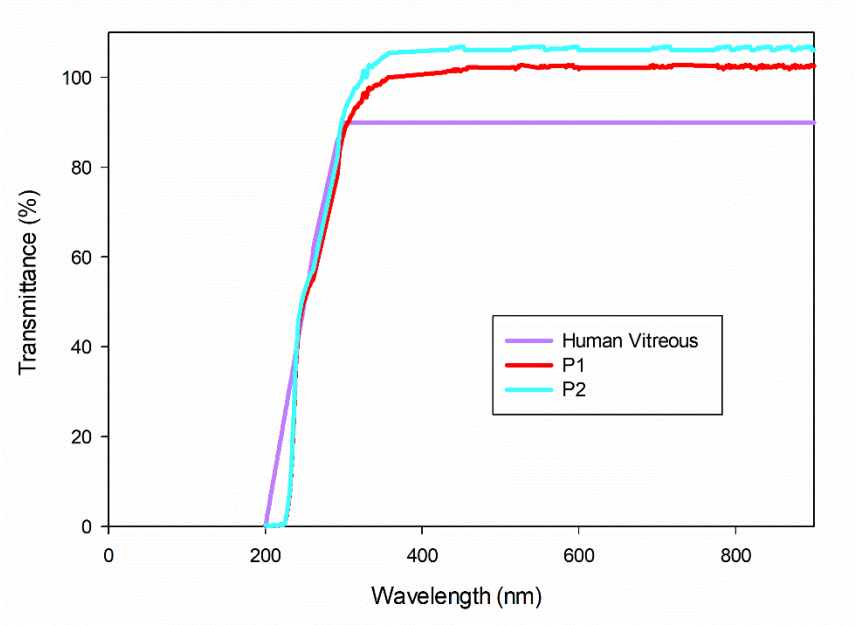

Figure 3.1 - Hydrogel transparency in comparison to the human vitreous.

P1 with a lower concentration of P188 had a faster gelling time of nine minutes, while P2 with a higher concentration of P188 had a gelling time of 16 minutes. These times were determined by placing 4 mL of the liquid hydrogel in a glass polytop (maintained for 2 hours at 4 °C) into an orbital Shaking Incubator (type LM-530-2, MRC Laboratory Instruments Ltd, Israel). Displayed in Figure 3.2Figure 3.2 are the hydrogels once the gel has formed. The formulations P1 and P2 were extruded into the glass polytops via a 26-gauge needle. Figure 3.2Figure 3.2 (A) shows the gel formed from formulation P1. The gel is transparent with no bubbles. Figure 3.2Figure 3.2 (B) shows that the gel formed by P2, although transparent, forms bubbles when injected via a needle due to poloxamer micelle formation as the total poloxamer concentration in P2 is higher than that in P1.

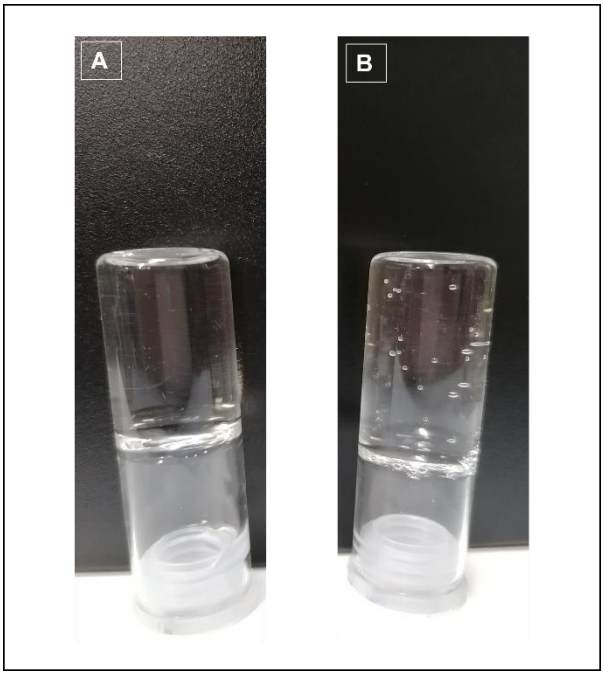

Figure 3.2 - Gel formation of each composite polymer blend. A) P1 B) P2.

These results indicate that P1, the hydrogel with a HA concentration of 0.5% $^{w}/_{v}$, a P407 concentration of 25% $^{w}/_{v}$ and a P188 concentration of 10% $^{w}/_{v}$, had favourable characteristics over P2 which had a higher P188 concentration. As such, P1 was selected for nanoparticle incorporation due to its thermo-responsive gel formation properties at physiological temperatures, its fast-gelling time, and its similarity to the human vitreous in its transparency and refractive index.

3.6. Conclusions

The development of an *in situ*-forming hydrogel as an ideal vitreous substitute presents many challenges. The choice of polymers for the fabrication of the hydrogel was based primarily on the thermo-responsiveness and transparency of the hydrogel that would form. In this chapter, various concentrations of two synthetic polymers (pNIPAAm and poloxamer) were tested with hyaluronic acid to form a composite polymer blend in an attempt to fabricate a transparent hydrogel that would function as a vitreous substitute.

PEGDA with a MW of 575 and 700 were tested at various concentrations with pNIPAAm, however, neither pNIPAAm-PEGDA copolymer exhibited favourable

hydrogel requirements. pNIPAAm formulations fabricated with both PEGDA 575 and PEGDA 700 at low concentrations did not form gels and when gels formed at higher concentrations, they were plagued by colour changes and gels that were unable to be extruded via a needle. Both these characteristics suggested that the pNIPAAm-PEGDA copolymer hydrogel would not form an ideal vitreous substitute and any further optimisation studies should be abandoned. It is likely, that with higher concentrations of the crosslinking agents (APS and TEMED), a successful hydrogel would form. However, the cytotoxicity of these agents at high concentrations would render the fabricated hydrogel toxic and incompatible with the sensitive ocular tissue.

A suitable candidate for further optimisation was ascertained with the poloxamer-based composite blend. An *in situ*-forming hydrogel fabricated from a blend of hyaluronic acid with a concentration of 0.5% $^{w}/_{v}$ and two poloxamers (poloxamer 407 and poloxamer 188 with concentrations of 25% and 10% $^{w}/_{v}$, respectively) proved to exhibit optical properties similar to the native human vitreous.

Since an ideal vitreous substitute is required to be a viscoelastic solid, transparent and have a refractive index similar to the natural vitreous, this initial pre-formulation study was necessary. Despite showing similar optical properties to the natural vitreous, further characterisation is needed to consider this composite polymer blend as an ideal vitreous substitute. These characterisations, followed by nanoparticle and drug loading are discussed in Chapter 4.

3.7. References

Alexandridis, P. & Alan Hatton, T. (1995) Poly(ethylene oxide)-poly(propylene oxide)-poly(ethylene oxide) block copolymer surfactants in aqueous solutions and at interfaces: thermodynamics, structure, dynamics, and modeling. *Colloids and Surfaces A: Physicochemical and Engineering Aspects*. 96 (1–2), 1–46. doi:10.1016/0927-7757(94)03028-X.

Almeida, H., Amaral, M.H. & Lobão, P. (2012) Temperature and pH stimuli-responsive polymers and their applications in controlled and self-regulated drug delivery. *Journal of Applied Pharmaceutical Science*. 2 (6), 01–10. doi:10.7324/JAPS.2012.2609.

Almeida, H., Amaral, M.H., Lobão, P. & Lobo, J.M.S. (2013) Applications of poloxamers in ophthalmic pharmaceutical formulations: an overview. *Expert Opinion on Drug Delivery*. 10 (9), 1223–1237. doi:10.1517/17425247.2013.796360.

Almeida, H., Amaral, M.H., Lobão, P. & Lobo, J.M.S. (2014) In situ gelling systems: a strategy to improve the bioavailability of ophthalmic pharmaceutical formulations. *Drug Discovery Today*. 19 (4), 400–412. doi:10.1016/j.drudis.2013.10.001.

Almeida, M., Magalhães, M., Veiga, F. & Figueiras, A. (2018) Poloxamers, poloxamines and polymeric micelles: Definition, structure and therapeutic applications in cancer. *Journal of Polymer Research*. 25 (1), 31. doi:10.1007/s10965-017-1426-x.

Al Khateb, K., Ozhmukhametova, E.K., Mussin, M.N., Seilkhanov, S.K., Rakhypbekov, T.K., Lau, W.M. & Khutoryanskiy, V. v. (2016) In situ gelling systems based on Pluronic F127/Pluronic F68 formulations for ocular drug delivery. *International Journal of Pharmaceutics*. 502 (1–2), 70–79. doi:10.1016/j.ijpharm.2016.02.027.

Al-Tahami, K. & Singh, J. (2007) Smart Polymer Based Delivery Systems for Peptides and Proteins. *Recent Patents on Drug Delivery & Formulation*. 1 (1), 65–71. doi:10.2174/187221107779814113.

Ankamah, E., Sebag, J., Ng, E. & Nolan, J.M. (2020) Vitreous antioxidants, degeneration, and vitreo-retinopathy: Exploring the links. *Antioxidants*.9 (1) p.7. doi:10.3390/antiox9010007.

Cooper, R.C. & Yang, H. (2019) Hydrogel-based ocular drug delivery systems: Emerging fabrication strategies, applications, and bench-to-bedside manufacturing considerations. *Journal of Controlled Release*. 306 (May), 29–39. doi:10.1016/j.jconrel.2019.05.034.

Da Silva, K., Kumar, P., Choonara, Y.E., du Toit, L.C. & Pillay, V. (2020) Three-dimensional printing of extracellular matrix (ECM)-mimicking scaffolds: A critical review of the current ECM materials. *Journal of biomedical materials research. Part A*. 108 (12), 2324–2350. doi:10.1002/jbm.a.36981.

de Smet, M.D., Gad Elkareem, A.M. & Zwinderman, A.H. (2013) The Vitreous, the Retinal Interface in Ocular Health and Disease. *Ophthalmologica*. 230 (4), 165–178. doi:10.1159/000353447.

Donati, S., Caprani, S.M., Airaghi, G., Vinciguerra, R., Bartalena, L., Testa, F., Mariotti, C., Porta, G., Simonelli, F. & Azzolini, C. (2014) Vitreous Substitutes: The Present and the Future. *BioMed Research International*. 2014 (May), 1–12. doi:10.1155/2014/351804.

Egbu, R., Brocchini, S., Khaw, P.T. & Awwad, S. (2018) Antibody loaded collapsible hyaluronic acid hydrogels for intraocular delivery. *European Journal of Pharmaceutics and Biopharmaceutics*. 124, 95–103. doi:10.1016/j.ejpb.2017.12.019.

Fathalla, Z.M.A., Vangala, A., Longman, M., Khaled, K.A., Hussein, A.K., El-Garhy, O.H. & Alany, R.G. (2017) Poloxamer-based thermoresponsive ketorolac tromethamine in situ gel preparations: Design, characterisation, toxicity and transcorneal permeation studies. *European Journal of Pharmaceutics and Biopharmaceutics*. 114, 119–134. doi:10.1016/j.ejpb.2017.01.008.

Fakhari, A., Corcoran, M. & Schwarz, A. (2017) Thermogelling properties of purified poloxamer 407. *Heliyon*. 3 (8), e00390. doi:10.1016/j.heliyon.2017.e00390.

Frost, B.A., Sutliff, B.P., Thayer, P., Bortner, M.J. & Foster, E.J. (2019) Gradient Poly(ethylene glycol) Diacrylate and Cellulose Nanocrystals Tissue Engineering Composite Scaffolds via Extrusion Bioprinting. *Frontiers in Bioengineering and Biotechnology*. 7. doi:10.3389/fbioe.2019.00280.

Gioffredi, E., Boffito, M., Calzone, S., Giannitelli, S.M., Rainer, A., Trombetta, M., Mozetic, P. & Chiono, V. (2016) Pluronic F127 Hydrogel Characterization and Biofabrication in Cellularized Constructs for Tissue Engineering Applications. *Procedia CIRP*. 49, 125–132. doi:10.1016/j.procir.2015.11.001.

Jeong, B., Kim, S.W. & Bae, Y.H. (2012) Thermosensitive sol–gel reversible hydrogels. *Advanced Drug Delivery Reviews*. 64 (SUPPL.), 154–162. doi:10.1016/j.addr.2012.09.012.

Kleinberg, T.T., Tzekov, R.T., Stein, L., Ravi, N. & Kaushal, S. (2011) Vitreous Substitutes: A Comprehensive Review. *Survey of Ophthalmology*. 56 (4), 300–323. doi:10.1016/j.survophthal.2010.09.001.

Lehmann, M., Krause, P., Miruchna, V. & von Klitzing, R. (2019) Tailoring PNIPAM hydrogels for large temperature-triggered changes in mechanical properties. *Colloid and Polymer Science*. 297 (4), 633–640. doi:10.1007/s00396-019-04470-0.

Lu, J., Zhu, W., Dai, L., Si, C. & Ni, Y. (2019) Fabrication of thermo- and pH-sensitive cellulose nanofibrils-reinforced hydrogel with biomass nanoparticles. *Carbohydrate Polymers*. 215 (29), 289–295. doi:10.1016/j.carbpol.2019.03.100.

Mahlumba, P., Choonara, Y.E., Kumar, P., du Toit, L.C. & Pillay, V. (2016) Stimuli-Responsive Polymeric Systems for Controlled Protein and Peptide Delivery: Future Implications for Ocular Delivery. *Molecules (Basel, Switzerland)*. 21 (8). doi:10.3390/molecules21081002.

McAvoy, K., Jones, D. & Thakur, R.R.S. (2018) Synthesis and Characterisation of Photocrosslinked poly(ethylene glycol) diacrylate Implants for Sustained Ocular Drug Delivery. *Pharmaceutical research*. 35 (2), 36. doi:10.1007/s11095-017-2298-9.

Mondal, S., Das, S. & Nandi, A.K. (2020) A review on recent advances in polymer and peptide hydrogels. *Soft Matter*. 16 (6), 1404–1454. doi:10.1039/C9SM02127B.

Moon, H.J., Ko, D.Y., Park, M.H., Joo, M.K. & Jeong, B. (2012) Temperature-responsive compounds as in situ gelling biomedical materials. *Chemical Society Reviews*. 41 (14), 4860. doi:10.1039/c2cs35078e.

Nickerson, C.S., Park, J., Kornfield, J.A. & Karageozian, H. (2008) Rheological properties of the vitreous and the role of hyaluronic acid. *Journal of biomechanics*. 41 (9), 1840–1846. doi:10.1016/j.jbiomech.2008.04.015.

Ow, V. & Loh, X.J. (2022) Recent developments of temperature-responsive polymers for ophthalmic applications. *Journal of Polymer Science*. 60 (9), 1429–1447. doi:10.1002/pol.20210907.

Qi, H., Chen, W., Huang, C., Li, L., Chen, C., Li, W. & Wu, C. (2007) Development of a poloxamer analogs/carbopol-based in situ gelling and mucoadhesive ophthalmic

delivery system for puerarin. *International Journal of Pharmaceutics*. 337 (1–2), 178–187. doi:10.1016/j.ijpharm.2006.12.038.

Russo, E. & Villa, C. (2019) Poloxamer Hydrogels for Biomedical Applications. *Pharmaceutics*. 11 (12), 671. doi:10.3390/pharmaceutics11120671.

Santhanam, S., Liang, J., Struckhoff, J., Hamilton, P.D. & Ravi, N. (2016) Biomimetic hydrogel with tunable mechanical properties for vitreous substitutes. *Acta Biomaterialia*. 43, 327–337. doi:10.1016/j.actbio.2016.07.051.

Sebag, J. (2002) Imaging vitreous. *Eye*. 16 (4), 429–439. doi:10.1038/sj.eye.6700201.

Sebag, J. (2018) Posterior Vitreous Detachment. *Ophthalmology*. 125 (9), 1384–1385. doi:10.1016/j.ophtha.2018.05.018.

Shastri, D., Prajapati, S. & Patel, L. (2010) Thermoreversible mucoadhesive ophthalmic in situ hydrogel: Design and optimization using a combination of polymers. *Acta Pharmaceutica*. 60 (3). doi:10.2478/v10007-010-0029-4.

Silva, A.F., Alves, M.A. & Oliveira, M.S.N. (2017) Rheological behaviour of vitreous humour. *Rheologica Acta*. 56 (4), 377–386. doi:10.1007/s00397-017-0997-0.

Singh-Joy, S.D. & McLain, V.C. (2008) Safety Assessment of Poloxamers 101, 105, 108, 122, 123, 124, 181, 182, 183, 184, 185, 188, 212, 215, 217, 231, 234, 235, 237, 238, 282, 284, 288, 331, 333, 334, 335, 338, 401, 402, 403, and 407, Poloxamer 105 Benzoate, and Poloxamer 182 Dibenzoate as Used in Cosmetics. *International Journal of Toxicology*. 27 (2_suppl), 93–128. doi:10.1080/10915810802244595.

Son, K. & Lee, J. (2016) Synthesis and Characterization of Poly(Ethylene Glycol) Based Thermo-Responsive Hydrogels for Cell Sheet Engineering. *Materials*. 9 (10), 854. doi:10.3390/ma9100854.

Tram, N.K., Jiang, P., Torres-Flores, T.C., Jacobs, K.M., Chandler, H.L. & Swindle-Reilly, K.E. (2020) A Hydrogel Vitreous Substitute that Releases Antioxidant. *Macromolecular Bioscience*. 20 (2), 1900305. doi:10.1002/mabi.201900305.

Tram, N.K. & Swindle-Reilly, K.E. (2018) Rheological properties and age-related changes of the human vitreous humor. *Frontiers in Bioengineering and Biotechnology*. 6 (DEC), 1–12. doi:10.3389/fbioe.2018.00199.

Wang, L., Liu, F., Qian, J., Wu, Z. & Xiao, R. (2021a) Multi-responsive PNIPAM-PEGDA hydrogel composite. *Soft matter*. 17 (46), 10421–10427. doi:10.1039/d1sm01178b.

Wang, T., Ran, R., Ma, Y. & Zhang, M. (2021b) Polymeric hydrogel as a vitreous substitute: current research, challenges, and future directions. *Biomedical Materials*. 16 (4), 042012. doi:10.1088/1748-605X/ac058e.

Yadav, I., Purohit, S.D., Singh, H., Bhushan, S., Yadav, M.K., Velpandian, T., Chawla, R., Hazra, S. & Mishra, N.C. (2021) Vitreous substitutes: An overview of the properties, importance, and development. *Journal of Biomedical Materials Research - Part B Applied Biomaterials*.109 (8) pp.1156–1176. doi:10.1002/jbm.b.34778.

Zellander, A., Zhao, C., Kotecha, M., Gemeinhart, R., Wardlow, M., Abiade, J. & Cho, M. (2014) Characterization of Pore Structure in Biologically Functional Poly(2-Hydroxyethyl Methacrylate) - Poly(Ethylene Glycol) Diacrylate (PHEMA-PEGDA) A.J. Engler (ed.). *PLoS ONE*. 9 (5), e96709. doi:10.1371/journal.pone.0096709.

Zhao, T., Zhang, H., Zhou, D., Gao, Y., Dong, Y., Greiser, U., Tai, H. & Wang, W. (2015) Water soluble hyperbranched polymers from controlled radical homopolymerization of PEG diacrylate. *RSC Advances*. 5 (43), 33823–33830. doi:10.1039/C5RA01253H.

Chapter 4 - A thermo-responsive, nanoparticle-loaded hydrogel for vitreous substitution and posterior segment disease treatment

4.1. Introduction

The vitreous is a clear, gel substance that occupies the majority of the posterior segment of the eye (Kleinberg *et al.*, 2011; Yadav *et al.*, 2020). It is considered to be an avascular and hydrated extracellular gel matrix (*Chirila and Hong, 1998; Silva et al*., 2017). This gel matrix is composed mainly of water, collagen, and hyaluronic acid (HA) constituting a volume of 4 mL (Swindle and Ravi, 2007; Donati *et al.*, 2014). Type II collagen, a fibrous extracellular matrix (ECM) protein, has a rigid structure that forms a network with HA in the vitreous (Le Goff and Bishop, 2008; Mishra *et al.*, 2022). HA is a glycosaminoglycan (GAG) that stabilises the collagen, creating an osmotic pressure that creates the tamponade effect holding the retina in place (Nickerson *et al.*, 2005; Santhanam *et al.*, 2016). This network formed by collagen and HA is responsible for the behaviour of the vitreous as a viscoelastic solid allowing for the absorption of shocks and vibrations experienced by the eye, thereby protecting the surrounding intraocular tissues (Lee *et al*., 1992; Baino, 2011).

As discussed in Chapter 2, the current treatment for various vitreoretinal diseases is vitrectomy, whereby the damaged vitreous is removed and replaced by silicone oil. Other substitutes such as perfluorocarbon liquids and air are also used, however, silicone oil is the first choice for substitution. Adverse effects associated with silicone oil substitution such as cataracts and cytotoxicity have resulted in a need for a substitute that can mimic the natural vitreous.

Vitreous substitution with *in situ*-forming hydrogels has been extensively studied. These hydrogels have been studied with natural polymers, such as HA (Schnichels *et al.*, 2017; Januschowski *et al.*, 2019; Raia *et al.*, 2020), gellan gum (Suri and Banerjee, 2006) and chitosan (Yang *et al.*, 2008; Jiang *et al.*, 2018), and synthetic polymers such as methylcellulose (Fernandez-Vigo *et al.*, 1990; Katagiri *et al.*, 2005), polyacrylamide (Foster *et al.*, 2006; Davis *et al.,* 2017), polyvinyl alcohol (Maruoka *et al.*, 2006; Leone *et al.*, 2010; Lamponi *et al.*, 2012), and polyethylene glycol (Hayashi *et al.*, 2017; Liu *et al.*, 2019; Tram *et al.*, 2020). Advantages of *in situ*-forming hydrogels include the ability to tune the mechanical and optical characteristics to mimic those of the natural

vitreous, and the easy injectability of the substitute using current vitrectomy procedures.

The *in situ* hydrogels for vitreous substitution studied to date have predominantly focussed on native vitreous mimicry. They have mimicked the mechanical and optical properties of the natural vitreous and the study by Tram *et al.* (2020) has also studied a PEG-based hydrogel that releases an antioxidant. However, these studies have not considered the treatment of any underlying posterior segment ocular diseases, or the inflammation (endophthalmitis) caused by pars plana vitrectomy (Dave *et al.*, 2014; Cunha *et al.*, 2021) that was observed as a result of those studies.

Intravitreal drug treatment is the most direct method of drug delivery to treat posterior segment diseases. Despite advantages such as increased drug concentration and decreased systemic effects (Edelhauser *et al.*, 2010; Thrimawithana *et al.*, 2011), intravitreal injections have to be given frequently to maintain the therapeutic drug window (Huang and Chau, 2019; Meng *et al.*, 2019). This results in a higher risk of ocular inflammation and cataracts. Therefore, long-term drug delivery using nano-systems and hydrogel systems is being investigated. However, studies based on the intravitreal delivery of drugs using hydrogels have focused on systems that combine with the natural vitreous and are not vitreous substitutes (Awwad *et al.*, 2019; Sapino *et al.*, 2019; Luaces-Rodríguez *et al.*, 2020). Therefore, the objective of this study was to fabricate a hydrogel with a dual purpose. The first is to function as a vitreous substitute and the second is to treat posterior segment diseases by acting as a drug reservoir with drug-loaded nanoparticles resulting in sustained drug release, thereby eliminating the need for frequent injections.

HA, a major component of the natural vitreous, is a linear polysaccharide that is composed of repeating disaccharide units (D-glucaronic acid and N-acetyl-D-glucosamine) that are linked via β-glycosidic bonds (Necas *et al.*, 2008; Zhang *et al.*, 2021). As it is an endogenous substance in the eye, HA and HA-based hydrogels have been widely studied for ocular administrations (Lajavardi *et al.*, 2009; Yu *et al.*, 2015; Tang *et al.*, 2019). HA-based hydrogels for vitreous substitution have been studied using non-modified and modified HA. The integration of HA into hydrogel systems via physical mixing can avoid cytotoxic effects that may occur due to crosslinkers in

modified-HA hydrogels (Schramm *et al.*, 2012; Zhang *et al.*, 2021). The mixing of HA with synthetic polymers that exhibit thermo-responsive properties can allow for HA-based *in situ*-forming hydrogels.

As discussed in the previous chapter, poloxamers are synthetic triblock copolymers composed of polyethylene oxide (PEO) and polypropylene oxide (PPO) (Gioffredi *et al.*, 2016; Russo and Villa, 2019). Poloxamers are available in a variety of molecular weights that modify their gelation behaviour (Alexandridis and Alan Hatton, 1995; Singh-Joy and McLain, 2008). Poloxamers undergo sol-gel phase transitions due to the formation of micelles as a result of the organisation of monomers into ordered structures as the temperature of the poloxamer solution increases (Dumortier *et al.*, 2006; Hsieh *et al.*, 2020). Poloxamers display a reversible thermo-responsive behaviour, whereby a sol-gel phase transition occurs around physiological temperature (~37 °C) and a reverse gel-sol phase transition occurs around 50 °C (Alexandridis and Alan Hatton, 1995; Almeida *et al.*, 2018).

Vitreous substitutes composed of poloxamers have been studied. These studies were conducted only with P407 and required large concentrations of P407 resulting in the occurrence of ocular toxicity (Davidorf *et al.*, 1990; Hwang *et al.*, 2013; Lin *et al*., 2013). Poloxamer-based hydrogels for ophthalmic administration with a combination of P407 and P188 were formulated and found to be non-toxic and non-irritating (Al Khateb *et al.*, 2016; Fathalla *et al.*, 2017). This is likely because the addition of P188 will require a lower concentration of P407 reducing the ocular toxicity of P407 (Kim *et al.*, 2002; Qi *et al.*, 2007; Almeida *et al.*, 2014).

Polymeric nanoparticles have been used for drug delivery for a considerable time as they are relatively easy to prepare, they can efficiently incorporate a variety of drugs and bioactive compounds within them and provide a controlled release of those substances (Manzoor *et al.*, 2012; Senapati *et al.*, 2018). Poly(DL-lactic-co-glycolic) acid (PLGA) is a biodegradable and biocompatible, FDA-approved polymer that has displayed great potential in drug delivery (Danhier *et al.*, 2012; Essa *et al.*, 2020) and it has been used to deliver many ocular therapeutic agents (Abrego *et al.*, 2015; Elsaid *et al.*, 2016; Yan *et al.*, 2018; Zhang *et al.*, 2018). PLGA nanoparticles can control and extend the release of drugs and biomolecules in the eye, however, intravitreal

nanoparticles are free-moving within the vitreous resulting in an increased clearance of the drugs (Sakurai *et al.*, 2001; Wang *et al.*, 2018; Huang and Chau, 2019). Encapsulation of nanoparticles within hydrogels can provide the NPs with a stable platform within the vitreous. This double-drug delivery system can also reduce the initial burst release of drugs normally observed with nanoparticle drug delivery (Thoniyot *et al.*, 2015; Bisht *et al*., 2017; Osswald *et al.*, 2017).

This study, therefore, formulated an *in situ*-forming hydrogel composed of the natural polymer, HA, and a blend of different molecular weight poloxamers (P188 and P407). Drug-loaded PLGA nanoparticles were then encapsulated in the formulated hydrogel. Triamcinolone acetonide, a corticosteroid drug used in the treatment and management of uveitis, proliferative diabetic vitreoretinopathy and macular degeneration was used for this study as a model drug (Munir *et al.*, 2005; Gillies and Larsson, 2007; Couch and Bakri, 2008). Thereafter, the nanoparticles and the hydrogel (unloaded and nanoparticle-loaded) were characterised and assessed for viscoelastic properties, optical properties, nanoparticle size and morphology, drug release characteristics, and lastly, biocompatibility.

4.2. Materials and Methods

4.2.1. Materials

The materials used in this research were bought from Sigma-Aldrich (St Louis, MO, USA). These materials include Poly(D,L-lactide-co-glycolide) (PLGA) (LA/GA=50/50, MW=45 000), Poly(vinyl alcohol) (PVA) (MW=85 000-124 000, 99+% hydrolysed), Dichloromethane, Ethyl Acetate, Triamcinolone acetonide, Poloxamer 407 (Pluronic ® F-127), Poloxamer 188 (Pluronic ® F-68), Hyaluronic acid sodium salt (from *Streptococcus equi*), and Lysozyme (from chicken egg white) (~70000 U/mg).

4.2.2. Synthesis of the poloxamer and hyaluronic acid hydrogel

The thermo-responsive hydrogel optimised in the previous chapter was formulated according to the cold method. Briefly, known concentrations of Poloxamer 188, Poloxamer 407 and Hyaluronic acid were mixed in deionised water on magnetic stirring at 4 °C for 12 hours. The solution was kept at 4 °C overnight for complete homogenisation.

The solution was then equilibrated before visual inspection of gelation, after which a vial inversion test was performed. For the inversion test (Niu *et al.,* 2019), 4 mL of the prepared formulation was placed in a 10 mL glass vial. It was then immersed in a water bath with a temperature of 37 °C. The time at which no flow of the sample was observed was considered to be the formation of the gel and the sol-gel phase change was visualised by the inversion of the vial. The temperature of gelation was also measured. The sample (4 mL) was placed in a transparent 10 mL vial with a magnetic bar. The temperature at which the bar stopped moving signified the gelation temperature. The gelation temperature was further confirmed as the temperature at which the gel remained intact after the vial was inverted for 60 seconds.

4.2.3. Preparation of PLGA nanoparticles and loading of nanoparticles in the hydrogel

Triamcinolone acetonide was encapsulated into PLGA nanoparticles using a double-emulsion solvent evaporation method. Various formulations were prepared and screened to determine the correct organic mixture ratio for nanoparticle synthesis. Triamcinolone acetonide of known mass was added to 2 mL of an organic mixture of ethyl acetate and dichloromethane (various ratios of 1:1, 1:2, 1:3, 2:1, and 3:1) containing 10 mg PLGA (slow stirring). This prepared solution was transferred, dropwise with a 26-gauge needle, into a 20 mL PVA solution (1% $^{w}/_{v}$) and stirred for 5 minutes. The solution was sonicated in an ice bath for 6, 20-second cycles (130 Watt, 20kHz, 50% Amplitude) with a probe sonicator (Sonics, Ultrasonic Processor, VCX130, Newtown, CT, USA). Thereafter, the solution was stirred for 48 hours for evaporation and the hardening of the triamcinolone acetonide-loaded nanoparticles. The nanoparticles were collected via centrifugation and washed with deionised water after which they were lyophilised (Labconco FreeZone 12 Console Freeze Dry, Kansas City, USA).

For nanoparticle loading within the hydrogel, the optimised nanoparticles were prepared as above. Following lyophilisation, nanoparticles were resuspended in deionised water. The polymers for the hydrogel were mixed in the resuspended nanoparticle solution rather than deionised water, as above.

4.2.4. Nanoparticle characterisation

Triamcinolone acetonide-loaded nanoparticles and unloaded nanoparticles were screened based on their diameter size, particle dispersity, surface charge, and encapsulation and loading of the drug. The Zetasizer NanoZS (Malvern Instruments Ltd., Worcestershire, UK) was used to determine the nanoparticle size, polydispersity index (PDI) and surface charge. The PDI was used as an indicator of dispersity where values ≤ 0.5 indicate monodisperse particles and ≥ 0.5 indicated polydisperse particles. The nanoparticle formulations were resuspended in deionised water (1 mg of the formulation in 1 mL water) and analysed using dynamic light scattering (DLS). The sample temperature was maintained at 25 °C and samples were diluted and sonicated prior to the measurement. The nanoparticle formulations were screened based on their size, PDI and surface charge. Formulations with favourable results, namely particle size < 200 nm, PDI ≤ 0.2, and a negative surface charge, were then screened based on the encapsulation efficacy and drug loading capacity. All measurements were conducted in triplicate.

The encapsulation efficiency of the nanoparticles was calculated using Equation 4-1.

$$Encapsulation\ efficiency\ (\%) = \frac{W_L}{W_O} \times 100 \qquad \text{Equation 4-1}$$

Where W_0 is the initial mass of triamcinolone acetonide and W_L is the mass of triamcinolone acetonide loaded in the nanoparticles. Encapsulation efficiency is the percentage of drug that is entrapped in the nanoparticle with respect to the amount of drug that was used in the nanoparticle preparation. Quantification of encapsulation efficiency via determination of the W_L was performed using a UV/Vis spectrophotometer (Lambda 25, PerkinElmer, MA, USA).

The surface morphology of the formulation selected (based on the above parameters) was then determined. Lyophilised samples of the drug-loaded, and unloaded nanoparticles were redispersed in deionised water and one drop was placed on an aluminium stub and allowed to dry for 24 hours. Samples were coated in a vacuum with one layer of gold using a sputter coater to induce induction. A field emission

scanning electron microscope (Zeiss, Jena, Germany) under an argon atmosphere was used to analyse the morphology of each sample.

4.2.5. Physicochemical characteristics of the nanoparticles and the hydrogel

4.2.5.1. Molecular transition and interaction analysis

Fourier Transform Infra-Red (FTIR) analysis was conducted on all pure polymers, lyophilised unloaded and loaded nanoparticles, and unloaded and loaded hydrogels. The molecular transitions and interactions were identified using a PerkinElmer ATR-FTIR (Spectrum 2000, Waltham, MA, USA) fitted with a single reflection diamond MIRTGS detector. FTIR spectra (20 scans per spectrum) were obtained using a wavelength range of 4000-650 cm^{-1}, a resolution of 4 cm^{-1}, and a constant pressure of 110 psi.

4.2.5.2. Thermal transitions and properties analysis

The thermal properties of the pure polymers, the lyophilised unloaded and loaded nanoparticles, and the lyophilised unloaded and loaded hydrogels were determined using a Differential Scanning Calorimeter (DSC) (Mettler Toledo DSC, STARe system, Schwerzenback, Switzerland) and a Thermogravimetric analyser (TGA) (PerkinElmer, TGA 4000, Llantrisant, Wales, UK). Thermally-induced phase transitions of the samples were determined using the DSC in an inert N^2 atmosphere. Samples were prepared and weighed into aluminium crucibles (3-10 mg), sealed (with a small, pierced hole to allow for pressure dissipation) and lastly, heated at a rate of 10 °C/minute over a range of 0-300 °C. The thermograms were plotted as a function of heat flow against temperature. Degradation temperatures of the samples were determined using the TGA as the percentage weight change over a temperature range of 30-900 °C with a heating rate of 10 °C/minute. Samples were maintained in an inert N^2 environment and degradation thermograms were plotted as percentage weight against temperature.

4.2.5.3. Crystallinity analysis

The crystallinity of the samples was determined using a benchtop MiniFlex 600 X-Ray Diffractometer (Rigaku, Tokyo, Japan). The pure polymers, the lyophilised unloaded and loaded nanoparticles, and the lyophilised unloaded and loaded hydrogels were

finely packed onto the sample holders with double-sided tape. CuKα radiation (15 mA, 40kV) was employed on the samples which underwent a 2θ scan range between 5-60° at a rate of 5°/minute.

4.2.6. Viscoelastic measurements of the hydrogel

The viscoelastic properties of the loaded and unloaded hydrogels were determined using the ThermoHaake MARS Modular Advanced Rheometer (Thermo Fischer Scientific, Karlsruhe, Germany) pre-equipped with a temperature-controlled bath allowing for temperature control of the sample chamber. Strain sweep, shear rate ramp, frequency sweep and temperature ramp measurements were conducted. All measurements were conducted in triplicate using a parallel plate with a gap measurement of 0.052 mm and measuring geometry of C35/1° T_1.

Hydrogel formation in the simulated vitreous humour (SVH) was evaluated using the ElastoSens^{TM} Bio2 (Rheolution, Montreal, Quebec, Canada). The real-time *in situ* formation of both hydrogels was evaluated in triplicate to assess the soft mechanical properties of each hydrogel. The experiment was conducted by placing 3 mL of formulated hydrogel (unloaded and loaded) in 1 mL of SVH to mimic the *in vitro* environment during administration. The shear storage (G') and loss (G") modulus of both hydrogels was measured as a function of time at a constant temperature of 37 °C.

The injectability of the hydrogels with a 26-gauge (26G) and 31-gauge (31G) needle was studied using the TA-XT2 Texture Analyser (Stable Micro Systems, Surrey, UK). All measurements were conducted in triplicate with the sample temperature at 10 °C (refrigerator storage temperature) in compression mode. A needle (26G or 31G) was fitted into a 3 mL luer-lock syringe and placed vertically in the holder with the needle facing downwards. Manual syringe injection was mimicked using a P/50R cylinder probe aligned to the plunger plate for volume displacement. Compression of the syringe plunger using the probe (compression speed of 1 mm/s and distance of 20 mm) expels the hydrogel from the syringe and the maximum force was recorded (Cilurzo *et al.*, 2011; Zhang *et al.*, 2018).

4.2.7. Optical properties of the hydrogel

The refractive index of the unloaded and loaded hydrogels was measured in triplicate using the Anton Paar refractometer (Anton Paar OptoTec GmbH, Germany) and the transmittance of the hydrogels was determined using the Implen Nanophotometer (NP80, UV//Vis spectrophotometer, Munich, Germany). The transmittance of the hydrogels was measured at 37 °C at a wavelength range of 200–950 nm.

4.2.8. *In vitro* drug release studies

In vitro drug release analysis was done using dialysis membranes in a simulated vitreous humour (SVH) buffer solution (4 mL). Analysis was conducted on drug release from the nanoparticle-loaded hydrogel as well as the loaded nanoparticles alone until an equilibrium release state was reached.

4.2.8.1. Preparation of standard solutions for the construction of a standard curve

A serial dilution of Triamcinolone acetonide (TA) was carried out in 40% ethanol at known concentrations (0.04 – 0.0009375 mg/mL). Full ultraviolet spectroscopy (UV-Vis) absorbance readings were taken on a spectrophotometer (Lambda 25 UV/Vis spectrophotometer, PerkinElmer, MA, USA) and the lambda-max (λ-max) of TA was confirmed at 240 nm. Thereafter, the absorbance of the aliquots from the TA dilutions was read (n=3).

4.2.8.2. In vitro drug release

An orbital shaker incubator was used to incubate all samples for the duration of the drug release studies at a constant temperature of 37 °C. Samples of 1 mL were withdrawn at each time point for analysis and replaced with 1 mL of fresh SVH solution to maintain sink conditions. Samples were analysed using a spectrophotometer (Lambda 25 UV/Vis spectrophotometer, PerkinElmer, MA, USA) in the same conditions used for the preparation of the calibration curve. The concentration of Triamcinolone acetonide released was determined using a calibration curve constructed from absorbance measurements of known drug concentrations.

4.2.9. Swelling and degradation profile determination

The swelling behaviour of the unloaded and loaded hydrogel was studied with all experiments conducted in triplicate. The swelling ratio of the hydrogels was measured by the immersion of the hydrogels in SVH at 37 °C in an orbital shaker. The weights of the swollen hydrogels (W_S) were measured every hour until equilibrium was reached and each sample was allowed to dry (W_D). The swelling ratio was calculated according to Equation 4-2, and the equilibrium ratio was determined as the ratio at which no further change in hydrogel mass occurred.

The degradation profiles of the unloaded and loaded hydrogel were determined with experiments conducted in triplicate. The degradation of the hydrogels was determined by immersing the hydrogel in SVH with lysozyme solution (10000 U/mL) at 37 °C in an orbital shaker. The weights of the hydrogels were measured at a specific time point for 60 days. The lysozyme-SVH was replaced every 48 hours. Degradation of the hydrogels was determined using Equation 4-3.

$$Swelling\ ratio = \frac{W_S - W_D}{W_D}$$ Equation 4-2

$$Degradation\ (\%) = \frac{W_t - W_0}{W_0} \times 100$$ Equation 4-3

Where W_0 is the initial weight of the hydrogels prior to immersion and W_t is the weight of the hydrogels at each time point after immersion.

4.2.10. *In vitro* cell biocompatibility

Biocompatibility of the drug and the unloaded and loaded hydrogels was evaluated in an NIH/3T3 (mouse fibroblast) (ATCC) and an hRPE (human retinal pigment epithelium) (ATCC) cell culture. NIH/3T3 cell maintenance was achieved in Dulbecco's Modified Eagle Medium (DMEM), with 10% Fetal Bovine Serum (FBS) and 1% penicillin/streptomycin antibiotic at 37 °C, 95% humidity and 5% CO_2. hRPE cell maintenance was achieved in DMEM/Hams F12 containing 10% FBS and 1% penicillin/streptomycin antibiotic at the same environmental conditions as the NIH/3T3

cell line. Culture mediums were replaced every 2 days until cell confluence (90%) was reached. Cell lines were seeded with a seeding density of $5x10^4$ cells/mL.

The sterile hydrogels (0.5 mL) and drug solution (UV sterilisation for 12 hours) at various concentrations were incubated for 48 hours and 72 hours with the cells in 96-well plates at 37 °C, 95% humidity and 5% CO_2. An MTT cell viability assay was conducted using an MTT-based Roche Cell Proliferation kit. 10 µL MTT solution was added to each well and the plates were incubated at 37 °C, 95% humidity and 5% CO_2 for 4 hours. Thereafter, 100 µL MTT solubilising agent was added to dissolve the formazan crystals overnight. A multi-plate reader (BioTek, USA) was used to determine the absorbance of the plates at 570 nm. The relative cell viability was calculated using Equation 4-4.

$$Cell\ Viability\ (\%) = \frac{Abs_S}{Abs_C} \times 100 \qquad \text{Equation 4-4}$$

Where Abs_S is the absorbance of the sample and Abs_C is the absorbance of the control (no treatment).

4.2.11. Statistical analysis

All analyses were conducted in triplicate (n = 3). All results were expressed as the mean and standard deviation and data was analysed using Microsoft EXCEL. The level of significance was determined using a student t-test. P values of less than 0.05 ($p < 0.05$) were considered as an indication of statistically significant differences. All graphs were plotted using SigmaPlot 12.0.

4.3. Results and Discussion

A nanoparticle-loaded hydrogel was successfully fabricated. An optically transparent and clear soft-gel (Figure 4.1) was obtained that underwent sol-gel phase transition at physiological temperatures.

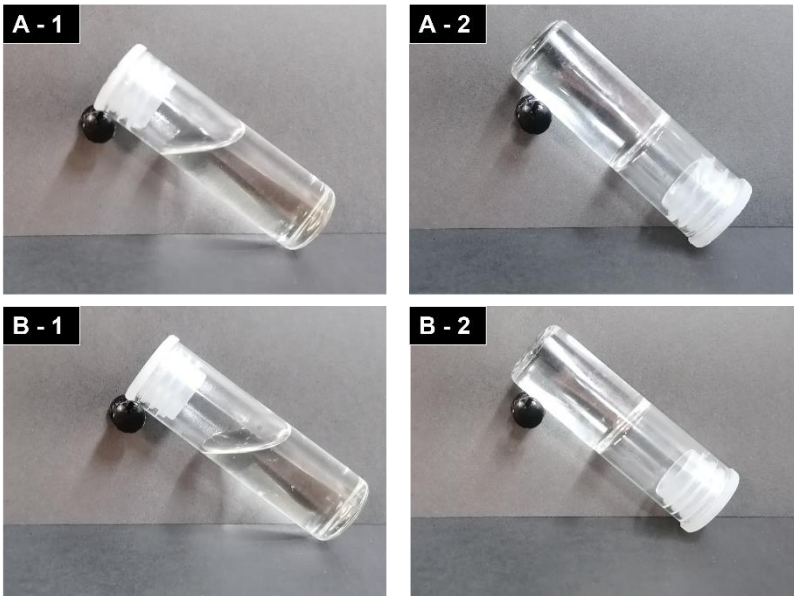

Figure 4.1 - Sol-gel phase transition with the vial inversion method. A) Sol-gel transition of the unloaded hydrogel B) Sol-gel of the nanoparticle loaded hydrogel.

Gel formation was observed to occur at ~33 °C for the unloaded hydrogel and ~36 °C for the nanoparticle-loaded hydrogel. The temperature of gel formation for the nanoparticle-loaded hydrogel is favourable as it is similar to physiological temperatures. Gel formation of the nanoparticle-loaded hydrogel occurred at a higher temperature than that for the unloaded hydrogel due to interactions between the nanoparticles and the micelles formed during the sol-gel transition. A higher temperature is needed to overcome these interactions for gel formation. Figure 4.2 displays the time taken for gel formation at 37 °C from 10 °C. These times of nine minutes (±0.6 minutes) for the unloaded hydrogel, and eight minutes (±0.2 minutes) for the loaded hydrogel, are clinically advantageous. Vitreous substitution with current tamponades requires patients to remain face-down post-vitrectomy (Kim and Baumal, 2004; Kleinberg *et al.*, 2011). This fabricated hydrogel would form almost immediately post-vitrectomy increasing patient compliance.

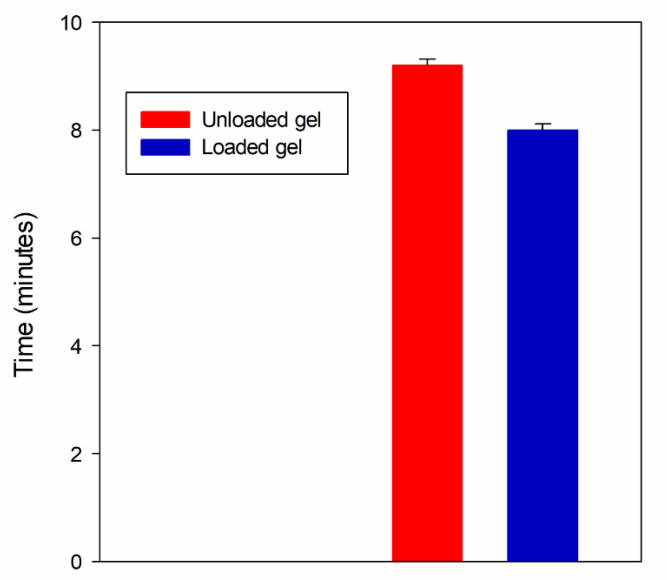

Figure 4.2 - Time required for gel formation at 37 °C.

4.3.1. Nanoparticle size, surface charge and surface morphology

Particles with a diameter of less than 200 nm have been proven to penetrate from the vitreous to the retinal layers (Huang and Chau, 2019). Therefore, nanoparticles formed were screened to have a diameter of < 200 nm with a PDI of ≤ 0.2.

Previously, PLGA nanoparticles for ocular administration (< 200 nm) were prepared for lipophilic drugs using the solvent-evaporation method (Esmaeili *et al.*, 2007; Javadzadeh *et al.*, 2010). Various solvents have been used for the fabrication of PLGA nanoparticles and PLGA nanoparticles for ocular administration utilising acetone, ethyl acetate and dichloromethane (Ding and Zhu, 2018). Acetone was not used in this study as particles formed with acetone would likely yield larger particles than those formed with dichloromethane due to the water miscibility of acetone (Essa *et al.*, 2020). Dichloromethane is reported to be a favourable solvent in the formation of PLGA nanoparticles (Mohammadi-Samani and Taghipour, 2015; Abd El Hady *et al.*, 2019), however, due to the cytotoxic nature of dichloromethane, ethyl acetate was used to decrease the concentration of dichloromethane in the formulation. Table 4.1 includes the various solvent ratios used and shows that lower dichloromethane concentrations with ethyl acetate are favourable for the fabrication of nanoparticles with a size < 200

nm and a PDI < 0.2. The negative surface charge observed for all the nanoparticle formulations is attributed to the carboxylic acid end groups of PLGA.

Table 4.1 - Size, dispersity, and surface charge of PLGA nanoparticles in various solvent ratios.

PVA concentration	Organic mixture ratio (EA: DCM)	Particle size (diameter) (nm)	PDI	Particle surface charge (mV)
1% $^{w}/_{v}$	1:1	184 ± 4.1	0.205 ± 0.035	-31.3 ± 0.8
	1:2	245 ± 2.6	0.247 ± 0.005	-43.5 ± 0.2
	1:3	235 ± 3.4	0.263 ± 0.003	-26.4 ± 0.4
	2:1	145 ± 2.5	0.187 ± 0.020	-26.3 ± 0.1
	3:1	134 ± 1.0	0.155 ± 0.006	-25.1 ± 0.5

Nanoparticles with a solvent ratio of 2:1 and 3:1 (ethyl acetate: dichloromethane) both had the necessary particle size and PDI. Thus, to choose the formulation for entrapment within the hydrogel, the encapsulation efficiency with triamcinolone acetonide (TA) of both formulations was tested. Figure 4.3, illustrates that the formulation with a 3:1 ratio of ethyl acetate: dichloromethane had better drug encapsulation of 97.500% (± 1.523%) while encapsulation within the 2:1 formulation was 78.123% (± 2.271%).

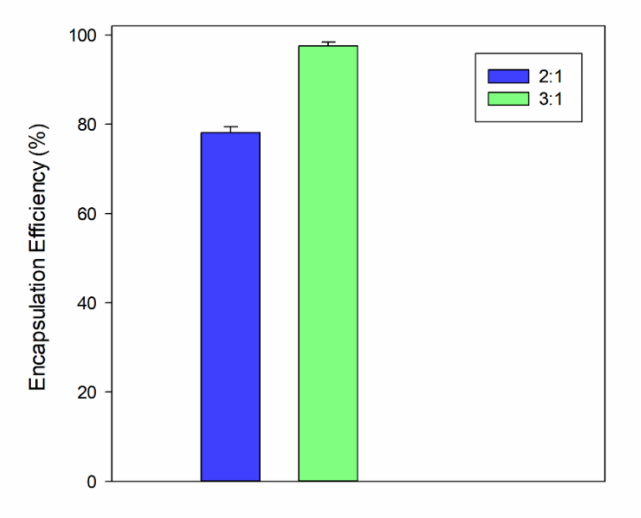

Figure 4.3 - Encapsulation efficiency of the 2:1 and 3:1 (EA: DCM) nanoparticle formulations.

The PLGA nanoparticle formulation with a 3:1 solvent ratio (ethyl acetate: dichloromethane) was chosen for encapsulation within the hydrogel. The particle size and PDI of the unloaded nanoparticles (Figure 4.4A) and the TA-loaded nanoparticles (Figure 4.4 B) were 133.7 nm (± 1.0 nm) PDI = 0.155 (± 0.006) and 153.1 nm (± 2.4 nm) PDI = 0.179 (± 0.020), respectively. The surface charge of both the unloaded and loaded nanoparticles was negative due to the PLGA (Figure 4.4C & D).

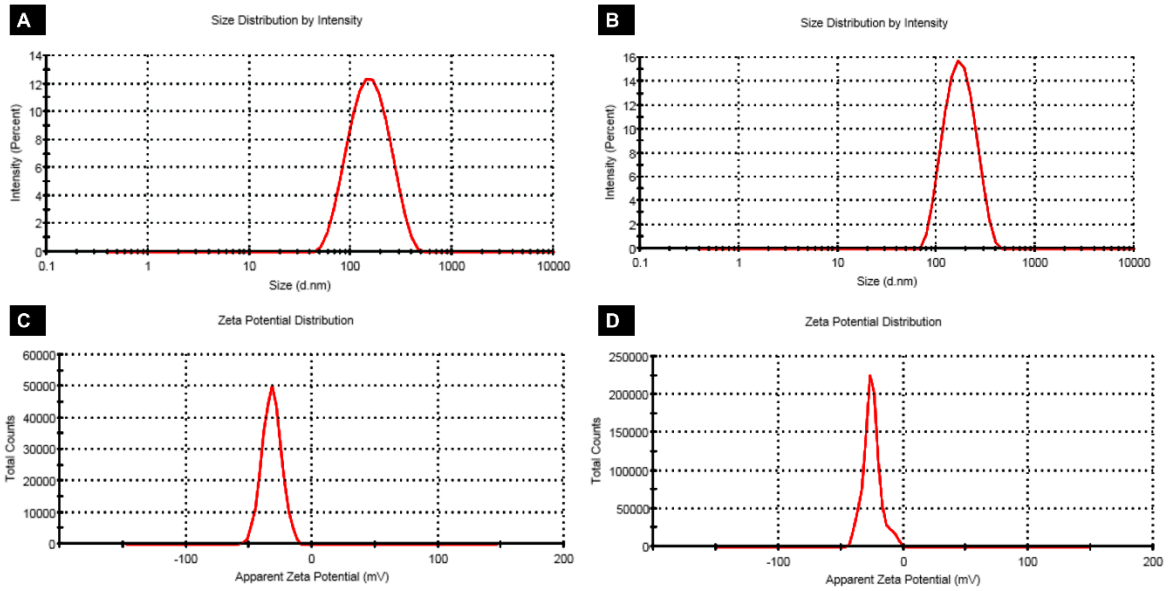

Figure 4.4 - A, B) Particle size distribution and C, D) Zeta potential distribution of the: A, C) unloaded and B, D) TA loaded PLGA nanoparticles.

SEM micrographs, Figure 4.5, show the spherical morphology of the fabricated nanoparticles. Slight particle size increases are noted between the unloaded nanoparticles (Figure 4.5 A) and the drug-loaded nanoparticles (Figure 4.5 B). The particles are visualised to be dispersed with no drug crystals visible unlike those noted by Gómez-Gaete and co-workers in 2007. The lack of drug crystals shows entrapment of the drug and this should eliminate the burst release of the drug from the nanoparticles as reported in previous PLGA nanoparticle studies (Gómez-Gaete *et al.*, 2007; Javadzadeh *et al.*, 2010; Sabzevari *et al.*, 2013).

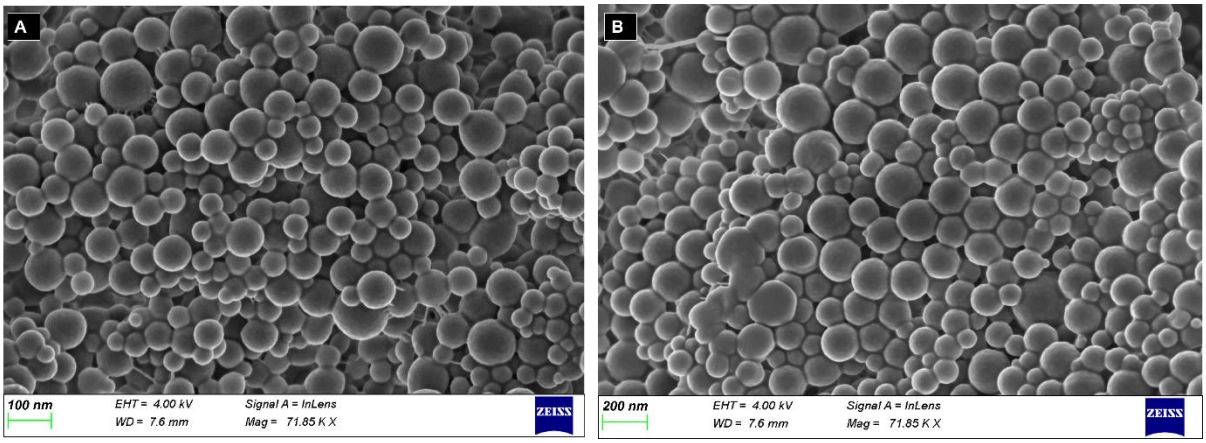

Figure 4.5 - SEM micrographs of the A) unloaded PLGA nanoparticles and B) TA-loaded PLGA nanoparticles.

4.3.2. Physicochemical properties of the nanoparticles and the hydrogel

FTIR spectra of the PLGA nanoparticles, and native triamcinolone acetonide and PLGA are shown in Figure 4.6. Triamcinolone acetonide (TA) nanoparticle fabrication was confirmed by FTIR. Unloaded and TA-loaded PLGA nanoparticles displayed IR absorption bands characteristic of the PLGA polymer (indicated by the black arrows). These bands include C-H bending at 3002 cm^{-1} and 2956 cm^{-1}, the C-O ester double bond at 1760 cm^{-1}, and C-O stretching at 1091 cm^{-1}. Lactide-lactide (1456 cm^{-1}), glycolide-glycolide (1429 cm^{-1}) and lactide-glycolide (1394 cm^{-1}) bands of the PLGA monomers were also visible as a triple-peak (marked by the black box).

The FTIR spectrum of pure TA showed the characteristic H-bond hydroxyl stretching IR absorption band at 3398 cm^{-1}, carbonyl stretching at 1706 cm^{-1} and C-F stretching at 1057 cm^{-1}. These TA IR absorption bands (indicated by red arrows) are also visible in the TA-loaded nanoparticles. Polymer and drug interactions did not take place as new peaks were not visible and shifts in existing peaks were not observed. The presence of these peaks suggests that TA was successfully encapsulated in the PLGA nanoparticles.

FTIR spectra of the hydrogels and their polymers are shown in Figure 4.7. Poloxamer 407 and Poloxamer 188 displayed similar FTIR profiles due to their similarities in their composition. Both showed characteristic hydroxyl stretching bands at 3400 cm^{-1} and C-O-C stretching at 1085 cm^{-1}. These bands (indicated by the light green arrows) were also prominent in the final unloaded and nanoparticle-loaded hydrogels. The FTIR

spectrum of HA displays characteristic IR absorption bands at 3318 cm^{-1} (hydroxyl stretching), C-O-C stretching at 1151 cm^{-1} and 1024 cm^{-1}, amide bands at 1530 cm^{-1} and 1565 cm^{-1}, and carboxylic bands at 1605 cm^{-1} and 1405 cm^{-1}. HA hydroxy groups and a carboxylic band are visible in the unloaded and loaded nanoparticle spectra (purple arrows) indicative of the presence of HA in the hydrogels. The nanoparticle-loaded hydrogel also displays a peak at 1760 cm^{-1} (yellow arrow) indicative of a C-O ester bond related to the PLGA within the nanoparticle system. HA and nanoparticle bands in the hydrogels had lower transmittance values due to the high amount of poloxamer in comparison to HA. Similar results have also been observed in physically mixed poloxamer gels (Rangabhatla *et al.*, 2016). Shifts in peaks were not visible and new peaks were absent. This confirms that chemical interactions between the hydrogel and nanoparticles did not take place.

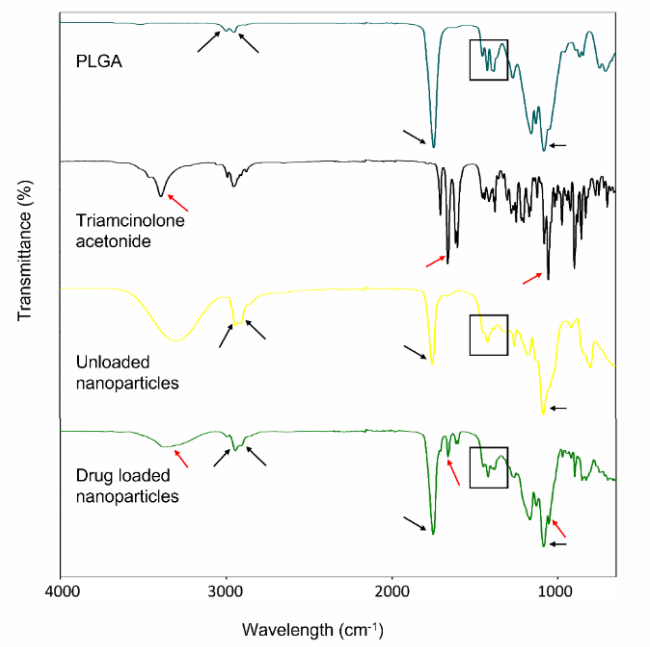

Figure 4.6 - FTIR spectra of PLGA, triamcinolone acetonide and the unloaded and loaded nanoparticles.

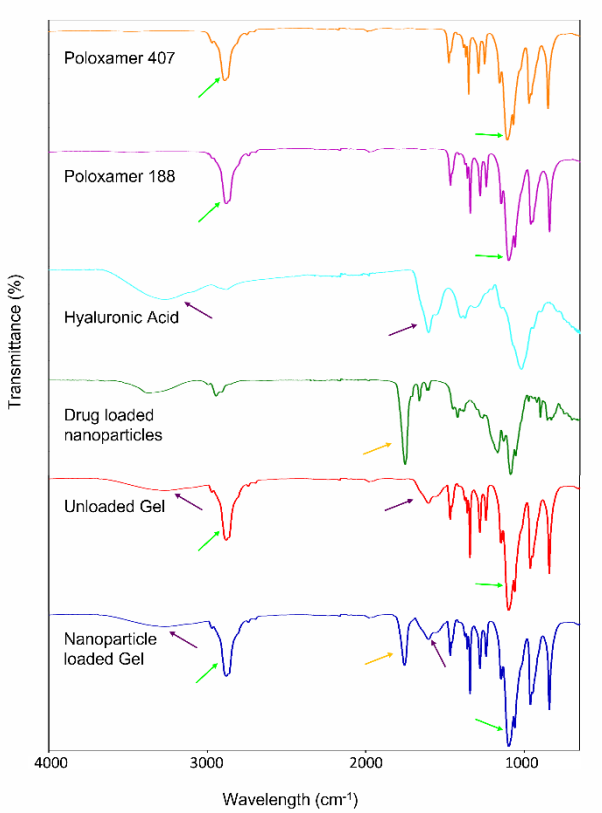

Figure 4.7 - FTIR spectra of both poloxamers, hyaluronic acid, the loaded nanoparticles and the unloaded and loaded hydrogels.

DSC analysis was performed on the unloaded and loaded PLGA nanoparticles, TA, and PLGA (Figure 4.8). PLGA displayed an endothermic peak at 51.14 °C indicative of its glass transition (D'Avila Carvalho Erbetta *et al.*, 2012). PVA displayed an endothermic peak at 227.84 °C associated with the melting point. This endothermic peak was then visible in the unloaded and loaded PLGA nanoparticles. A sharp endothermic peak at 295.87 °C was observed for TA due to the melting point of the crystalline state of TA (García-Millán *et al.*, 2017). This sharp endothermic peak was not visible in the TA-loaded PLGA nanoparticles, which may indicate a shift to a more amorphous form leading to increased solubility of the drug in the nanoparticle (Salama *et al.*, 2016; García-Millán *et al.*, 2017) or due to solid state interaction by heating (Pandit *et al.*, 2017; Alkholief *et al.*, 2019).

The DSC thermograms of the hydrogels and their constituents are shown in Figure 4.8. The DSC thermograms of Poloxamer 407 and Poloxamer 188 displayed endothermic peaks at 57.66 °C and 55.27 °C respectively. These are indicative of the melting temperature of poloxamers. The unloaded and loaded hydrogels displayed the

same peak. However, these peaks had slight shifts in comparison to the pure polymers. This would be a result of the physical mixing of HA and the nanoparticles in the hydrogels. The DSC thermogram of HA displays a gentle endothermic peak at 133 °C and a steep exothermic peak at 238 °C indicative of the degradation of HA. This exothermic peak is visible in the unloaded and loaded hydrogel thermograms and the PLGA nanoparticle degradation is also visible in the thermogram of the loaded hydrogel. The high concentration of poloxamer, as with the FTIR spectra, reduces and masks peaks that were visible in the thermogram of the nanoparticles.

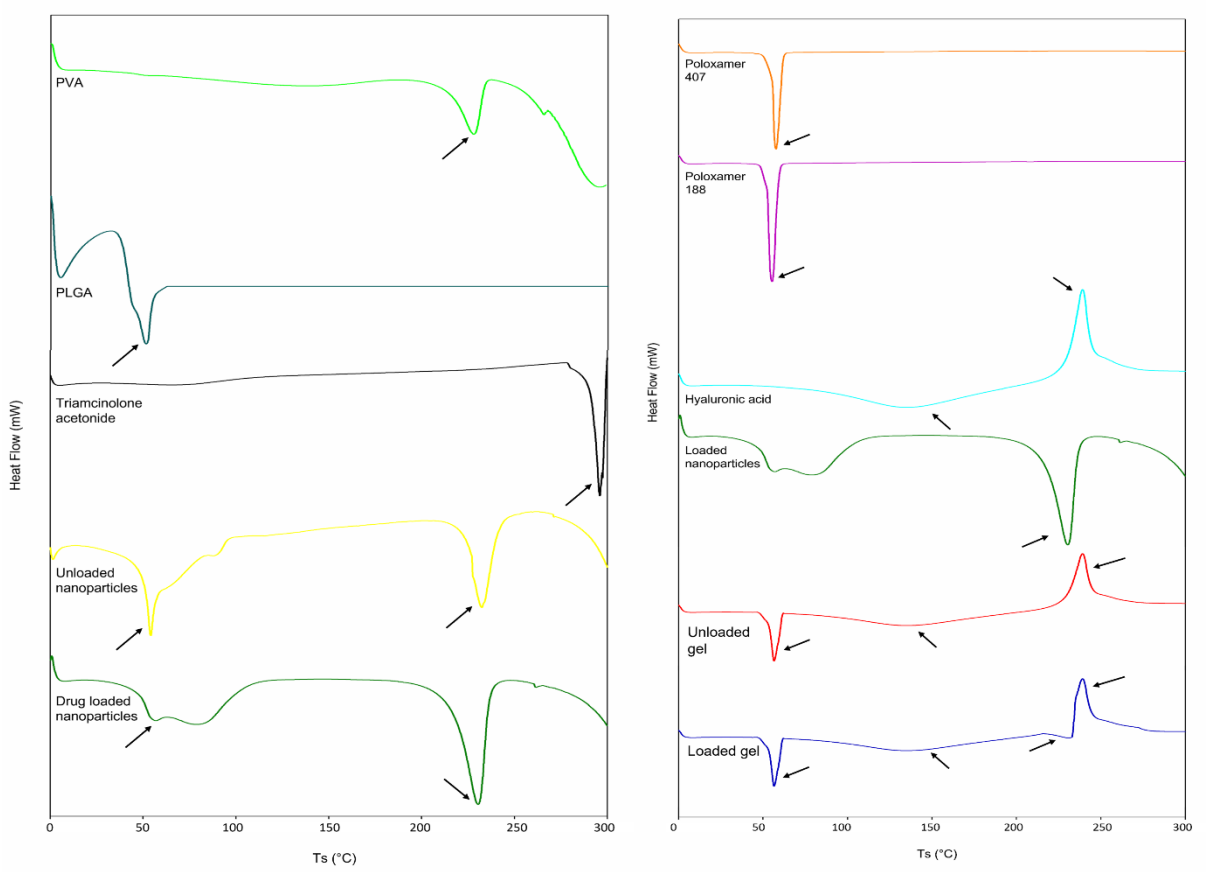

Figure 4.8 - DSC thermograms of all polymers, triamcinolone acetonide and all nanoparticle and hydrogel formulations.

TGA thermograms (Figure 4.9) were then correlated to the DSC thermograms. Complete degradation of all prepared formulations (nanoparticles and hydrogels) occurred with major weight loss occurring between 270 °C and 500 °C for both nanoparticle formulations and between 375 °C and 500 °C for both hydrogel

formulations. The degradation of the nanoparticle formulations is congruent with the DSC thermograms where the start of an endothermic peak is visible towards 300 °C in the thermograms. The TGA thermograms also display a decreased degradation rate for the nanoparticle-loaded hydrogel in comparison to the unloaded hydrogel.

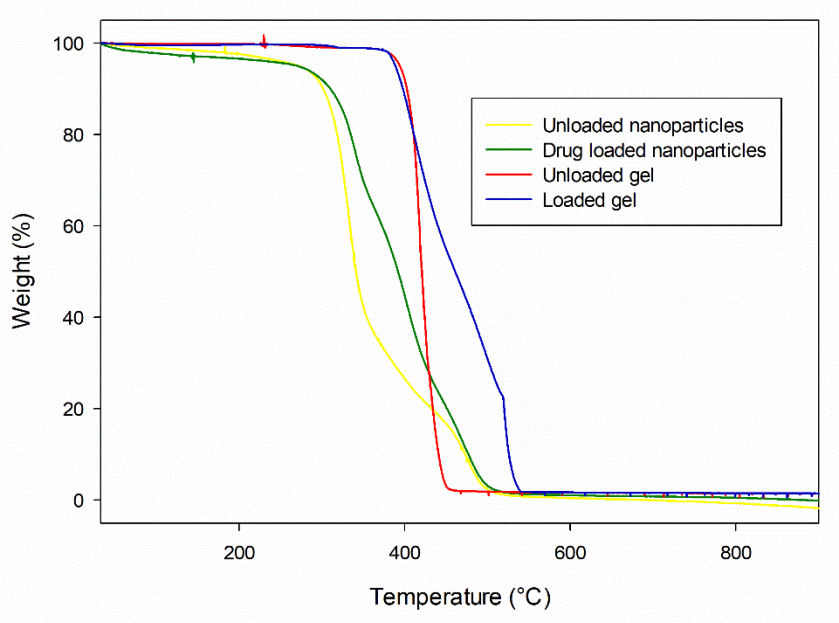

Figure 4.9 - TGA thermograms of the unloaded and loaded nanoparticles and the unloaded and loaded hydrogels.

The XRD patterns of the prepared nanoparticle formulations, TA and the pristine polymers are shown in Figure 4.10. PLGA and PVA display amorphous surface characteristics while TA shows various crystalline peaks. The unloaded nanoparticles display an amorphous structure similar to the structure seen with pure PLGA. An amorphous structure is also visible for the drug-loaded nanoparticles; however, some TA peaks were visible. This amorphous structure of the loaded nanoparticles is attributed to the decreased drug crystallinity and solubilisation in PLGA during the synthesis of the nanoparticles.

The XRD pattern of the unloaded hydrogel displayed in Figure 4.10 is very similar to that of the pure poloxamer polymers. However, differences in structure are visible between 23° and 29°. The loaded hydrogel displays characteristics similar to the unloaded hydrogel except for changes visible between 30° and 54°. The changes in the unloaded hydrogel are attributed to HA while changes in the loaded hydrogel are due to the presence of the nanoparticles. The intensity of these changes is low, likely

due to the lower HA and nanoparticle concentrations in comparison to that of the poloxamers.

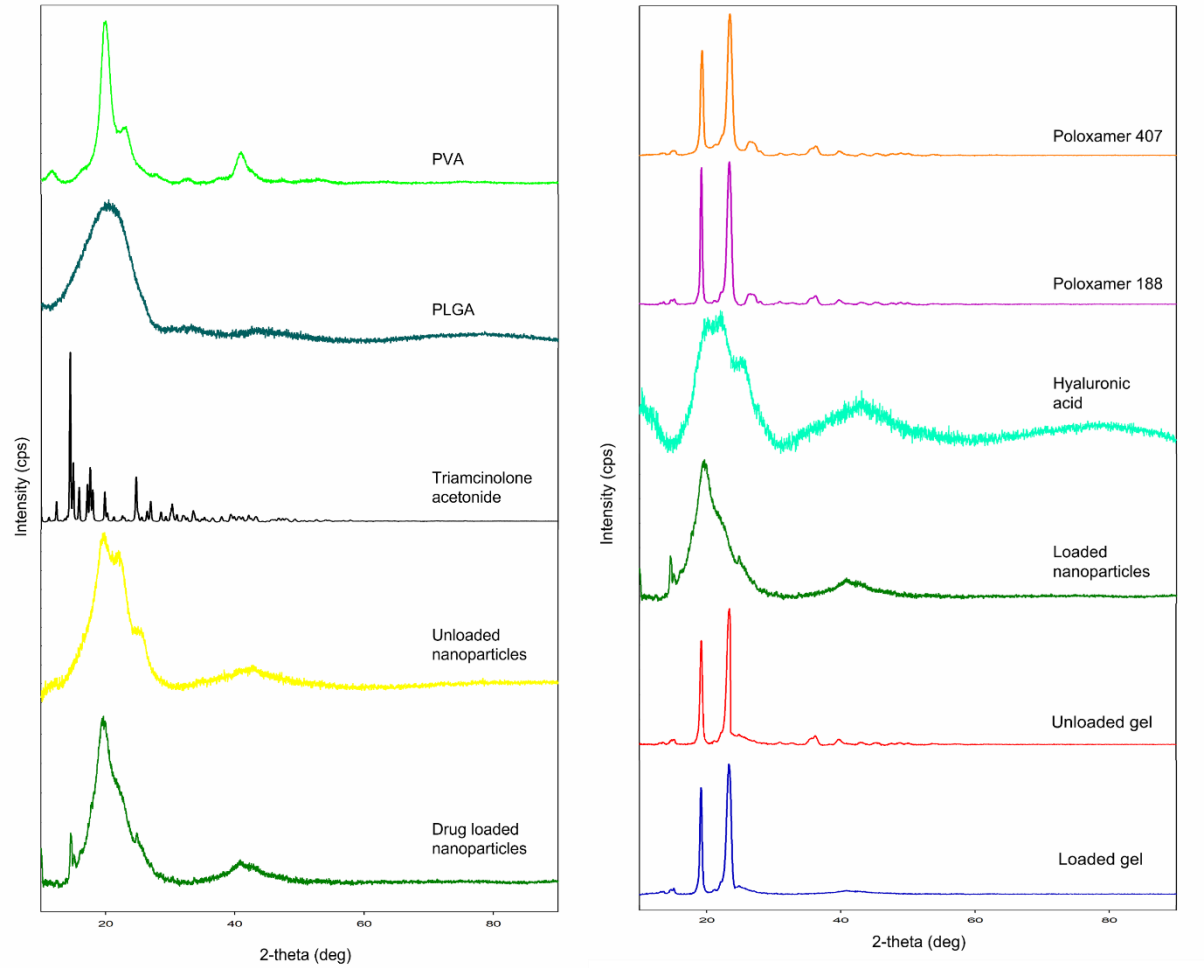

Figure 4.10 - X-Ray Diffractograms of the polymers, drug and nanoparticle and hydrogel formulations.

4.3.3. Viscoelastic measurements of the hydrogel

The unloaded and loaded hydrogels displayed similar viscoelastic properties to the natural vitreous. It is necessary to determine the Linear viscoelastic range (LVR) to better understand the linear behaviour of the hydrogels. A strain sweep analysis was conducted to find the LVR of both hydrogels. Figure 4.11 (A) shows that the LVR for both hydrogels was below a strain of 10%. The study was conducted at a constant frequency of 1 Hz as variations in modulus are easily detected at this frequency. G' (storage modulus) and G" (loss modulus) decreased above a 10% strain and the loss

modulus for the loaded hydrogel became larger than the storage modulus. This suggests that the hydrogel became more liquid. As a result, a 1% strain was used to conduct all subsequent rheology studies on both hydrogels.

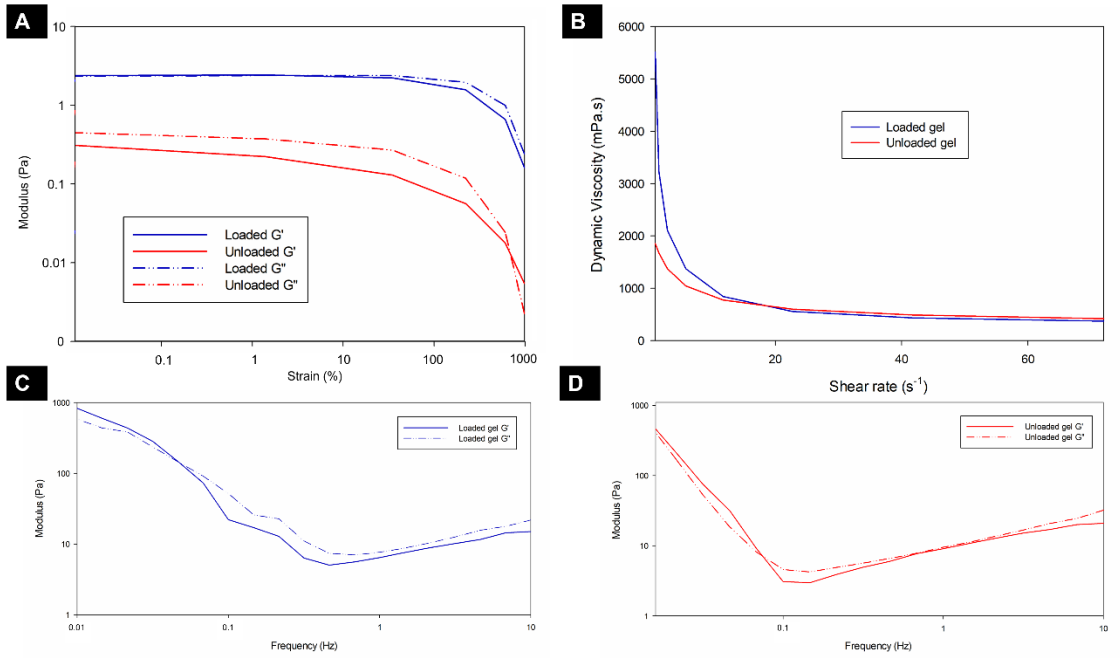

Figure 4.11 - Rheological data for the unloaded and loaded hydrogels. A) Strain sweep experiments, B) Shear rate ramp experiments, C) Frequency sweep of the loaded hydrogel and D) Frequency sweep of the unloaded hydrogel.

Shear thinning of both hydrogels was observed with a decrease in viscosity as the shear rate increased (Figure 4.11 B). This behaviour is ideal for extrusion via a needle for the administration of the gels.

The storage modulus of the natural vitreous is reported to range from 1-7 Pa while the loss modulus is reported to range between 0.3 and 1 Pa (Tram and Swindle-Reilly, 2018; Schulz *et al.*, 2019). However, these studies were conducted on the *in vitro* vitreous and do not represent the modulus of the *in vivo* vitreous. The properties of the human vitreous change after removal from the eye (Santhanam *et al.*, 2016) and a study conducted by Zimberlin and co-workers (2010) demonstrated that the modulus of the *in vivo* vitreous is higher than that of the *in vitro* vitreous. The study by Santhanam *et al.* (2016) shows that a suitable vitreous substitute should have a

modulus above 100 Pa. Frequency sweep studies were conducted on both hydrogels at a constant temperature of 37 °C (Figure 4.11 C & D). Table 4.2, displays that the average modulus of both hydrogels is > 100 Pa. These modulus values are also favourable for vitreous substitutes as they indicate that the hydrogels would not pass through retinal tears (Yadav *et al.*, 2021).

Table 4.2 - Average storage and loss moduli of the unloaded and loaded hydrogels.

	Storage modulus (G') (Pa)	**Loss modulus (G") (Pa)**
Loaded hydrogel	132.593 ± 0.320	110.889 ± 0.038
Unloaded hydrogel	99.503 ± 0.024	108.581 ± 0.011

Temperature ramp studies were conducted on both hydrogels to assess their behaviour with changes in temperature (Figure 4.12). The storage modulus (G'), loss modulus (G"), and viscosity of the hydrogels were assessed at a temperature range of 10-50 °C. The loaded hydrogel (Figure 4.12 A & C) displays a cross-over of G' and G" at 36.496 °C (± 0.014 °C). this cross-over is indicative of the temperature at which the behaviour of the hydrogel becomes that of a gel rather than a solution. Between temperatures of 33 °C and 35 °C an increase in G' and viscosity show the beginning of the sol-gel phase change. This phase change is visible in Figure 4.12 B and C for the unloaded hydrogel between 29 °C and 32 °C, with a G'-G" cross-over occurring at a temperature of 33.688 °C (± 0.021 °C). The crossover temperature of the nanoparticle-loaded hydrogel is favourable over that of the unloaded hydrogel as it is similar to physiological temperature demonstrating gel formation at physiological temperature.

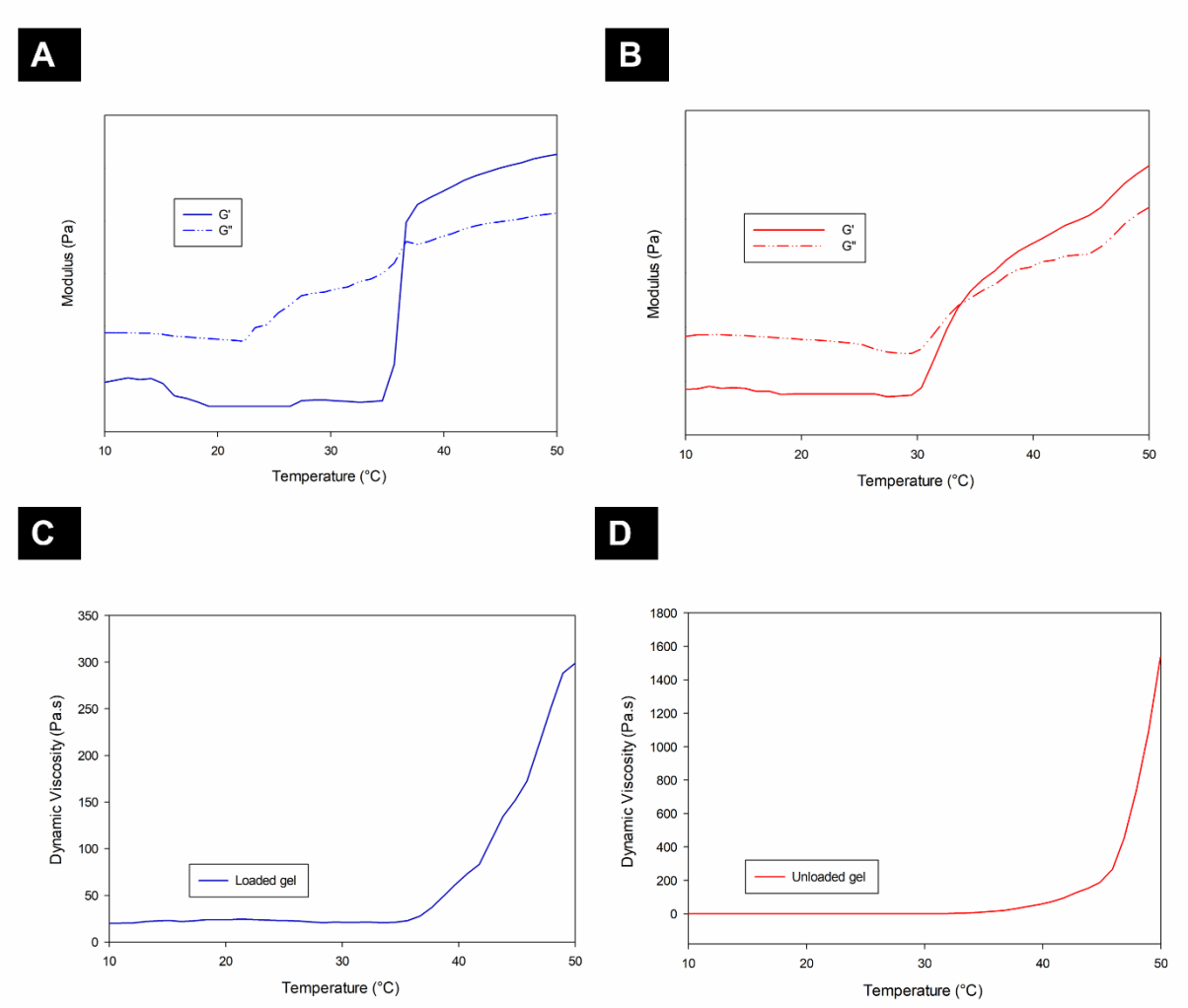

Figure 4.12 - Temperature ramp data of both hydrogels between 10 °C and 50 °C. A) Modulus of the loaded hydrogel, B) modulus of the unloaded hydrogel, C) viscosity of the loaded hydrogel and D) viscosity of the unloaded hydrogel.

The ElastoSens™ Bio2 technique for rheological studies measures the real-time properties of the hydrogel in a non-destructive manner. The analysis of the hydrogels is conducted via gentle mechanical vibrations passing through the hydrogel samples that are held within confined holders and the response to the vibrations is detected by a laser. It is important to assess the interaction between the hydrogel (unloaded and loaded) and the native vitreous. Therefore, SVH was prepared to assess this interaction. Figure 4.13 shows the storage modulus (G') and loss modulus (G") of both hydrogels in SVH over 3 hours. The initial increase of the shear storage modulus and loss modulus of both hydrogels shows the mixing of both hydrogels with the SVH which is evidence of *in situ* hydrogel formation. The unloaded hydrogel ($G'_{average}$ = 467.01 Pa ± 1.286 Pa) and the loaded hydrogel ($G'_{average}$ = 600.62 Pa ± 2.356 Pa) display

properties of soft hydrogels as their modulus was less than 1 kPa. Both hydrogels formed immediately after exposure to the SVH at 37 °C. Maximum gelling and modulus values were achieved in 10 minutes (± 0.885 minutes) for the unloaded hydrogel and 18 minutes (± 1.05 minutes) for the loaded hydrogel. This was then maintained for the duration of the experiment. These results are for real-time experiments and are thus incomparable to those obtained via the rheometer. However, the gelling times are comparable to those observed in the vial inversion test.

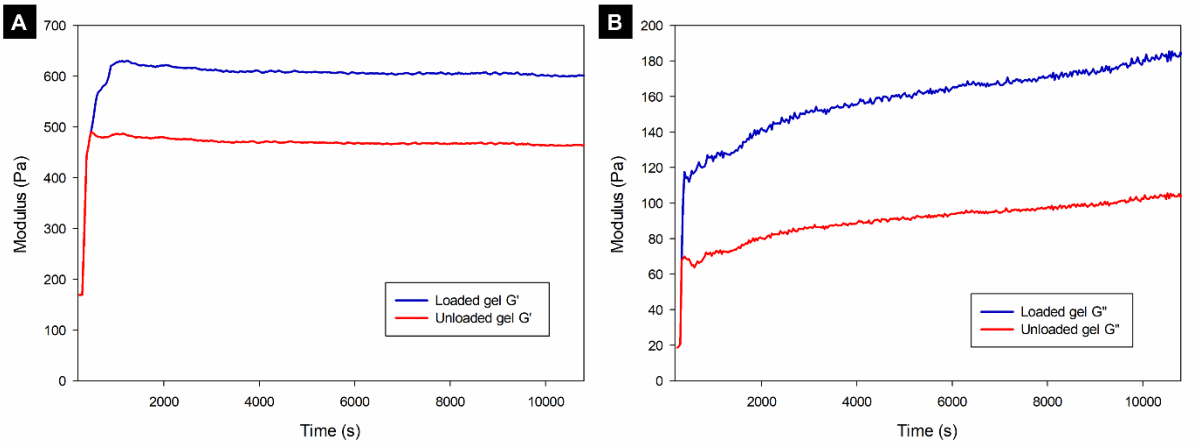

Figure 4.13 - Real-time modulus changes of the unloaded and loaded hydrogels. (A) Storage modulus (G'), (B) Loss modulus (G")

The injectability of both hydrogels (Figure 4.14) was conducted with 26-gauge (26G) and 31-gauge (31G) needles. Pars plana vitrectomy is commonly conducted using 23-, 25- and 27-gauge needles (Schweitzer *et al.*, 2009; Rizzo *et al.*, 2015; Otsuka *et al.*, 2018) and intravitreal injections are commonly administered with 26-, 27-, 30- and 31-gauge needles (Pulido *et al.*, 2007; Haas *et al.*, 2016; Loureiro *et al.*, 2017). Due to availability, 26G and 31G needles were used for this study. Figure 4.14 shows that injection of the hydrogels was possible with both needles, however, a greater force was required for administration with the 31G needle (Figure 4.14 B) than with the 26G needle (Figure 4.14 A). As pars plana vitrectomy and intravitreal injections utilise 26G needles and for ease of administration, injection of the hydrogels via 26G needles is preferable.

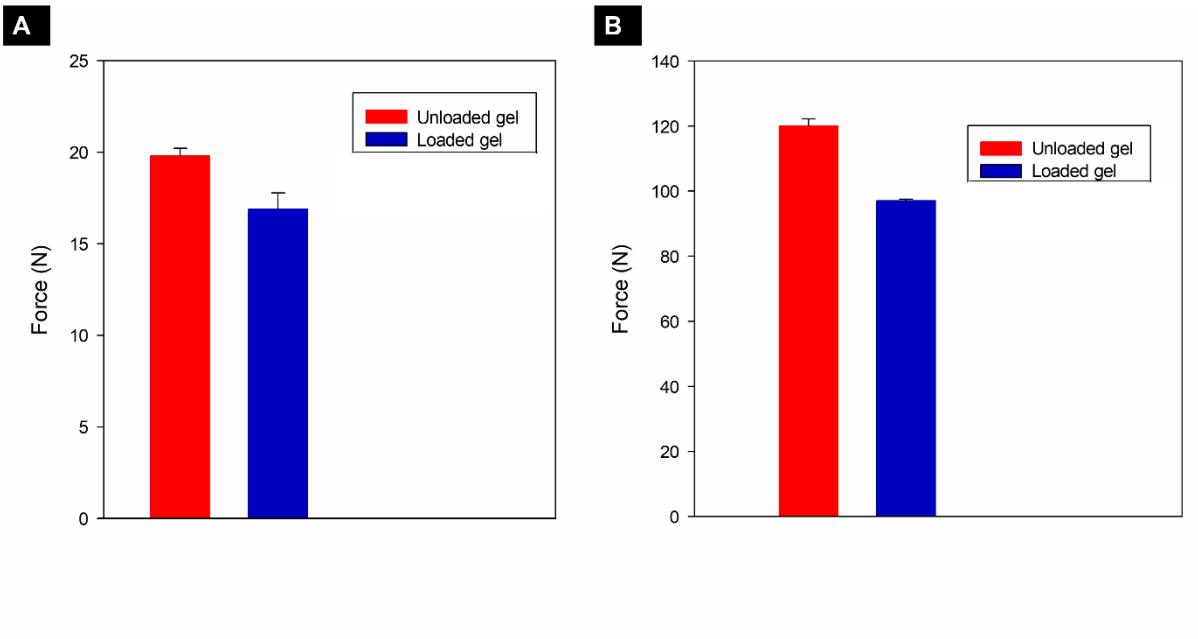

Figure 4.14 - Maximum force required by A) 26G and B) 31G needles for hydrogel administration.

4.3.4. Optical properties of the hydrogel

The hydrogels had a transparency of >90% ($p < 0.05$) at 37 °C within the visible wavelengths (Figure 4.15). Although the unloaded hydrogel had a higher transmittance than the loaded hydrogel (most probably due to slight nanoparticle interference), both were optically similar to the natural vitreous which allows for 90% of light between 300 and 1400 nm (Boettner and Wolter, 1962). The transmittance of both hydrogels also behaved similarly to the natural vitreous with a drop in transmittance between a UV range of 0-230 nm.

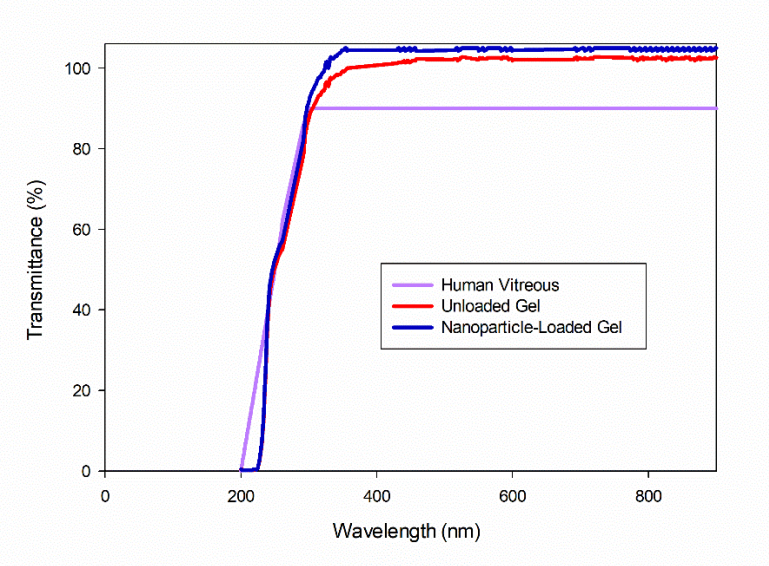

Figure 4.15 - The transmittance of the hydrogels between 200 and 900 nm.

The refractive index of the unloaded hydrogel was 1.3350 (± 0.002) and the refractive index of the loaded hydrogel was 1.3352 (± 0.003). Both of these are similar to 1.3349 which is the refractive index of the natural vitreous. Silicone oil, the most used vitreous substitute (Thacker *et al.*, 2021), has a refractive index of 1.405 (Smith *et al.*, 1990). This has resulted in refractive errors in patients receiving silicone oil as a substitute post-vitrectomy (Eibenberger *et al.*, 2020).

4.3.5. *In vitro* drug release

Drug release studies were conducted to determine the release profile of TA from the PLGA nanoparticles and the nanoparticle-loaded hydrogel. A calibration curve (Figure 4.16) was constructed to determine the release concentrations of TA.

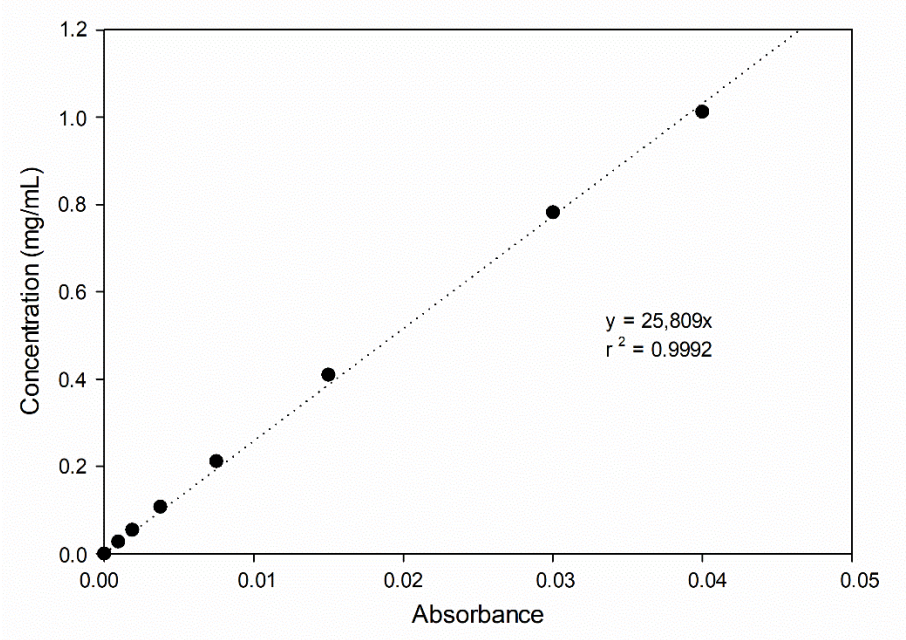

Figure 4.16 - Calibration curve of triamcinolone acetonide.

Figure 4.17 shows the *in vitro* release profiles of TA from the nanoparticles and the nanoparticle-loaded hydrogel. The drug release profiles show that release of TA from the nanoparticle-loaded hydrogel is slower and over an extended period; whereas the release of TA was faster from the nanoparticles alone which would result in faster clearance of the drug from the vitreous (Huang and Chau, 2019).

50% of TA was released from the nanoparticles within the first day of administration while the remaining TA was released over 7 days. Vitreous substitution can cause inflammation post-vitrectomy (Dave *et al.*, 2014; Cunha *et al.*, 2021) and an initial burst release ensued by a slow release of TA from a vitreous substitute would be advantageous for the treatment of the initial acute inflammation. Inflammation due to long-term substitution may also occur and the steady, long-term TA release observed in the loaded hydrogel would allow for treatment of the inflammation. Vitreoretinal diseases such as uveitis, proliferative diabetic vitreoretinopathy and macular degeneration require treatment with TA. Therefore, TA release from the hydrogel is beneficial.

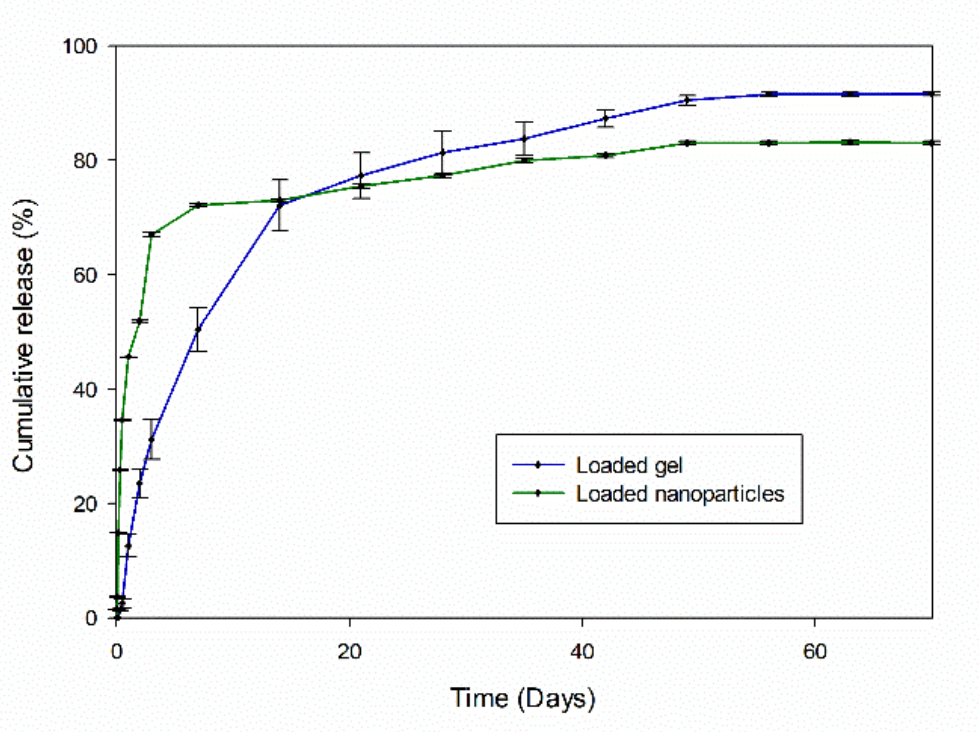

Figure 4.17 - Drug release profiles from the nanoparticles and the loaded hydrogel.

4.3.6. Swelling and degradation

The swelling ratio of the unloaded and loaded hydrogels was determined after incubation of the hydrogels in simulated vitreous humour (SVH) buffer solution at 37 °C. This was continued until equilibrium swelling was reached as shown in Figure 4.18. Equilibrium swelling was reached within 12 hours for the unloaded hydrogel and 8 hours for the loaded hydrogel. The loaded hydrogel reached equilibrium swelling in less time than the unloaded hydrogel due to the presence of the nanoparticles. The total hydrogel volume in the nanoparticle-loaded hydrogel is marginally less attributed to the decreased time taken for equilibrium swelling. This is advantageous as the administration of the hydrogel into the vitreous body should not affect intraocular pressure.

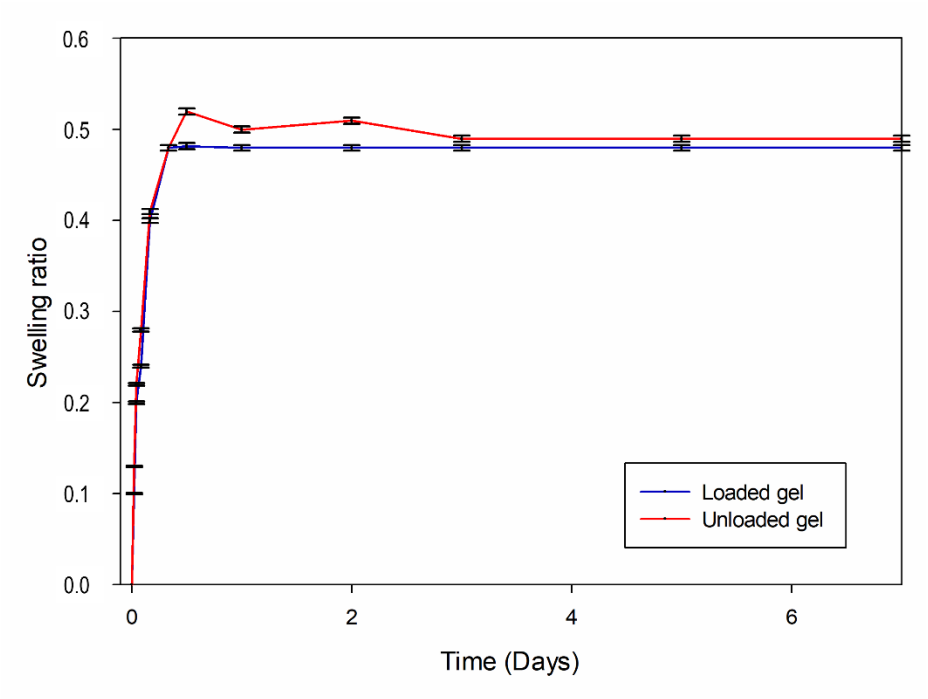

Figure 4.18 - Swelling ratio profile of the unloaded and loaded hydrogels in simulated vitreous humour at 37 °C.

Biodegradation studies (Figure 4.19) were conducted with the use of lysozyme which acts as a general ocular enzyme at 37 °C. The studies were conducted for up to 63 days to assess the long-term degradation behaviour of both hydrogels. Although a weight loss of the hydrogels was observed, this degradation was less than vitreous substitutes reported by Baker *et al*. (2021) and Yu *et al*. (2022) where the hydrogel mass decreased by 60% in 56 days and 40% in 14 days, respectively. The long-term stability of hydrogels as vitreous substitutes is important to avoid frequent injections and degradation *in vitro*. Resistance to enzymes as shown with both hydrogels is essential for long-term administration.

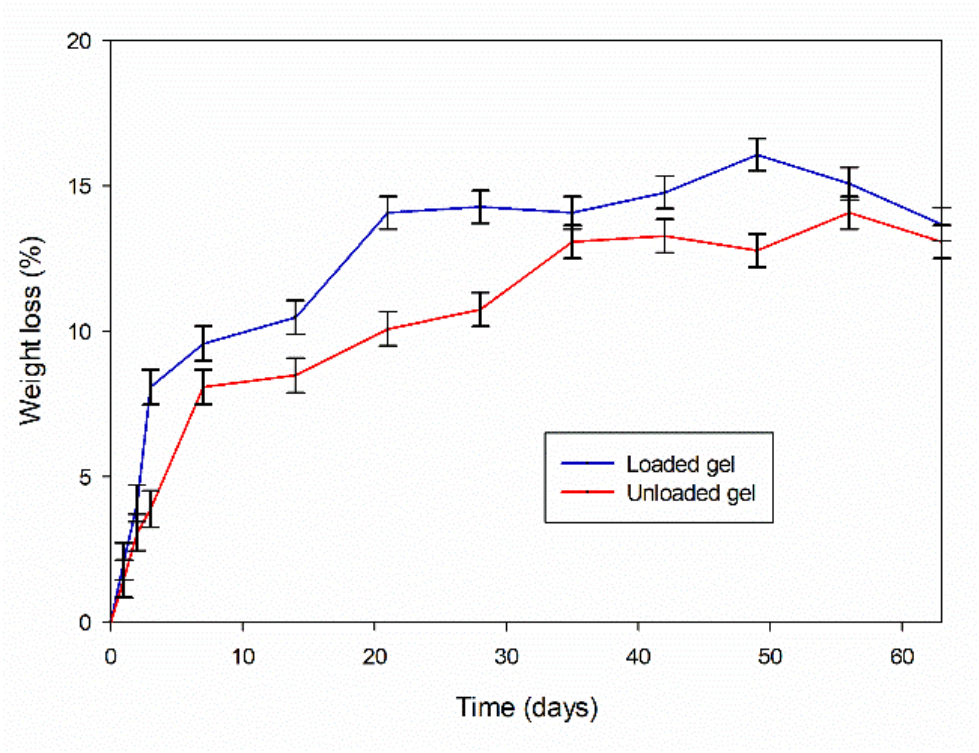

Figure 4.19 - Degradation profiles of unloaded and loaded hydrogels at 37 °C.

4.3.7. *In vitro* cell biocompatibility

Biocompatibility studies were conducted on 3T3 and hRPE cell lines. Both cell lines were utilised as previous studies of potential vitreous substitutes have used both cell lines (Santhanam *et al.*, 2016; Lin *et al.*, 2017; Jiang *et al.*, 2018; Yadav *et al.*, 2021). Studies with the hRPE cell line are particularly important as clinical administration of the hydrogels in the vitreous body would result in direct contact between the substitute and retinal pigment epithelium. The MTT cell viability assays (Figure 4.20) showed that the unloaded and loaded hydrogels were not toxic to either cell line over 48- and 72 hours. Particularly noteworthy, is the promotion of cell growth with the 3T3 cell lines.

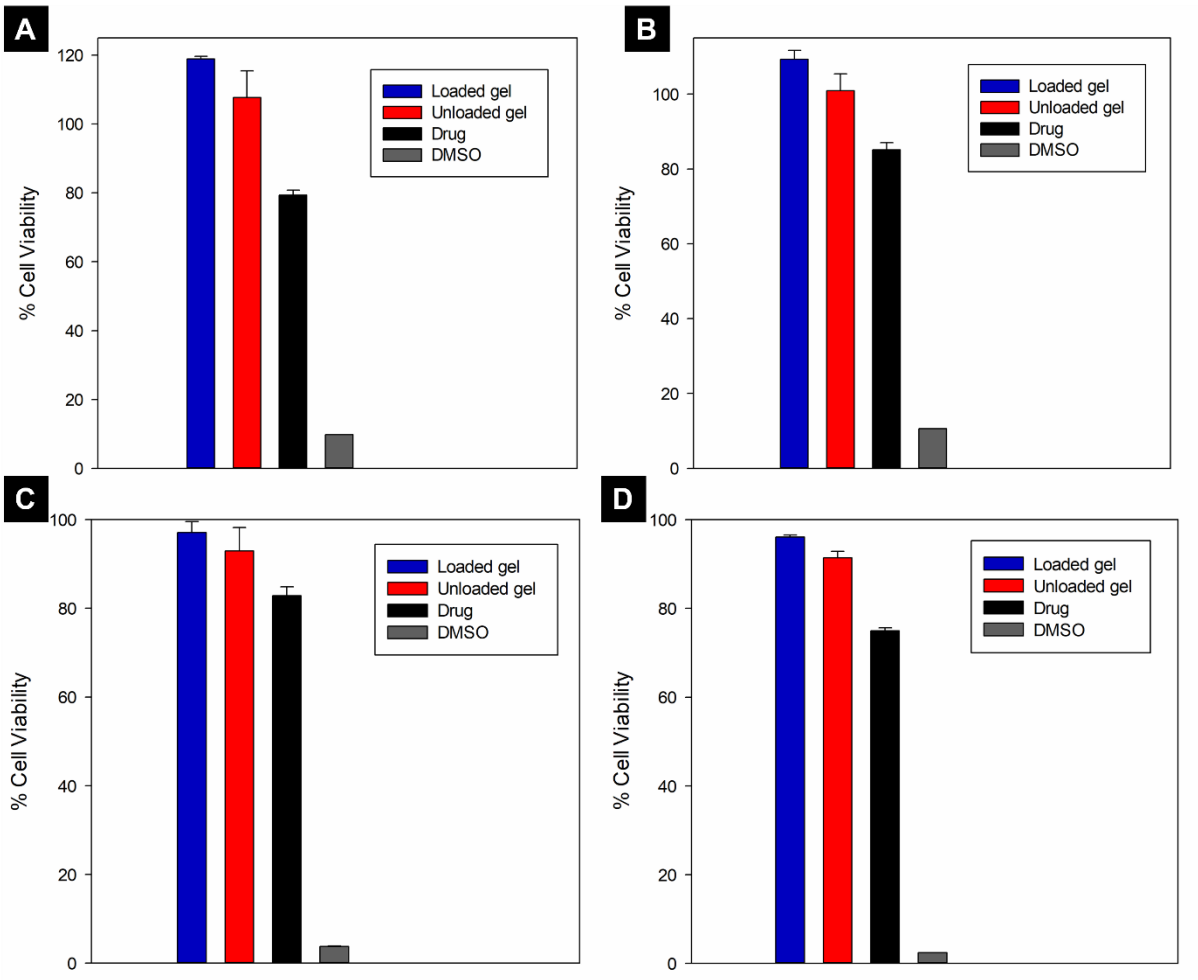

Figure 4.20 - Cell biocompatibility with A) 3T3 cells after 48 hours, B) 3T3 cells after 72 hours, C) hRPE cells after 48 hours and, D) hRPE cells after 72 hours.

4.4. Conclusions

The study assessed the potential of PLGA nanoparticles entrapped in a hyaluronic acid-poloxamer blend hydrogel as a vitreous substitute. The study prepared unloaded and nanoparticle-loaded hydrogels that displayed similar optical and viscoelastic properties to the natural vitreous. Rheological studies showed the ability of the hydrogels to form *in situ*, and both hydrogels can be injected via similar gauge needles as those currently used clinically. Furthermore, the hydrogels demonstrate excellent swelling and degradation behaviour furthering their potential to be suited as vitreous substitutes. Additionally, the nanoparticle-loaded hydrogel showed long-term drug release of TA and thus has the potential for delivery of other ocular therapeutics for the treatment of posterior segment diseases. Lastly, both hydrogels displayed biocompatibility with two cell lines including a retinal cell line. It is concluded that the

developed nanoparticle-loaded hydrogel has the potential as a long-term drug delivery system and both hydrogels (the unloaded and loaded) have the potential to act as vitreous substitutes.

4.5. References

Abd El Hady, W.E., Mohamed, E.A., Soliman, O.A.E.-A. & El-Sabbagh, H.M. (2019) In vitro-in vivo evaluation of chitosan-PLGA nanoparticles for potentiated gastric retention and anti-ulcer activity of diosmin. *International journal of nanomedicine*. 14, 7191–7213. doi:10.2147/IJN.S213836.

Abrego, G., Alvarado, H., Souto, E.B., Guevara, B., Bellowa, L.H., Parra, A., Calpena, A. & Garcia, M.L. (2015) Biopharmaceutical profile of pranoprofen-loaded PLGA nanoparticles containing hydrogels for ocular administration. *European Journal of Pharmaceutics and Biopharmaceutics*. 95, 261–270. doi:10.1016/j.ejpb.2015.01.026.

Al Khateb, K., Ozhmukhametova, E.K., Mussin, M.N., Seilkhanov, S.K., Rakhypbekov, T.K., Lau, W.M. & Khutoryanskiy, V. v. (2016) In situ gelling systems based on Pluronic F127/Pluronic F68 formulations for ocular drug delivery. *International Journal of Pharmaceutics*. 502 (1–2), 70–79. doi:10.1016/j.ijpharm.2016.02.027.

Alexandridis, P. & Alan Hatton, T. (1995) Poly(ethylene oxide)-poly(propylene oxide)-poly(ethylene oxide) block copolymer surfactants in aqueous solutions and at interfaces: thermodynamics, structure, dynamics, and modeling. *Colloids and Surfaces A: Physicochemical and Engineering Aspects*. 96 (1–2), 1–46. doi:10.1016/0927-7757(94)03028-X.

Alkholief, M., Albasit, H., Alhowyan, A., Alshehri, S., Raish, M., Abul Kalam, M. & Alshamsan, A. (2019) Employing a PLGA-TPGS based nanoparticle to improve the ocular delivery of Acyclovir. *Saudi Pharmaceutical Journal*. 27 (2), 293–302. doi:10.1016/j.jsps.2018.11.011.

Almeida, H., Amaral, M.H., Lobão, P. & Lobo, J.M.S. (2014) In situ gelling systems: a strategy to improve the bioavailability of ophthalmic pharmaceutical formulations. *Drug Discovery Today*. 19 (4), 400–412. doi:10.1016/j.drudis.2013.10.001.

Almeida, M., Magalhães, M., Veiga, F. & Figueiras, A. (2018) Poloxamers, poloxamines and polymeric micelles: Definition, structure and therapeutic applications in cancer. *Journal of Polymer Research*. 25 (1), 31. doi:10.1007/s10965-017-1426-x.

Awwad, S., Abubakre, A., Angkawinitwong, U., Khaw, P.T. & Brocchini, S. (2019) In situ antibody-loaded hydrogel for intravitreal delivery. *European Journal of Pharmaceutical Sciences*. 137 (March), 104993. doi:10.1016/j.ejps.2019.104993.

Baino, F. (2011) Towards an ideal biomaterial for vitreous replacement: Historical overview and future trends. *Acta biomaterialia*. 7 (3), 921–935. doi:10.1016/j.actbio.2010.10.030.

Baker, A.E.G., Cui, H., Ballios, B.G., Ing, S., Yan, P., Wolfer, J., Wright, T., Dang, M., Gan, N.Y., Cooke, M.J., Ortín-Martínez, A., Wallace, V.A., van der Kooy, D., Devenyi, R. & Shoichet, M.S. (2021) Stable oxime-crosslinked hyaluronan-based hydrogel as a biomimetic vitreous substitute. *Biomaterials*. 271, 120750. doi:10.1016/j.biomaterials.2021.120750.

Bisht, R., Jaiswal, J.K. & Rupenthal, I.D. (2017) Nanoparticle-loaded biodegradable light-responsive in situ forming injectable implants for effective peptide delivery to the posterior segment of the eye. *Medical Hypotheses*. 103, 5–9. doi:10.1016/j.mehy.2017.03.033.

Boettner, E.A. & Wolter, J.R. (1962) Transmission of the Ocular Media. *Investigative Ophthalmology & Visual Science*. 1 (6), 776–783.

Chirila, T. v. & Hong, Y. (1998) The Vitreous Humor. In: *Handbook of Biomaterial Properties*. Boston, MA, Springer US. pp. 125–131. doi:10.1007/978-1-4615-5801-9_12.

Cilurzo, F., Selmin, F., Minghetti, P., Adami, M., Bertoni, E., Lauria, S. & Montanari, L. (2011) Injectability Evaluation: An Open Issue. *AAPS PharmSciTech*. 12 (2), 604–609. doi:10.1208/s12249-011-9625-y.

Couch, S.M., Bakri, S.J. (2008) Intravitreal triamcinolone for intraocular inflammation and associated macular edema. *Clinical Ophthalmology*. 41. doi:10.2147/OPTH.S4477.

Cunha, A.M., Iglésias, M.M., Rocha-Sousa, A., Falcão-Reis, F. & Falcão, M. (2021) Endophthalmitis following Intravitreal Injection, Cataract Surgery, and Vitrectomy: Clinical Features and Visual Outcomes A. Meduri (ed.). *Journal of Ophthalmology*. 2021, 1–8. doi:10.1155/2021/9985821.

Danhier, F., Ansorena, E., Silva, J.M., Coco, R., le Breton, A. & Préat, V. (2012) PLGA-based nanoparticles: an overview of biomedical applications. *Journal of controlled release : official journal of the Controlled Release Society*. 161 (2), 505–522. doi:10.1016/j.jconrel.2012.01.043.

Dave, V.P., Pathengay, A., Schwartz, S.G. & Flynn, H.W. (2014) Endophthalmitis following pars plana vitrectomy: a literature review of incidence, causative organisms, and treatment outcomes. *Clinical ophthalmology (Auckland, N.Z.)*. 8, 2183–2188. doi:10.2147/OPTH.S71293.

Davidorf, F.H., Chambers, R.B., Kwon, O.W., Doyle, W., Gresak, P. & Frank, S.G. (1990) Ocular toxicity of vitreal pluronic polyol F-127. *Retina (Philadelphia, Pa.)*. 10 (4), 297–300. doi:10.1097/00006982-199010000-00013.

D'Avila Carvalho Erbetta, C., Alves, R.J., Resende, J.M., de Souza Freitas, R.F. & de Sousa, R.G. (2012) Synthesis and Characterization of Poly(D,L-Lactide-co-Glycolide) Copolymer. *Journal of Biomaterials and Nanobiotechnology*. 03 (02), 208–225. doi:10.4236/jbnb.2012.32027.

Davis, J.T., Hamilton, P.D. & Ravi, N. (2017) Poly(acrylamide co-acrylic acid) for use as an in situ gelling vitreous substitute. *Journal of Bioactive and Compatible Polymers*. 32 (5), 528–541. doi:10.1177/0883911516688482.

Ding, D. & Zhu, Q. (2018) Recent advances of PLGA micro/nanoparticles for the delivery of biomacromolecular therapeutics. *Materials Science and Engineering: C*. 92 (December 2017), 1041–1060. doi:10.1016/j.msec.2017.12.036.

Donati, S., Caprani, S.M., Airaghi, G., Vinciguerra, R., Bartalena, L., Testa, F., Mariotti, C., Porta, G., Simonelli, F. & Azzolini, C. (2014) Vitreous Substitutes: The Present and the Future. *BioMed Research International*. 2014 (May), 1–12. doi:10.1155/2014/351804.

Dumortier, G., Grossiord, J.L., Agnely, F. & Chaumeil, J.C. (2006) A Review of Poloxamer 407 Pharmaceutical and Pharmacological Characteristics. *Pharmaceutical Research*. 23 (12), 2709–2728. doi:10.1007/s11095-006-9104-4.

Edelhauser, H.F., Rowe-Rendleman, C.L., Robinson, M.R., Dawson, D.G., Chader, G.J., et al. (2010) Ophthalmic Drug Delivery Systems for the Treatment of Retinal Diseases: Basic Research to Clinical Applications. *Investigative Opthalmology & Visual Science*. 51 (11), 5403. doi:10.1167/iovs.10-5392.

Eibenberger, K., Sacu, S., Rezar-Dreindl, S., Schmidt-Erfurth, U. & Georgopoulos, M. (2020) Silicone Oil Tamponade in Rhegmatogenous Retinal Detachment: Functional and Morphological Results. *Current Eye Research*. 45 (1), 38–45. doi:10.1080/02713683.2019.1652917.

Elsaid, N., Jackson, T.L., Elsaid, Z., Alqathama, A. & Somavarapu, S. (2016) PLGA Microparticles Entrapping Chitosan-Based Nanoparticles for the Ocular Delivery of Ranibizumab. *Molecular Pharmaceutics*. 13 (9), 2923–2940. doi:10.1021/acs.molpharmaceut.6b00335.

Esmaeili, F., Atyabi, F. & Dinarvand, R. (2007) Preparation of PLGA nanoparticles using TPGS in the spontaneous emulsification solvent diffusion method. *Journal of Experimental Nanoscience*. 2 (3), 183–192. doi:10.1080/17458080701393137.

Essa, D., Choonara, Y.E., Kondiah, P.P.D. & Pillay, V. (2020a) Comparative Nanofabrication of PLGA-Chitosan-PEG Systems Employing Microfluidics and Emulsification Solvent Evaporation Techniques. *Polymers*. 12 (9), 1882. doi:10.3390/polym12091882.

Essa, D., Kondiah, P.P.D., Choonara, Y.E. & Pillay, V. (2020b) The Design of Poly(lactide-co-glycolide) Nanocarriers for Medical Applications. *Frontiers in Bioengineering and Biotechnology*. 8. doi:10.3389/fbioe.2020.00048.

Fathalla, Z.M.A., Vangala, A., Longman, M., Khaled, K.A., Hussein, A.K., El-Garhy, O.H. & Alany, R.G. (2017) Poloxamer-based thermoresponsive ketorolac tromethamine in situ gel preparations: Design, characterisation, toxicity and transcorneal permeation studies. *European Journal of Pharmaceutics and Biopharmaceutics*. 114, 119–134. doi:10.1016/j.ejpb.2017.01.008.

Fernandez-Vigo, J., Sabugal, J.F., Diaz Rey, A., Concheiro, A. & Martinez, R. (1990) Molecular weight dependence of the pharmacokinetic of hydroxypropyl methylcellulose in the vitreous. *Journal of ocular pharmacology*. 6 (2), 137–142. doi:10.1089/jop.1990.6.137.

Foster, W.J., Aliyar, H.A., Hamilton, P. & Ravi, N. (2006) Internal Osmotic Pressure as a Mechanism of Retinal Attachment in a Vitreous Substitute. *Journal of Bioactive and Compatible Polymers*. 21 (3), 221–235. doi:10.1177/0883911506064368.

García-Millán, E., Quintáns-Carballo, M. & Otero-Espinar, F.J. (2017) Solid-state characterization of triamcinolone acetonide nanosuspensiones by X-ray spectroscopy, ATR Fourier transforms infrared spectroscopy and differential scanning calorimetry analysis. *Data in Brief*. 15, 133–137. doi:10.1016/j.dib.2017.09.002.

Gillies, M.C. & Larsson, J. (2007) The Effect of Intravitreal Triamcinolone on Foveal Edema in Exudative Macular Degeneration. *American Journal of Ophthalmology*. 144 (1), 134–136. doi:10.1016/j.ajo.2007.03.019.

Gioffredi, E., Boffito, M., Calzone, S., Giannitelli, S.M., Rainer, A., Trombetta, M., Mozetic, P. & Chiono, V. (2016) Pluronic F127 Hydrogel Characterization and Biofabrication in Cellularized Constructs for Tissue Engineering Applications. *Procedia CIRP*. 49, 125–132. doi:10.1016/j.procir.2015.11.001.

Gómez-Gaete, C., Tsapis, N., Besnard, M., Bochot, A. & Fattal, E. (2007) Encapsulation of dexamethasone into biodegradable polymeric nanoparticles. *International journal of pharmaceutics*. 331 (2), 153–159. doi:10.1016/j.ijpharm.2006.11.028.

Haas, P., Falkner-Radler, C., Wimpissinger, B., Malina, M. & Binder, S. (2016) Needle size in intravitreal injections - pain evaluation of a randomized clinical trial. *Acta Ophthalmologica*. 94 (2), 198–202. doi:10.1111/aos.12901.

Hayashi, K., Okamoto, F., Hoshi, S., Katashima, T., Zujur, D.C., Li, X., Shibayama, M., Gilbert, E.P., Chung, U., Ohba, S., Oshika, T. & Sakai, T. (2017) Fast-forming hydrogel with ultralow polymeric content as an artificial vitreous body. *Nature Biomedical Engineering*. 1 (3), 0044. doi:10.1038/s41551-017-0044.

Hsieh, H.-Y., Lin, W.-Y., Lee, A.L., Li, Y.-C., Chen, Y., Chen, K.-C. & Young, T.-H. (2020) Hyaluronic acid on the urokinase sustained release with a hydrogel system composed of poloxamer 407: HA/P407 hydrogel system for drug delivery J.-Y. Lai (ed.). *PLOS ONE*. 15 (3), e0227784. doi:10.1371/journal.pone.0227784.

Huang, X. & Chau, Y. (2019) Intravitreal nanoparticles for retinal delivery. *Drug Discovery Today*. 24 (8), 1510–1523. doi:10.1016/j.drudis.2019.05.005.

Hwang, Y.-S., Chiang, P.-R., Hong, W.-H., Chiao, C.-C., Chu, I.-M., Hsiue, G.-H. & Shen, C.-R. (2013) Study In Vivo Intraocular Biocompatibility of In Situ Gelation Hydrogels: Poly(2-Ethyl Oxazoline)-Block-Poly(ε-Caprolactone)-Block-Poly(2-Ethyl Oxazoline) Copolymer, Matrigel and Pluronic F127 W.-C. Chin (ed.). *PLoS ONE*. 8 (7), e67495. doi:10.1371/journal.pone.0067495.

Januschowski, K., Schnichels, S., Hurst, J., Hohenadl, C., Reither, C., Rickmann, A., Pohl, L., Bartz-Schmidt, K.-U. & Spitzer, M.S. (2019) Ex vivo biophysical characterization of a hydrogel-based artificial vitreous substitute T. Langmann (ed.). *PLOS ONE*. 14 (1), e0209217. doi:10.1371/journal.pone.0209217.

Javadzadeh, Y., Ahadi, F., Davaran, S., Mohammadi, G., Sabzevari, A. & Adibkia, K. (2010) Preparation and physicochemical characterization of naproxen-PLGA nanoparticles. *Colloids and surfaces. B, Biointerfaces*. 81 (2), 498–502. doi:10.1016/j.colsurfb.2010.07.047.

Jiang, X., Peng, Y., Yang, C., Liu, W. & Han, B. (2018) The feasibility study of an in situ marine polysaccharide-based hydrogel as the vitreous substitute. *Journal of biomedical materials research. Part A*. 106 (7), 1997–2006. doi:10.1002/jbm.a.36403.

Katagiri, Y., Iwasaki, T., Ishikawa, T., Yamakawa, N., Suzuki, H. & Usui, M. (2005) Application of Thermo-setting Gel as Artificial Vitreous. *Japanese Journal of Ophthalmology*. 49 (6), 491–496. doi:10.1007/s10384-005-0255-3.

Kim, E.-Y., Gao, Z.-G., Park, J.-S., Li, H. & Han, K. (2002) rhEGF/HP-β-CD complex in poloxamer gel for ophthalmic delivery. *International Journal of Pharmaceutics*. 233 (1–2), 159–167. doi:10.1016/S0378-5173(01)00933-4.

Kim, R. & Baumal, C. (2004) Anterior segment complications related to vitreous substitutes. *Ophthalmology Clinics of North America*. 17 (4), 569–576. doi:10.1016/j.ohc.2004.06.011.

Kleinberg, T.T., Tzekov, R.T., Stein, L., Ravi, N. & Kaushal, S. (2011) Vitreous Substitutes: A Comprehensive Review. *Survey of Ophthalmology*. 56 (4), 300–323. doi:10.1016/j.survophthal.2010.09.001.

Lajavardi, L., Camelo, S., Agnely, F., Luo, W., Goldenberg, B., Naud, M.-C., Behar-Cohen, F., de Kozak, Y. & Bochot, A. (2009) New formulation of vasoactive intestinal peptide using liposomes in hyaluronic acid gel for uveitis. *Journal of Controlled Release*. 139 (1), 22–30. doi:10.1016/j.jconrel.2009.05.033.

Lamponi, S., Leone, G., Consumi, M., Greco, G. & Magnani, A. (2012) In Vitro Biocompatibility of New PVA-Based Hydrogels as Vitreous Body Substitutes. *Journal of Biomaterials Science, Polymer Edition*. 23 (1–4), 555–575. doi:10.1163/092050611X554499.

Le Goff, M.M. & Bishop, P.N. (2008) Adult vitreous structure and postnatal changes. *Eye*. 22 (10), 1214–1222. doi:10.1038/eye.2008.21.

Lee, B., Litt, M. & Buchsbaum, G. (1992) Rheology of the vitreous body. Part I: Viscoelasticity of human vitreous. *Biorheology*. 29 (5–6), 521–533. doi:10.3233/BIR-1992-295-612.

Leone, G., Consumi, M., Aggravi, M., Donati, A., Lamponi, S. & Magnani, A. (2010) PVA/STMP based hydrogels as potential substitutes of human vitreous. *Journal of Materials Science: Materials in Medicine*. 21 (8), 2491–2500. doi:10.1007/s10856-010-4092-7.

Lin, Y.-K., Chen, K.-H. & Kuan, C.-Y. (2013) The synthesis and characterization of a thermally responsive hyaluronic acid/Pluronic copolymer and an evaluation of its potential as an artificial vitreous substitute. *Journal of Bioactive and Compatible Polymers*. 28 (4), 355–367. doi:10.1177/0883911513491181.

Lin, Y.-K., Sharma, R., Ma, H., Chen, W.-S. & Yao, C.-L. (2017) In situ polymerizable hydrogel incorporated with specific pathogen-free porcine platelet-rich plasma for the

reconstruction of the corneal endothelium. *Journal of the Taiwan Institute of Chemical Engineers*. 78, 65–74. doi:10.1016/j.jtice.2017.06.006.

Liu, Z., Liow, S.S., Lai, S.L., Alli-Shaik, A., Holder, G.E., et al. (2019) Retinal-detachment repair and vitreous-like-body reformation via a thermogelling polymer endotamponade. *Nature biomedical engineering*. 3 (8), 598–610. doi:10.1038/s41551-019-0382-7.

Loureiro, M., Matos, R., Sepulveda, P. & Meira, D. (2017) Intravitreal Injections of Bevacizumab: The Impact of Needle Size in Intraocular Pressure and Pain. *Journal of Current Glaucoma Practice*. 11 (2), 38–41. doi:10.5005/jp-journals-10028-1220.

Luaces-Rodríguez, A., Mondelo-García, C., Zarra-Ferro, I., González-Barcia, M., Aguiar, P., Fernández-Ferreiro, A. & Otero-Espinar, F.J. (2020) Intravitreal anti-VEGF drug delivery systems for age-related macular degeneration. *International Journal of Pharmaceutics*. 573 (August 2019), 118767. doi:10.1016/j.ijpharm.2019.118767.

Manzoor, A.A., Lindner, L.H., Landon, C.D., Park, J.-Y., Simnick, A.J., Dreher, M.R., Das, S., Hanna, G., Park, W., Chilkoti, A., Koning, G.A., ten Hagen, T.L.M., Needham, D. & Dewhirst, M.W. (2012) Overcoming Limitations in Nanoparticle Drug Delivery: Triggered, Intravascular Release to Improve Drug Penetration into Tumors. *Cancer Research*. 72 (21), 5566–5575. doi:10.1158/0008-5472.CAN-12-1683.

Maruoka, S., Matsuura, T., Kawasaki, K., Okamoto, M., Yoshiaki, H., Kodama, M., Sugiyama, M. & Annaka, M. (2006) Biocompatibility of Polyvinylalcohol Gel as a Vitreous Substitute. *Current Eye Research*. 31 (7–8), 599–606. doi:10.1080/02713680600813854.

Meng, T., Kulkarni, V., Simmers, R., Brar, V. & Xu, Q. (2019) Therapeutic implications of nanomedicine for ocular drug delivery. *Drug discovery today*. 24 (8), 1524–1538. doi:10.1016/j.drudis.2019.05.006.

Mishra, D., Gade, S., Glover, K., Sheshala, R. & Singh, T.R.R. (2023) Vitreous Humor: Composition, Characteristics and Implication on Intravitreal Drug Delivery. *Current eye research*. 48 (2), 208–218. doi:10.1080/02713683.2022.2119254.

Mohammadi-Samani, S. & Taghipour, B. (2015) PLGA micro and nanoparticles in delivery of peptides and proteins; problems and approaches. *Pharmaceutical Development and Technology*. 20 (4), 385–393. doi:10.3109/10837450.2014.882940.

Munir, W.M., Pulido, J.S., Sharma, M.C. & Buerk, B.M. (2005) Intravitreal triamcinolone for treatment of complicated proliferative diabetic retinopathy and proliferative vitreoretinopathy. *Canadian Journal of Ophthalmology*. 40 (5), 598–604. doi:10.1016/S0008-4182(05)80052-3.

Necas, J., Bartosikova, L., Brauner, P. & Kolar, J. (2008) Hyaluronic acid (hyaluronan): a review. *Veterinarni Medicina*.53 (8).

Nickerson, C.S., Karageozian, H.L., Park, J. & Kornfield, J.A. (2005) Internal Tension: A Novel Hypothesis Concerning the Mechanical Properties of the Vitreous Humor. *Macromolecular Symposia*. 227 (1), 183–190. doi:10.1002/masy.200550918.

Niu, C., Li, X., Wang, Y., Liu, X., Shi, J. & Wang, X. (2019) Design and performance of a poly(vinyl alcohol)/silk fibroin enzymatically crosslinked semi-interpenetrating hydrogel for a potential hydrophobic drug delivery. *RSC Advances*. 9 (70), 41074–41082. doi:10.1039/c9ra09344c.

Osswald, C.R., Guthrie, M.J., Avila, A., Valio, J.A., Mieler, W.F. & Kang-Mieler, J.J. (2017) In Vivo Efficacy of an Injectable Microsphere-Hydrogel Ocular Drug Delivery System. *Current Eye Research*. 42 (9), 1293–1301. doi:10.1080/02713683.2017.1302590.

Otsuka, K., Imai, H., Fujii, A., Miki, A., Tagami, M., Azumi, A. & Nakamura, M. (2018) Comparison of 25- and 27-Gauge Pars Plana Vitrectomy in Repairing Primary Rhegmatogenous Retinal Detachment. *Journal of Ophthalmology*. 2018, 1–5. doi:10.1155/2018/7643174.

Pandit, J., Sultana, Y. & Aqil, M. (2017) Chitosan-coated PLGA nanoparticles of bevacizumab as novel drug delivery to target retina: optimization, characterization, and *in vitro* toxicity evaluation. *Artificial Cells, Nanomedicine, and Biotechnology*. 45 (7), 1397–1407. doi:10.1080/21691401.2016.1243545.

Pulido, J.S., Pulido, C.M., Bakri, S.J., McCannel, C.A. & Cameron, J.D. (2007) The use of 31-gauge needles and syringes for intraocular injections. *Eye (London, England)*. 21 (6), 829–830. doi:10.1038/sj.eye.6702514.

Qi, H., Chen, W., Huang, C., Li, L., Chen, C., Li, W. & Wu, C. (2007) Development of a poloxamer analogs/carbopol-based in situ gelling and mucoadhesive ophthalmic delivery system for puerarin. *International Journal of Pharmaceutics*. 337 (1–2), 178–187. doi:10.1016/j.ijpharm.2006.12.038.

Raia, N.R., Jia, D., Ghezzi, C.E., Muthukumar, M. & Kaplan, D.L. (2020) Characterization of silk-hyaluronic acid composite hydrogels towards vitreous humor substitutes. *Biomaterials*. 233 (July 2019), 119729. doi:10.1016/j.biomaterials.2019.119729.

Rangabhatla, A.S.L., Tantishaiyakul, V., Oungbho, K. & Boonrat, O. (2016) Fabrication of pluronic and methylcellulose for etidronate delivery and their application for osteogenesis. *International Journal of Pharmaceutics*. 499 (1–2), 110–118. doi:10.1016/j.ijpharm.2015.12.070.

Rizzo, S., Barca, F., Caporossi, T. & Mariotti, C. (2015) Twenty-Seven–Gauge Vitrectomy for Various Vitreoretinal Diseases. *Retina*. 35 (6), 1273–1278. doi:10.1097/IAE.0000000000000545.

Russo, E. & Villa, C. (2019) Poloxamer Hydrogels for Biomedical Applications. *Pharmaceutics*. 11 (12), 671. doi:10.3390/pharmaceutics11120671.

Sabzevari, A., Adibkia, K., Hashemi, H., Hedayatfar, A., Mohsenzadeh, N., Atyabi, F., Ghahremani, M.H. & Dinarvand, R. (2013) Polymeric triamcinolone acetonide nanoparticles as a new alternative in the treatment of uveitis: In vitro and in vivo studies. *European Journal of Pharmaceutics and Biopharmaceutics*. 84 (1), 63–71. doi:10.1016/j.ejpb.2012.12.010.

Sakurai, E., Ozeki, H., Kunou, N. & Ogura, Y. (2001) Effect of Particle Size of Polymeric Nanospheres on Intravitreal Kinetics. *Ophthalmic Research*. 33 (1), 31–36. doi:10.1159/000055638.

Salama, A.H., Mahmoud, A.A. & Kamel, R. (2016) A Novel Method for Preparing Surface-Modified Fluocinolone Acetonide Loaded PLGA Nanoparticles for Ocular Use: In Vitro and In Vivo Evaluations. *AAPS PharmSciTech*. 17 (5), 1159–1172. doi:10.1208/s12249-015-0448-0.

Santhanam, S., Liang, J., Struckhoff, J., Hamilton, P.D. & Ravi, N. (2016) Biomimetic hydrogel with tunable mechanical properties for vitreous substitutes. *Acta Biomaterialia*. 43, 327–337. doi:10.1016/j.actbio.2016.07.051.

Sapino, S., Peira, E., Chirio, D., Chindamo, G., Guglielmo, S., Oliaro-Bosso, S., Barbero, R., Vercelli, C., Re, G., Brunella, V., Riedo, C., Fea, A.M. & Gallarate, M. (2019) Thermosensitive Nanocomposite Hydrogels for Intravitreal Delivery of Cefuroxime. *Nanomaterials*. 9 (10), 1461. doi:10.3390/nano9101461.

Schnichels, S., Schneider, N., Hohenadl, C., Hurst, J., Schatz, A., Januschowski, K. & Spitzer, M.S. (2017) Efficacy of two different thiol-modified crosslinked hyaluronate formulations as vitreous replacement compared to silicone oil in a model of retinal detachment A. Wedrich (ed.). *PLOS ONE*. 12 (3), e0172895. doi:10.1371/journal.pone.0172895.

Schramm, C., Spitzer, M.S., Henke-Fahle, S., Steinmetz, G., Januschowski, K., Heiduschka, P., Geis-Gerstorfer, J., Biedermann, T., Bartz-Schmidt, K.U. & Szurman, P. (2012) The Cross-linked Biopolymer Hyaluronic Acid as an Artificial Vitreous Substitute. *Investigative Opthalmology & Visual Science*. 53 (2), 613. doi:10.1167/iovs.11-7322.

Schulz, A., Wahl, S., Rickmann, A., Ludwig, J., Stanzel, B. v., von Briesen, H. & Szurman, P. (2019) Age-Related Loss of Human Vitreal Viscoelasticity. *Translational Vision Science & Technology*. 8 (3), 56. doi:10.1167/tvst.8.3.56.

Schweitzer, C., Delyfer, M.-N., Colin, J. & Korobelnik, J.-F. (2009) 23-Gauge transconjunctival sutureless pars plana vitrectomy: results of a prospective study. *Eye*. 23 (12), 2206–2214. doi:10.1038/eye.2008.431.

Senapati, S., Mahanta, A.K., Kumar, S. & Maiti, P. (2018) Controlled drug delivery vehicles for cancer treatment and their performance. *Signal Transduction and Targeted Therapy*. 3 (1), 7. doi:10.1038/s41392-017-0004-3.

Silva, A.F., Alves, M.A. & Oliveira, M.S.N. (2017) Rheological behaviour of vitreous humour. *Rheologica Acta*. 56 (4), 377–386. doi:10.1007/s00397-017-0997-0.

Singh-Joy, S.D. & McLain, V.C. (2008) Safety Assessment of Poloxamers 101, 105, 108, 122, 123, 124, 181, 182, 183, 184, 185, 188, 212, 215, 217, 231, 234, 235, 237, 238, 282, 284, 288, 331, 333, 334, 335, 338, 401, 402, 403, and 407, Poloxamer 105 Benzoate, and Poloxamer 182 Dibenzoate as Used in Cosmetics. *International Journal of Toxicology*. 27 (2_suppl), 93–128. doi:10.1080/10915810802244595.

Smith, R.C., Smith, G.T. & Wong, D. (1990) Refractive changes in silicone filled eyes. *Eye*. 4 (1), 230–234. doi:10.1038/eye.1990.32.

Suri, S. & Banerjee, R. (2006) In vitro evaluation of in situ gels as short term vitreous substitutes. *Journal of biomedical materials research. Part A*. 79 (3), 650–664. doi:10.1002/jbm.a.30917.

Swindle, K.E. & Ravi, N. (2007) Recent advances in polymeric vitreous substitutes. *Expert Review of Ophthalmology*. 2 (2), 255–265. doi:10.1586/17469899.2.2.255.

Tang, Z., Jiang, F., Zhang, Y., Zhang, Y., YuanYang, Huang, X., Wang, Y., Zhang, D., Ni, N., Liu, F., Luo, M., Fan, X., Zhang, W. & Gu, P. (2019) Mussel-inspired injectable hydrogel and its counterpart for actuating proliferation and neuronal differentiation of retinal progenitor cells. *Biomaterials*. 194, 57–72. doi:10.1016/j.biomaterials.2018.12.015.

Thacker, M., Tseng, C.-L. & Lin, F.-H. (2020) Substitutes and Colloidal System for Vitreous Replacement and Drug Delivery: Recent Progress and Future Prospective. *Polymers*. 13 (1), 121. doi:10.3390/polym13010121.

Thoniyot, P., Tan, M.J., Karim, A.A., Young, D.J. & Loh, X.J. (2015) Nanoparticle-Hydrogel Composites: Concept, Design, and Applications of These Promising, Multi-Functional Materials. *Advanced Science*. 2 (1–2), 1400010. doi:10.1002/advs.201400010.

Thrimawithana, T.R., Young, S., Bunt, C.R., Green, C. & Alany, R.G. (2011) Drug delivery to the posterior segment of the eye. *Drug Discovery Today*. 16 (5–6), 270–277. doi:10.1016/j.drudis.2010.12.004.

Tram, N.K., Jiang, P., Torres-Flores, T.C., Jacobs, K.M., Chandler, H.L. & Swindle-Reilly, K.E. (2020) A Hydrogel Vitreous Substitute that Releases Antioxidant. *Macromolecular Bioscience*. 20 (2), 1900305. doi:10.1002/mabi.201900305.

Tram, N.K. & Swindle-Reilly, K.E. (2018) Rheological properties and age-related changes of the human vitreous humor. *Frontiers in Bioengineering and Biotechnology*. 6 (DEC), 1–12. doi:10.3389/fbioe.2018.00199.

Wang, K., Mitra, R.N., Zheng, M. & Han, Z. (2018) Nanoceria-loaded injectable hydrogels for potential age-related macular degeneration treatment. *Journal of Biomedical Materials Research Part A*. 106 (11), 2795–2804. doi:10.1002/jbm.a.36450.

Yadav, I., Purohit, S.D., Singh, H., Bhushan, S., Yadav, M.K., Velpandian, T., Chawla, R., Hazra, S. & Mishra, N.C. (2021a) Vitreous substitutes: An overview of the properties, importance, and development. *Journal of Biomedical Materials Research Part B: Applied Biomaterials*. 109 (8), 1156–1176. doi:10.1002/jbm.b.34778.

Yadav, I., Purohit, S.D., Singh, H., Das, N., Roy, P. & Mishra, N.C. (2021b) A highly transparent tri-polymer complex in situ hydrogel of HA, collagen and four-arm-PEG as potential vitreous substitute. *Biomedical Materials*. 16 (6), 065018. doi:10.1088/1748-605X/ac2714.

Yan, J., Peng, X., Cai, Y. & Cong, W. (2018) Development of facile drug delivery platform of ranibizumab fabricated PLGA-PEGylated magnetic nanoparticles for age-related macular degeneration therapy. *Journal of Photochemistry and Photobiology B: Biology*. 183 (February), 133–136. doi:10.1016/j.jphotobiol.2018.04.033.

Yang, H., Wang, R., Gu, Q. & Zhang, X. (2008) Feasibility study of chitosan as intravitreous tamponade material. *Graefe's Archive for Clinical and Experimental Ophthalmology*. 246 (8), 1097–1105. doi:10.1007/s00417-008-0813-8.

Yu, S., Wang, S., Xia, L., Hu, H., Zou, M., Jiang, Z., Chi, J., Zhang, Y., Li, H., Yang, C., Liu, W. & Han, B. (2022) Injectable self-crosslinking hydrogels based on hyaluronic acid as vitreous substitutes. *International Journal of Biological Macromolecules*. 208, 159–171. doi:10.1016/j.ijbiomac.2022.03.046.

Yu, Y., Lau, L.C.M., Lo, A.C. & Chau, Y. (2015) Injectable Chemically Crosslinked Hydrogel for the Controlled Release of Bevacizumab in Vitreous: A 6-Month In Vivo Study. *Translational Vision Science & Technology*. 4 (2), 5. doi:10.1167/tvst.4.2.5.

Zhang, Q., Fassihi, M.A. & Fassihi, R. (2018) Delivery Considerations of Highly Viscous Polymeric Fluids Mimicking Concentrated Biopharmaceuticals: Assessment of Injectability via Measurement of Total Work Done “WT”. *AAPS PharmSciTech*. 19 (4), 1520–1528. doi:10.1208/s12249-018-0963-x.

Zhang, X., Wei, D., Xu, Y. & Zhu, Q. (2021) Hyaluronic acid in ocular drug delivery. *Carbohydrate Polymers*.264. doi:10.1016/j.carbpol.2021.118006.

Zhang, X.-P., Sun, J.-G., Yao, J., Shan, K., Liu, B.-H., Yao, M.-D., Ge, H.-M., Jiang, Q., Zhao, C. & Yan, B. (2018) Effect of nanoencapsulation using poly (lactide-co-glycolide) (PLGA) on anti-angiogenic activity of bevacizumab for ocular angiogenesis therapy. *Biomedicine & Pharmacotherapy*. 107 (August), 1056–1063. doi:10.1016/j.biopha.2018.08.092.

Zimberlin, J.A., McManus, J.J. & Crosby, A.J. (2010) Cavitation rheology of the vitreous: mechanical properties of biological tissue. *Soft Matter*. 6 (15), 3632. doi:10.1039/b925407b.

5.1. Introduction

In vitro results of toxicity, biodegradation and cell behaviour are known to vary under *in vivo* settings (Jurga *et al.*, 2011). *In vivo* analysis enables the assessment of the clinical translational potential of the fabricated nanoparticle-loaded hydrogel under *in vivo* conditions. To assess the full safety of the hydrogel an *in vivo* assessment is essential. *In vivo* pilot studies, such as the study reported in this Chapter, allow for the assessment of the biocompatibility of therapeutic agents while minimising the number of animals used.

Studies on the vitreous of various animals have been conducted to assess their nature and composition in relation to the human vitreous (Suri and Banerjee, 2006; Silva *et al.*, 2017; Shafaie *et al.*, 2018; Tram and Swindle-Reilly, 2018). These studies have shown that the vitreous humour of the rabbit has many similarities to the human vitreous. Additionally, the rabbit model has been used for various ophthalmic surgery evaluations as the rabbit eye is larger than the rodent eye and, thus, the ocular tissues, including the vitreous, are larger allowing for easier surgical procedures (Abdo *et al.*, 2017; Clippinger *et al.*, 2021; Daniels *et al.*, 2021). This is especially advantageous for surgeries involving the posterior segment of the eye. *In vivo* studies of various intravitreal injections as well as pars plana vitrectomies with polymeric vitreous substitutes have been conducted using the New Zealand White (NZW) rabbit model (Du Toit *et al.*, 2014; Yu *et al.*, 2015; Yang *et al.*, 2019; Kim *et al.*, 2020; Xue *et al.*, 2020; Huang *et al.*, 2021). Therefore, established protocols and data are available for comparative analysis to determine the efficacy of the fabricated hydrogel. Thus, NZW rabbits were used as the animal model for this study.

The purpose of this chapter was to conduct a pilot, *in vivo* study of the nanoparticle-loaded hydrogel. The unloaded hydrogel was not assessed as the purpose of the pilot study was to assess the preliminary biocompatibility of the entire system (nanoparticle-loaded hydrogel). The study assessed the biocompatibility and *in vivo* drug release profile of the hydrogel over 28 days.

5.2. Materials and Methods

5.2.1. Animal Procurement

The New Zealand White (NZW) rabbits (male and female, weight 2.5-4.5 kg) utilised in this study were procured from the Wits Research Animal Facility (WRAF) of the University of the Witwatersrand. Ethics clearance for this study was obtained from the Wits Animal Ethics Screening Committee, ethics clearance number: 2021/03/07/C (Appendix A). Ethics clearance for this pilot study was granted through umbrella ethics granted to Mrs Uwaezuoke as a co-worker.

5.2.2. Animal preparation and care

Fifteen NZW rabbits of both sexes were used for the pilot *in vivo* study involving intravitreal vitreous removal, vitreous replacement, and subsequent biocompatibility testing. NZW rabbits were individually housed, and cages were maintained at room temperature (25 °C). The rabbits were fed a commercial diet and water was given ad libitum. The NZW rabbits were allowed to acclimatise to the environment one week before the surgery and weighed weekly. A weight loss of 15% or more of its body weight would result in the removal of the rabbit from the study. All procedures conformed to the South African standard for the use and care of animals for scientific purposes and were conducted following the standard operating procedures (SOPs) of the WRAF.

5.2.3. Experimental design and surgical protocol

Rabbits were grouped according to their similarity in weight in groups of three for each time point (Days 5, 7, 14, 21 and 28). Surgery and intervention were conducted in the left eye and the right eye of each rabbit would serve as the negative control (no intervention). Each rabbit was injected with 500 µL of the formulated hydrogel after the removal of the same amount of native vitreous with the procedure discussed henceforth.

All surgeries were performed with sterile technique and with sterile equipment (Figure 5.1 A) as used routinely for human subjects, by an ophthalmologist. An ophthalmological examination of the rabbit eyes was conducted prior to the surgery to ensure that no ocular abnormalities were observed. General anaesthesia was induced with an intramuscular (IM) combination of ketamine and xylazine (40 mg/kg and 10

mg/kg respectively). The rabbits were then appropriately positioned on the operating table. The body temperature of the rabbit was maintained by a heating cushion and skin electrodes were placed to monitor physiological parameters. A wire speculum was inserted in the left eye (Figure 5.1 B) after which the eye was washed with several drops of 5% povidone/iodine and 0.2 mL lignocaine, local anaesthetic was instilled. A 26-gauge needle and 1 mL syringe were used to puncture the eye, 2.0 mm posterior to the superior-temporal limbus where the needle would be visible in the pupil area. Vitreous humour (500 µL) was gently aspirated (Figure 5.1 C) after which the syringe was replaced with a 1 mL syringe containing 500 µL of the loaded hydrogel (Figure 5.1 D). The needle and syringe were held in place for about 30 seconds to allow for the hydrogel to increase in viscosity, to prevent reflux, and to ensure no vitreous haemorrhage occurred. Once the needle was withdrawn, direct pressure was placed on the site of injection. All formulations were sterilised via UV sterilisation overnight. An anaesthetic reversal agent was administered IM to each rabbit, and they were then placed in their cage for recovery. Following surgery, qualitative cage-side observations were conducted following the rabbit grimace scale (Figure 5.2) (Keating *et al.*, 2012) and their weight was measured weekly.

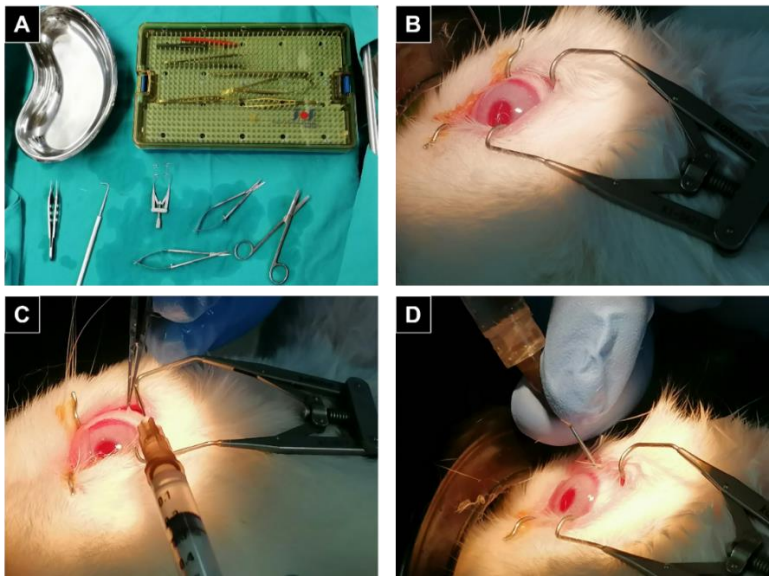

Figure 5.1 - Surgical procedure for intravitreal injection of the loaded hydrogel. A) Sterilised surgical equipment, B) Wire speculum in the left eye to enable better visual field for aspiration and administration, C) Aspiration of native rabbit vitreous, D) Administration of the loaded hydrogel.

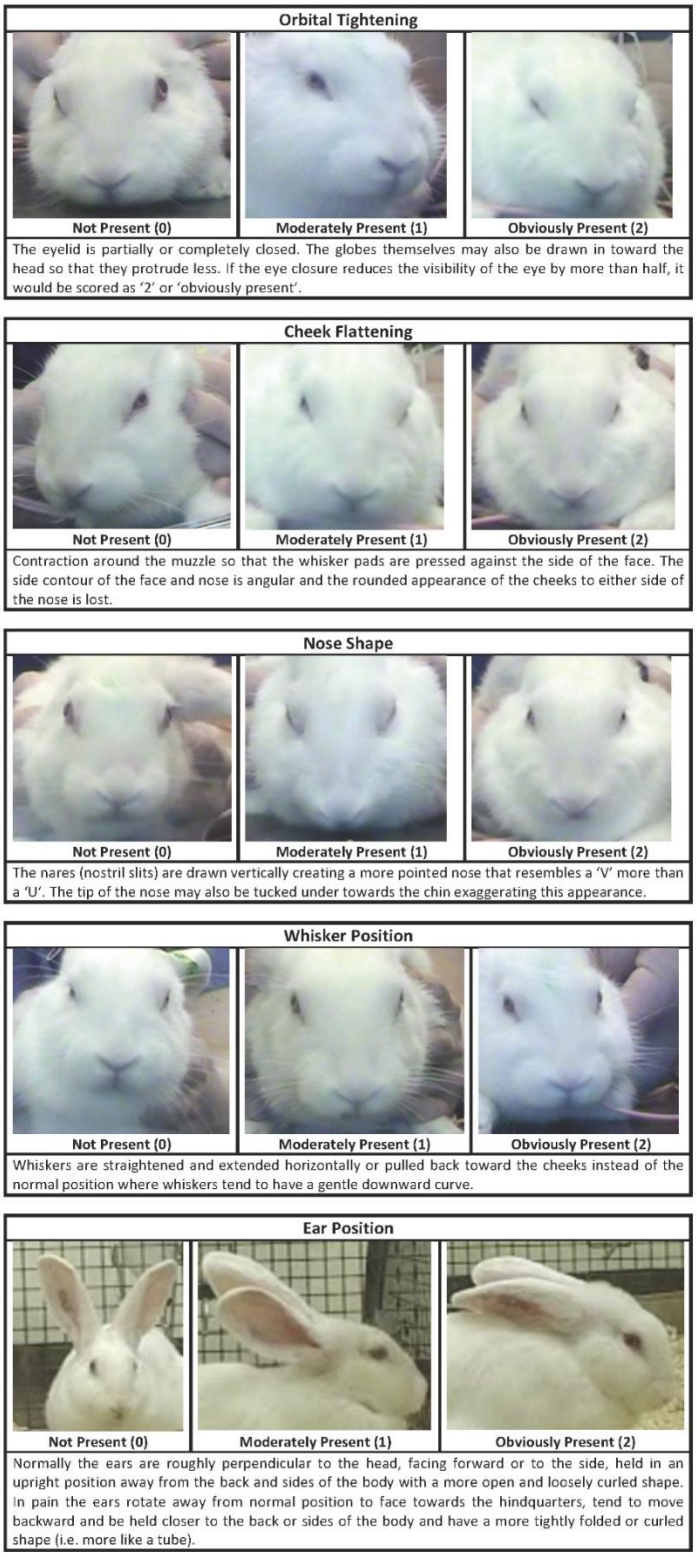

Figure 5.2 - Rabbit Grimace Scale. This image was reused from Keating *et al*. (2012) under the terms of the Creative Commons Attribution License (http://creativecommons.org/licenses/by/2.0).

5.2.4. Euthanisation

Three NZW rabbits were euthanised at each time point (day 5, day 7, day 14, day 21 and day 28). Before euthanisation, 1 mL of blood was taken from each rabbit and centrifuged (Eppendorf centrifuge 5804, Hamburg, Germany) for blood serum drug release studies. An overdose of IV sodium pentobarbital (> 50 mg/kg, 2 mL) was administered via the ear marginal vein for euthanisation followed by enucleation (removal of the eyeball) of the control eye (right eye) and the treated left eye. Aqueous humour and vitreous humour were aspirated from the treated eye and maintained at -80 °C for analysis. The remaining enucleated ocular tissue was immersed and fixed in 10% $^{v}/_{v}$ buffered formalin for histomorphological analysis.

5.2.5. Histomorphological analysis

The enucleated eyes (fixed in 10% $^{v}/_{v}$ formalin) were sent for analysis to IDEXX laboratories (Johannesburg, South Africa). The eyes were cut according to the IDEXX SOP (IdexxSA-AP-SOP-26) and processed in an automated tissue processor according to the histological tissue processing SOP (IdexxSA-AP-SOP-27). Thereafter, sections of the tissue were cut (IdexxSA-AP-SOP-30) and the slides produced stained in an automated Haematoxylin and Eosin tissue stainer (IdexxSA-AP-SOP-205) prior to histological evaluation.

5.2.6 Drug release studies

5.2.6.1. Preparation of standard solutions for the construction of a standard curve

A serial dilution of TA was carried out in 40% $^{v}/_{v}$ ethanol at known concentrations (0.031 – 0.0062 mg/mL). A full ultraviolet spectroscopy (UV-Vis) absorbance reading was taken on the Implen Nanophotometer NP80 (Implen, München, Germany) and the lambda-max (λ-max) of TA was confirmed at 240nm. Thereafter, the absorbance of the aliquots from the TA dilutions was read (n=3).

5.2.6.2. In vivo drug release analysis

Aspirated and frozen blood serum, aqueous humour, and vitreous humour were thawed and centrifuged (Eppendorf centrifuge 5804, Hamburg, Germany). The concentration of TA was evaluated by UV-Vis (Implen Nanophotometer NP80, Implen,

München, Germany) at a wavelength of 240nm as established previously. The absorbance readings were used with the calibration curve to determine the release of TA.

5.2.7. Statistical analysis

All analyses were conducted in triplicate (n = 3). All results were expressed as the mean and standard deviation and data was analysed using Microsoft EXCEL. The level of significance was determined using a student t-test. P values of less than 0.05 ($p < 0.05$) were considered as an indication of statistically significant differences. All graphs were plotted using SigmaPlot 12.0.

5.3. Results and Discussion

5.3.1. Animal post-operative survival, recovery, and behaviour

All the animals survived the intravitreal administration of the loaded hydrogel. Rabbits were awake and responsive within an hour post-surgery and the lights of the room were left off to allow for acclimatisation of their treated eye. The rabbits were checked routinely, and no signs of infection were observed. Partial tightening of the orbit of the treated eye was observed in some rabbits on the first-day post-surgery, reducing thereafter within the first week and not present in the last 3 weeks of the study. This may be due to light sensitivity and tissue sensitivity as a result of the intravitreal injection. The rabbits did not lose weight throughout the study and no obvious markers of discomfort were observed. This substantiates that the intravitreal administration of the nanoparticle-loaded hydrogel is technically feasible in the New Zealand White rabbits, and it is tolerated by the animals.

Macroscopic changes in the treated eye at each timepoint shown in Figure 5.3 are easily compared to the normal untreated rabbit eye in Figure 5.4. The treated eye of the rabbits euthanised 5 days post-surgery displayed macroscopic signs of inflammation, retraction of the orbit, engorgement of the iris vessels, and small amounts of blood in the anterior chamber. These are likely due to trauma from the surgical procedure. Iris vessel engorgement was reduced in the treated eyes of the rabbits that were euthanised 7 days post-administration and no blood was seen in the anterior chamber of the eye. Inflammation was still macroscopically visible with a slight

retraction of the orbit of the treated eye. Inflammation was not macroscopically visible in the rabbits euthanised on days 14, 21 and 28 indicating that the inflammation seen in the first two groups may have been due to the surgical procedure and TA release from the hydrogel would have assisted in the decreased of inflammation. These results are comparable to those reported by Swindle-Reilly *et al*. (2009) and Uesugi *et al*. (2017) with no significant inflammation or gel opacity reported. One of the rabbits developed a cataract due to the perioperative touching of the lens while three rabbits developed a cataract likely due to the hydrogel causing protein or fibre breakdown in the lens of those eyes (Barth *et al.*, 2019).

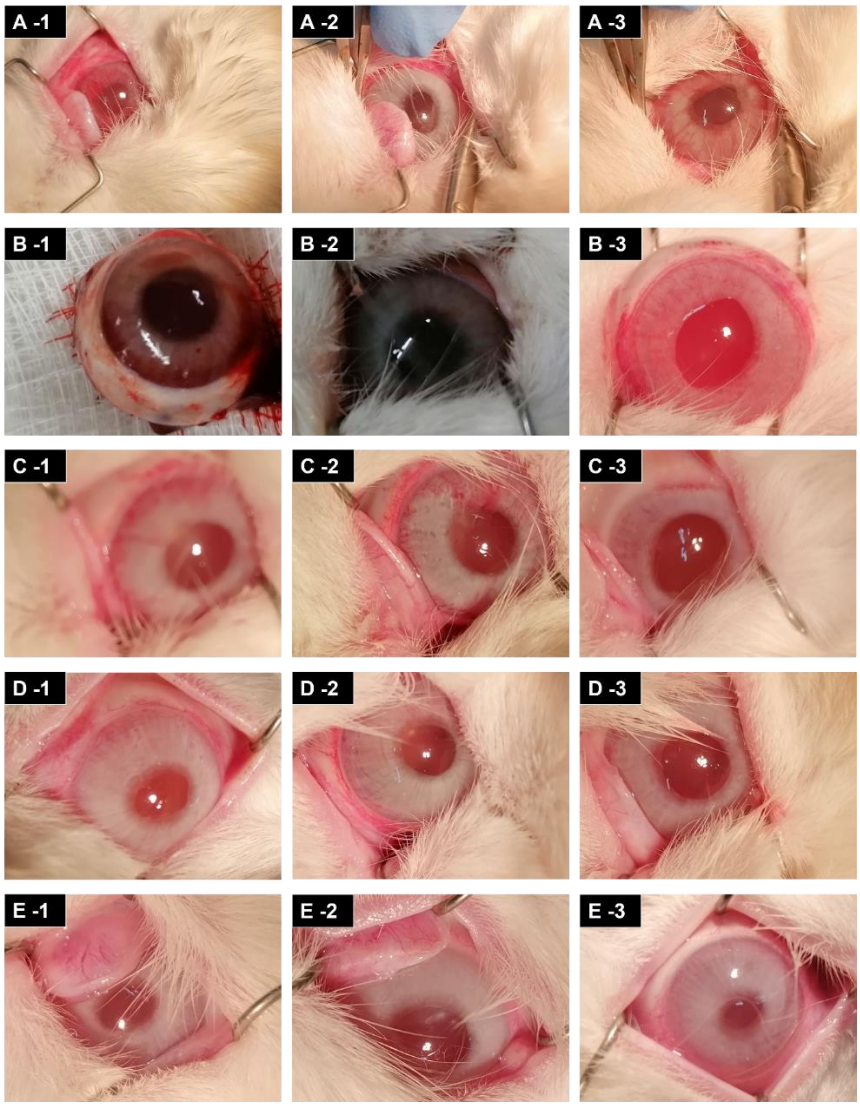

Figure 5.3 - Macroscopic view of the treated rabbit eye A 1-3) Day 5, B 1-3) Day 7, C 1-3) Day 14, D 1-3) Day 21 and E 1-3) Day 28

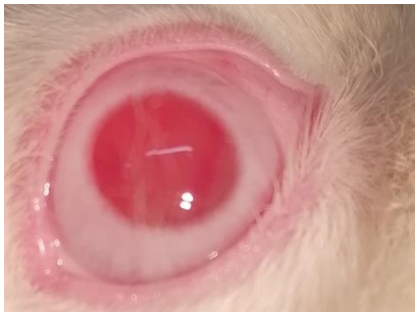

Figure 5.4 - Macroscopic view of the untreated rabbit eye.

5.3.2. Histomorphological analysis

Haematoxylin and eosin (H&E) staining was conducted for the histomorphological analysis and the general histologic observation of the enucleated ocular tissues (Figure 5.5). Morphological changes to the cornea were only observed in the enucleated eyes of the rabbits on day 5 suggesting this may relate to the surgical procedure. Mild inflammation was seen in the bulbar conjunctiva only in the eyes enucleated on day 5, likely due to the changes observed in the cornea. The sclera and periocular soft tissue of all the enucleated eyes were histologically normal and no signs of scleritis were observed. Changes to the choroid were observed for most of the eyes with mild to moderate choroiditis. These changes are proposedly due to ischaemia and not necrosis as typical necrosis signs were not observed. The surface and superficial layers of the optic disc displayed inflammation due to its contact with the vitreous. Lens capsule protein fibres were visible in the vitreous body in some eyes. This may be of surgical origin or due to the piercing of the globe for aspiration of aqueous humour and vitreous humour for *in vivo* drug release studies. Lastly, the inner retinal surfaces that are in close proximity to the vitreous body displayed retinitis. Figure 5.5 depicts the changes in the retina over the 28 days of the study. The retina showed mild inflammation on day 5 increasing to moderate inflammation by day 28. Five (5) enucleated eyes from day 7 to day 28 (two on day 7 and one each for days 14-28) displayed tombstoning of the outer retinal epithelial cells indicative of retinal detachment. Studies by Jakobsson *et al.* (2015), Ben Yahia *et al.* (2016), and Yasuda *et al.* (2016) reported retinal detachment following intravitreal injections. Inflammation to the ocular tissues occurs post-intravitreal surgery in the majority of the studies and

was expected (Swindle and Ravi, 2007; Barth *et al.*, 2019). Histomorphological analysis of rabbit eyes following vitreous substitution conducted by Swindle-Reilly *et al*. (2009), Uesugi *et al*. (2017), and Santhanam *et al*. (2019) demonstrated inflammatory cells localised to the site of vitrectomy and tissues in contact with the vitreous humour similar to those observed in this study. These studies also reported no degenerative changes observed in the retina with H&E staining.

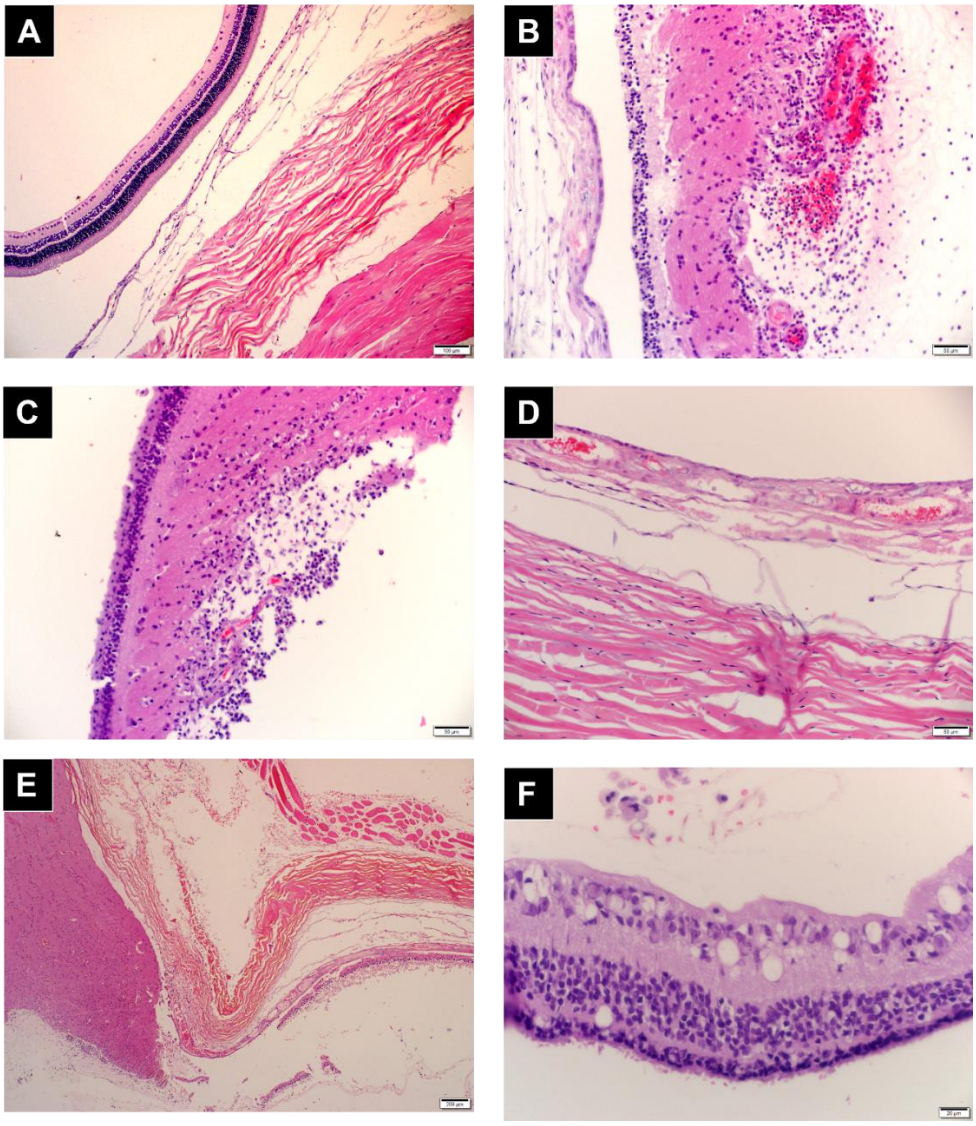

Figure 5.5 - Histological slides at each time point. A) Negative control eye showing the retina, choroid, and sclera at 10x magnification, B – F) hydrogel administered eyes. B) Day 5 shows the retina at 20x magnification, C) Day 7 shows the retina at 20x magnification, D) Day 14 shows the choroid and sclera at 20x magnification, E) Day 21 shows the optic nerve, retina, choroid and sclera at 4x magnification, F) Day 28 showing the retina at 40x magnification.

5.2.3. *In vivo* drug release

Figure 5.6 displays the calibration curve for TA used to analyse the UV-Vis absorbance readings obtained for the blood serum and aspirated vitreous humour and aqueous humour of the studied rabbits. Figure 5.7 depicts the concentration of drug measured in the blood serum, vitreous humour, and aqueous humour at all the euthanisation time points. Minimal amounts of drug were found in the blood indicative of localised drug release. Higher drug release in the blood serum on days 5 and 7 is likely due to perioperative bleeding leading to drug release in the systemic circulation. Drug release within the vitreous and aqueous humour indicates localised drug release with ocular tissues with a release for the duration of the study (28 days). Intravitreal TA has a minimum effective concentration (MEC) of 2 mg/ml (Williamson & O'Donnell, 2005) and a large therapeutic window (Tao & Jonas, 2011). Thus, the drug release levels achieved in this study are equal to or above the MEC and were maintained within the therapeutic window.

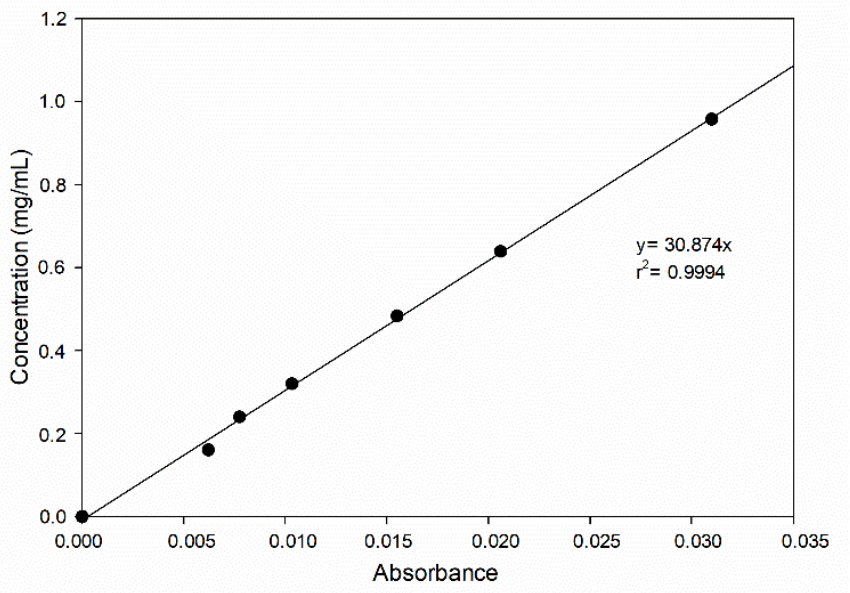

Figure 5.6 - Calibration curve of triamcinolone acetonide.

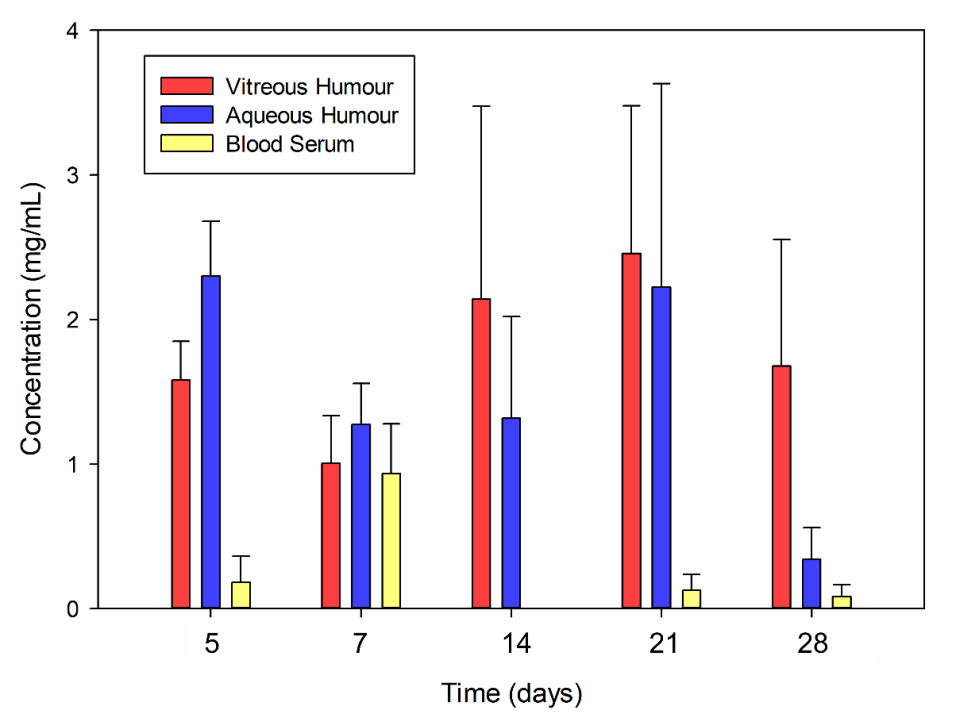

Figure 5.7 - *In vivo* drug release in the vitreous humour, aqueous humour, and blood serum.

5.4. Conclusions

The objective to inject the nanoparticle-loaded hydrogel into an NZW rabbit model was successfully achieved with no loss of life, no post-operative infection, no complete vision loss in the treated eye, and moderate inflammation. As noted in Chapter 4, the hydrogel was easily injectable with a 26-gauge needle and formed *in situ* (no leakage of the vitreous from the site of injection).

While the loaded hydrogel achieved success in many areas, the limitations with surgical equipment prevented the assessment of the potential of the hydrogel to function as a vitreous substitute. This also resulted in some issues with intraocular needle placement leading to post-operative inflammation.

In vivo drug release analysis showed the localised release of drug in the vitreous and aqueous humour throughout all the days of the study indicating that the hydrogel remained in the vitreous. Histomorphological analysis showed higher inflammation in the first week, reducing thereafter for the remaining 3 weeks. This may be due to the

initial inflammation as a result of the surgical procedure, followed by the anti-inflammatory effect with the release of the corticosteroid drug over the 28 days thus reducing intraocular inflammation.

Although these results are promising, a definitive conclusion on the *in vivo* behaviour of the hydrogel cannot be reached as the study was a pilot study. To fully understand the *in vivo* behaviour of the loaded hydrogel and to assess its ability to function as a long-term vitreous substitute, further comprehensive *in vivo* studies would need to be undertaken.

5.5. References

Abdo, M., Haddad, S. & Emam, M. (2017) Development of the New Zealand White Rabbit Eye: I. Pre- and Postnatal Development of Eye Tunics. *Anatomia, Histologia, Embryologia*. 46 (5), 423–430. doi:10.1111/ahe.12284.

Ben Yahia, S., Kahloun, R., Abroug, N., Kaibi, I., Laadhari, G., Jelliti, B. & Khairallah, M. (2016) Comparative effect of topical diclofenac and topical dexamethasone on anterior chamber flare and postoperative pain following rhegmatogenous retinal detachment surgery. *International Ophthalmology*. 36 (5), 623–628. doi:10.1007/s10792-015-0168-1.

Barth, H., Crafoord, S., Arnér, K. & Ghosh, F. (2019) Inflammatory responses after vitrectomy with vitreous substitutes in a rabbit model. *Graefe's Archive for Clinical and Experimental Ophthalmology*. 257 (4), 769–783. doi:10.1007/s00417-019-04242-0.

Clippinger, A.J., Raabe, H.A., Allen, D.G., Choksi, N.Y., van der Zalm, A.J., Kleinstreuer, N.C., Barroso, J. & Lowit, A.B. (2021) Human-relevant approaches to assess eye corrosion/irritation potential of agrochemical formulations. *Cutaneous and Ocular Toxicology*. 40 (2), 145–167. doi:10.1080/15569527.2021.1910291.

Daniels, A.B., Pierce, J.M. & Chen, S. (2021) Complete preclinical platform for intravitreal chemotherapy drug discovery for retinoblastoma: Assessment of pharmacokinetics, toxicity and efficacy using a rabbit model. *MethodsX*. 8, 101358. doi:10.1016/j.mex.2021.101358.

Du Toit, L.C., Carmichael, T., Govender, T., Kumar, P., Choonara, Y.E. & Pillay, V. (2014) In Vitro, In Vivo, and In Silico Evaluation of the Bioresponsive Behavior of an Intelligent Intraocular Implant. *Pharmaceutical Research*. 31 (3), 607–634. doi:10.1007/s11095-013-1184-3.

Huang, W.-C., Cheng, F., Chen, C.-C., Kuo, P.-H., Wang, Y.-J., Yin, S.-C., Tu, C.-M., Wu, M.-H., Wang, W.-Y. & Chen, S.-E. (2021) A Novel Eye Drop Formulation for Potential Treatment of Neovascular Age-Related Macular Degeneration. *Translational Vision Science & Technology*. 10 (14), 23. doi:10.1167/tvst.10.14.23.

Jakobsson, G., Sundelin, K., Zetterberg, H. & Zetterberg, M. (2015) Increased Levels of Inflammatory Immune Mediators in Vitreous From Pseudophakic Eyes. *Investigative Opthalmology & Visual Science*. 56 (5), 3407. doi:10.1167/iovs.15-16837.

Jurga, M., Dainiak, M.B., Sarnowska, A., Jablonska, A., Tripathi, A., Plieva, F.M., Savina, I.N., Strojek, L., Jungvid, H., Kumar, A., Lukomska, B., Domanska-Janik, K., Forraz, N. & McGuckin, C.P. (2011) The performance of laminin-containing cryogel scaffolds in neural tissue regeneration. *Biomaterials*. 32 (13), 3423–3434. doi:10.1016/j.biomaterials.2011.01.049.

Keating, S.C.J., Thomas, A.A., Flecknell, P.A. & Leach, M.C. (2012) Evaluation of EMLA Cream for Preventing Pain during Tattooing of Rabbits: Changes in Physiological, Behavioural and Facial Expression Responses G. Chapouthier (ed.). *PLoS ONE*. 7 (9), e44437. doi:10.1371/journal.pone.0044437.

Kim, H.M., Ha, S., Hong, H.K., Hwang, Y., Kim, P., Yang, E., Chung, J.Y., Park, S., Park, Y.J., Park, K.H., Kim, H. & Woo, S.J. (2020) Intraocular Distribution and Kinetics of Intravitreally Injected Antibodies and Nanoparticles in Rabbit Eyes. *Translational Vision Science & Technology*. 9 (6), 20. doi:10.1167/tvst.9.6.20.

Santhanam, S., Shui, Y.-B., Struckhoff, J., Karakocak, B.B., Hamilton, P.D., Harocopos, G.J. & Ravi, N. (2019) Bioinspired Fibrillary Hydrogel with Controlled Swelling Behavior: Applicability as an Artificial Vitreous. *ACS Applied Bio Materials*. 2 (1), 70–80. doi:10.1021/acsabm.8b00376.

Shafaie, S., Hutter, V., Brown, M.B., Cook, M.T. & Chau, D.Y.S. (2018) Diffusion through the ex vivo vitreal body – Bovine, porcine, and ovine models are poor surrogates for the human vitreous. *International Journal of Pharmaceutics*. 550 (1–2), 207–215. doi:10.1016/j.ijpharm.2018.07.070.

Silva, A.F., Alves, M.A. & Oliveira, M.S.N. (2017) Rheological behaviour of vitreous humour. *Rheologica Acta*. 56 (4), 377–386. doi:10.1007/s00397-017-0997-0.

Suri, S. & Banerjee, R. (2006) In vitro evaluation of in situ gels as short term vitreous substitutes. *Journal of biomedical materials research. Part A*. 79 (3), 650–664. doi:10.1002/jbm.a.30917.

Swindle, K.E. & Ravi, N. (2007) Recent advances in polymeric vitreous substitutes. *Expert Review of Ophthalmology*. 2 (2), 255–265. doi:10.1586/17469899.2.2.255.

Swindle-Reilly, K.E., Shah, M., Hamilton, P.D., Eskin, T.A., Kaushal, S. & Ravi, N. (2009) Rabbit Study of an In Situ Forming Hydrogel Vitreous Substitute. *Investigative Opthalmology & Visual Science*. 50 (10), 4840. doi:10.1167/iovs.08-2891.

Tao, Y. & Jonas, J.B. (2011) Intravitreal Triamcinolone. *Ophthalmologica*. 225 (1), 1–20. doi:10.1159/000317909.

Tram, N.K. & Swindle-Reilly, K.E. (2018) Rheological properties and age-related changes of the human vitreous humor. *Frontiers in Bioengineering and Biotechnology*. 6 (DEC), 1–12. doi:10.3389/fbioe.2018.00199.

Uesugi, K., Sakaguchi, H., Hayashida, Y., Hayashi, R., Baba, K., Suganuma, Y., Yokoi, H., Tsujikawa, M. & Nishida, K. (2017) A Self-Assembling Peptide Gel as a Vitreous Substitute: A Rabbit Study. *Investigative Opthalmology & Visual Science*. 58 (10), 4068. doi:10.1167/iovs.17-21536.

Williamson, T.H. & O'Donnell, A. (2005) Intravitreal Triamcinolone Acetonide for Cystoid Macular Edema in Nonischemic Central Retinal Vein Occlusion. *American Journal of Ophthalmology*. 139 (5), 860–866. doi:10.1016/j.ajo.2005.01.001.

Xue, K., Liu, Z., Jiang, L., Kai, D., Li, Z., Su, X. & Loh, X.J. (2020) A new highly transparent injectable PHA-based thermogelling vitreous substitute. *Biomaterials Science*. 8 (3), 926–936. doi:10.1039/C9BM01603A.

Yang, P., Dong, Y., Huang, D., Zhu, C., Liu, H., Pan, X. & Wu, C. (2019) Silk fibroin nanoparticles for enhanced bio-macromolecule delivery to the retina. *Pharmaceutical Development and Technology*. 24 (5), 575–583. doi:10.1080/10837450.2018.1545236.

Yasuda, K., Motohashi, R., Kotake, O., Nakagawa, H., Noma, H. & Shimura, M. (2016) Comparative Effects of Topical Diclofenac and Betamethasone on Inflammation After Vitrectomy and Cataract Surgery in Various Vitreoretinal Diseases. *Journal of Ocular Pharmacology and Therapeutics*. 32 (10), 677–684. doi:10.1089/jop.2016.0099.

Yu, Y., Lau, L.C.M., Lo, A.C. & Chau, Y. (2015) Injectable Chemically Crosslinked Hydrogel for the Controlled Release of Bevacizumab in Vitreous: A 6-Month In Vivo Study. *Translational Vision Science & Technology*. 4 (2), 5. doi:10.1167/tvst.4.2.5.

6.1. Conclusions

The vitreous is essential to the proper functioning of the eye. Various clinical vitreoretinal diseases such as posterior vitreous detachment, retinal detachment, vitreous haemorrhage, and uveitis are due to vitreous dysfunction. Vitrectomy is fast becoming the treatment of choice for these diseases making the need for a suitable vitreous substitute essential. Current substitutes work well as short-term tamponades, but an improved long-term tamponade is necessary.

The goal of this research was to design and fabricate a polymeric vitreous substitute that exhibited similar physicomechanical and optical properties to the natural vitreous. An additional aim was to entrap drug-loaded nanoparticles into the substitute to allow for the treatment of vitreoretinal diseases.

The literature review extensively discussed current clinically used vitreous substitutes along with experimental natural and synthetic polymer-based hydrogel substitutes. Using the review as a guide, a combination of natural and synthetic polymers was chosen for the design and fabrication of a new vitreous substitute. During the pre-formulation and optimisation phase, a composite hydrogel composed of hyaluronic acid and a poloxamer blend was formulated as a potential vitreous substitute.

The optimised hydrogel was further characterised and nano-enabled with drug-loaded PLGA nanoparticles. The hydrogel displayed *in situ*-forming properties and was transparent. FTIR, DSC and TGA analysis confirmed the formation of the hydrogel with hyaluronic acid, poloxamer and the PLGA nanoparticles. The physicomechanical and optical properties of the nanoparticle-loaded hydrogel also were similar to those of the natural vitreous. The hydrogel demonstrated injectability via a 26G needle and retained its properties post-injection. Cytocompatibility studies using 3T3 and hRPE cell lines demonstrated the biocompatibility of the nanoparticle-loaded hydrogel and this was further demonstrated with an *in vivo* rabbit model. All of these properties confer numerous advantages for the developed hydrogel to perform as a vitreous substitute.

6.2. Recommendations

The current dissertation provided a comprehensive evaluation of the design, fabrication and characterisation of a nanoparticle-loaded hydrogel that functions as a potential vitreous substitute. It is recommended that further studies of this hydrogel include the loading of collagen (type II) to further improve the biomimetic properties of the substitute. Studies may also be conducted to improve and decrease the degradation rate of the hydrogel. Other drugs, such as anti-VEGF drugs and peptides, may be loaded instead of triamcinolone acetonide (TA) or simultaneously with TA to evaluate the ability of the substitute as a tamponade and treatment for other vitreoretinal diseases.

Comprehensive *in vivo* rabbit studies are recommended. The studies may include a pars plana vitrectomy along with slit lamp, fundus, and ERG examinations. These studies may also be conducted in conjunction with current clinically used vitreous substitutes.

As discussed in Chapter 2, regeneration of the vitreous humour would allow for improved biocompatibility with surrounding ocular tissue and better biomechanical properties. Regeneration of the vitreous is complex and future studies should focus on this.

Appendix A

ANIMALS RESEARCH ETHICS COMMITTEE (AREC)

UNIVERSITY OF THE WITWATERSRAND, JOHANNESBURG

STRICTLY CONFIDENTIAL

CLEARANCE CERTIFICATE NUMBER: 2021/03/07/C

APPLICANT: Ms OJ Owaezuoke
School: School of Therapeutic Sciences; Department: N/A; Location: WRAF

PROJECT TITLE: In vivo evaluation of a bioinspired protein resistant ocular biomaterial (BioPROT) in Albino New Zealand rabbits
Category: C; Species and Numbers involved: *70X 2.5 - 3.5 kg male or female, Albino New Zealand rabbits*

Approval is hereby given for the use of animals for the research project named above and described in the application reviewed by a quorate meeting of the AREC held on 30 Mar 2021. This approval remains valid until 20 May 2021 and is conditional to the following (if blank there are no special conditions):

Condition 1	Condition 2	Condition 3	Condition 4
Liaise with the WRAF staff about the feasibility of using an Elizabethan collar if irritation of the eyes			

All material changes to the approved research must be reported to the AREC before they are implemented. Failure to do so will invalidate this clearance certificate.

An annual progress report must be provided to the AREC.

The use of these animals is subject to AREC guidelines on the use and care of laboratory animals, is limited to the procedures described in the application and is subject to additional conditions listed below:

I, the Chair of the AREC (or my designated representative) am satisfied that the proposed research is ethical as judged by local law, international standards and University policy.

Signed: _____ _____ Date: __21/05/2021_____
(Chairperson of the AREC)

I am satisfied that the persons listed in this application are competent to perform the procedures described in the application, in the context of Section 23 (1) (c) of the veterinary and Para-veterinary Professions Act (19 of 1982).

CC: Student supervisor: «Title1» «Initials1» «Supervisor_surname»
Director Wits Research Animal Facility (WRAF): Dr Kim Jardine

Appendix B

Design and engineering of a bio-responsive, nano-enabled vitreous substitute for the treatment of retinal diseases.

Naik, K.[1], Choonara, Y.E.[1], du Toit, L.C.[1] and Ally, N.[2]

[1]Wits Advanced Drug Delivery Platform Research Unit, Department of Pharmacy and Pharmacology, School of Therapeutic Sciences, Faculty of Health Sciences, University of the Witwatersrand, Johannesburg, 7 York Road, Parktown, 2193, South Africa
[2]Division of Ophthalmology, Department of Neurosciences, School of Clinical Medicine, Faculty of Health Sciences, University of the Witwatersrand, Johannesburg, 7 York Road, Parktown 2193, South Africa

Limitations with current vitreous substitutes have stimulated a need for new vitreous substitutes with reduced side effects. The ideal vitreous substitute should have similar viscoelastic properties to the natural vitreous. It should maintain intraocular pressure within a normal range, and it should be able to support surrounding ocular tissue such as the retina without causing toxicity. The thermoresponsive vitreous substitute formulated in this study is a hydrogel composed of a pluronic blend mixed with hyaluronic acid. Drug delivery to the retina is a challenge due to the position of the retina in the eye along with the blood-retinal barrier. Therefore, PLGA nanoparticles have been synthesised for the intravitreal delivery of drugs for retinal diseases. The nanoparticles possessed an average size of about 150nm and an average zeta potential of negative 25mV, and the hydrogel formed a gel at physiological temperatures (37°C). Nanoparticles were subsequently loaded into the hydrogel. The long-term vitreous substitute is proposed to function as a carrier and delivery system for drug-loaded nanoparticles with triamcinolone acetonide (a steroid used in the management of macular oedema) employed as a model drug. Temperature ramp studies of the loaded hydrogels demonstrated a solution to gel transition at physiological temperatures. Further studies are underway for the comprehensive evaluation of this system as a potential vitreous substitute.

Word count: 212 words

Acknowledgements: This research has been funded by grant #MND200602526843 from the National Research Foundation.

Presented online at - Annual Molecular Biosciences Research Trust (MBRT) Postgraduate Research Day 2021, University of the Witwatersrand

pharmaceutics

MDPI

Review

Advances in Polysaccharide- and Synthetic Polymer-Based Vitreous Substitutes

Kruti Naik [1], Lisa C. Du Toit [1], Naseer Ally [2] and Yahya E. Choonara [1,*]

[1] Wits Advanced Drug Delivery Platform Research Unit, Department of Pharmacy and Pharmacology, School of Therapeutic Sciences, Faculty of Health Sciences, University of the Witwatersrand, 7 York Road, Parktown, Johannesburg 2193, South Africa
[2] Division of Ophthalmology, Department of Neurosciences, School of Clinical Medicine, Faculty of Health Sciences, University of the Witwatersrand, 7 York Road, Parktown, Johannesburg 2193, South Africa
* Correspondence: yahya.choonara@wits.ac.za; Tel.: +27-11-717-2052

Abstract: The vitreous humour is a gel-like structure that composes the majority of each eye. It functions to provide passage of light, be a viscoelastic dampener, and hold the retina in place. Vitreous liquefaction causes retinal detachment and retinal tears requiring pars plana vitrectomy for vitreous substitution. An ideal vitreous substitute should display similar mechanical, chemical, and rheological properties to the natural vitreous. Currently used vitreous substitutes such as silicone oil, perfluorocarbon liquids, and gases cannot be used long-term due to adverse effects such as poor retention time, cytotoxicity, and cataract formation. Long-term, experimental vitreous substitutes composed of natural, modified and synthetic polymers are currently being studied. This review discusses current long- and short-term vitreous substitutes and the disadvantages of these that have highlighted the need for an ideal vitreous substitute. The review subsequently focuses specifically on currently used polysaccharide- and synthetic polymer-based vitreous substitutes, which may be modified or functionalised, or employed as the derivative, and discusses experimental vitreous substitutes in these classes. The advantages and challenges associated with the use of polymeric substitutes are discussed. Innovative approaches to vitreous substitution, namely a novel foldable capsular vitreous body, are presented, as well as future perspectives related to the advancement of this field.

Keywords: retinal detachment; vitrectomy; vitreous substitute; in situ hydrogel; polysaccharide; synthetic polymers; artificial vitreous

check for updates

Citation: Naik, K.; Du Toit, L.C.; Ally, N.; Choonara, Y.E. Advances in Polysaccharide- and Synthetic Polymer-Based Vitreous Substitutes. *Pharmaceutics* **2023**, *15*, 566. https://doi.org/10.3390/pharmaceutics15020566

Academic Editors: Paolo Lanzetta and Anna Drabczyk

Received: 12 January 2023
Revised: 1 February 2023
Accepted: 5 February 2023
Published: 8 February 2023

1. Introduction

The World Health Organisation (WHO) estimates that 2.2 billion people suffer from vision impairment or blindness globally. Of these 2.2 billion, 1 billion people have preventable causes of blindness or visual impairment [1]. Blindness and visual impairment can be caused by, cataracts, glaucoma, diabetic retinopathy, age-related macular degeneration (AMD), and retinal detachment (RD) [1,2]. The leading cause of global blindness is cataracts, while glaucoma is the leading cause of irreversible visual loss and is second to cataracts as a cause of blindness globally [3,4]. Worldwide, an estimated 14 million people are affected by age-related macular degeneration [5] and one-third of people suffering from diabetes mellitus (285 million) are affected by diabetic retinopathy [6]. Pars plana vitrectomy (PPV) is one of the most commonly used treatments for many retinal diseases, especially RD [7]. During PPV the vitreous body is removed and replaced with a vitreous substitute [8]. Certain types of RD can also be treated with pneumatic retinopexy (PR) [9]. PR is an outpatient procedure that involves the induction of retinopexy around the retinal breaks or tears and intravitreal injection of a long-acting expansive gas (Figure 1) [10].